POLITECNICO
MILANO 1863

SCUOLA DI INGEGNERIA INDUSTRIALE
E DELL'INFORMAZIONE

Electric Vehicle Modelling, Simulation and Validation on Real Driving Conditions

TESI DI LAUREA MAGISTRALE IN
MECHANICAL ENGINEERING

Author: **Antonio Covello**

Student ID: 970240
Advisor: Ch.ma Prof.sa Michela Longo
Co-advisor: Ing. Alessandro Saldarini
Academic Year: 2022-2023

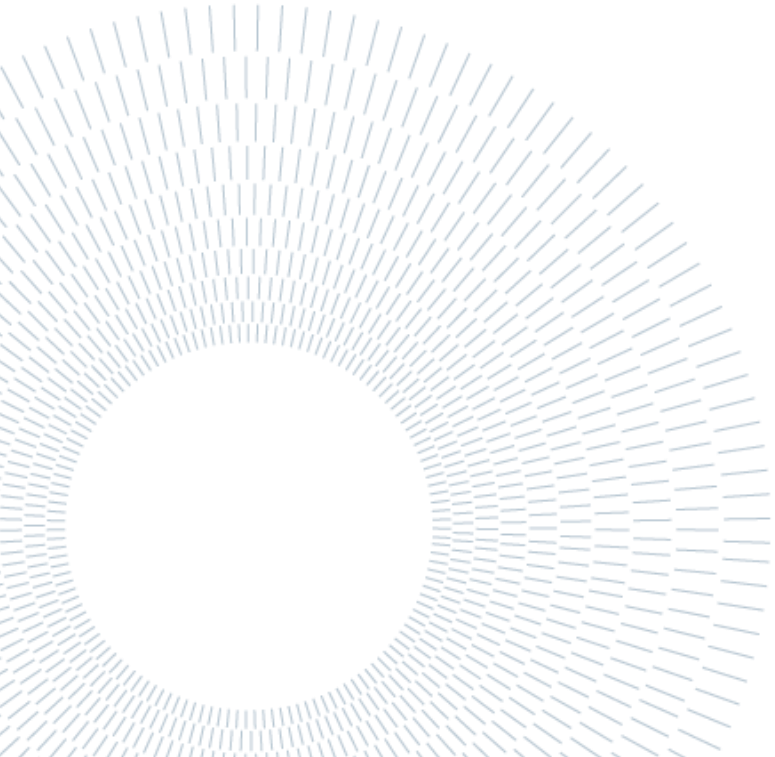

Abstract

Climate change and environmental concerns are now putting a higher focus than ever on sustainability in all aspects of modern life. The transition towards green energy and electrification must also involve the transportation sector, which is one of the major causes of emission all over the world. In this sense, great technological advancements have been in the road transports in modern years, with the development and evolution of Electric Vehicles (EV). This background represents the starting point of the work of this thesis. The purpose of this work is the development and the validation of an EV model. The first part deals with the presentation of the model, which starts from the definition of the route, and so the speed profile, and the choice of the vehicle, which are the main inputs of the model; the output is instead the energy consumption. Furthermore, the experimental campaign has been presented. In particular, fifty experimental tests has been conducted divided into two groups of twenty-five each. The differences between two groups and the experimental parameters have been explored. Finally, the both model and experimental results have been analyzed in detail and compared according to the level of auxiliaries power and to the type of the road.

Key-words: Sustainable transport, Electric Vehicle, EV model, experimental campaign.

Abstract in lingua italiana

Il cambiamento climatico e gli interessi per l'ambiente hanno posto un interesse sempre maggiore verso la sostenibilità in tutti gli aspetti della vita moderna. La transizione verso le energie rinnovabili non può non coinvolgere anche il settore dei trasporti, che risulta essere una delle maggiori cause di inquinamento nel mondo. In questa direzione, grandi evoluzioni tecnologiche sono state avanzate nei trasporti stradali negli ultimi anni, tra cui lo sviluppo e il miglioramento dei veicoli ibridi ed elettrici. Tale background rappresenta il punto di partenza di questo lavoro di tesi, il cui scopo è quello di sviluppare un modello di un veicolo elettrico validandolo attraverso una mirata campagna sperimentale. Come si può immaginare, il cuore pulsante del veicolo è lo stato di carica della batteria, il cui consumo dipende da molti aspetti (per es. accensione aria condizionata, pendenza del territorio, ecc.). Input del modello sono le informazioni inerenti al tragitto e la velocità del veicolo e ovviamente le caratteristiche tecniche del veicolo stesso. Il modello è stato sviluppato attraverso l'ausilio di Matlab/Simulink e validato con dati reali raccolti su campo. I risultati raccolti hanno mostrato come il modello risulti essere molto accurato e facilmente scalabile in altri contesti.

Parole chiave: Mobilità sostenibile, veicolo elettrico, modello di veicolo elettrico, campagna sperimentale.

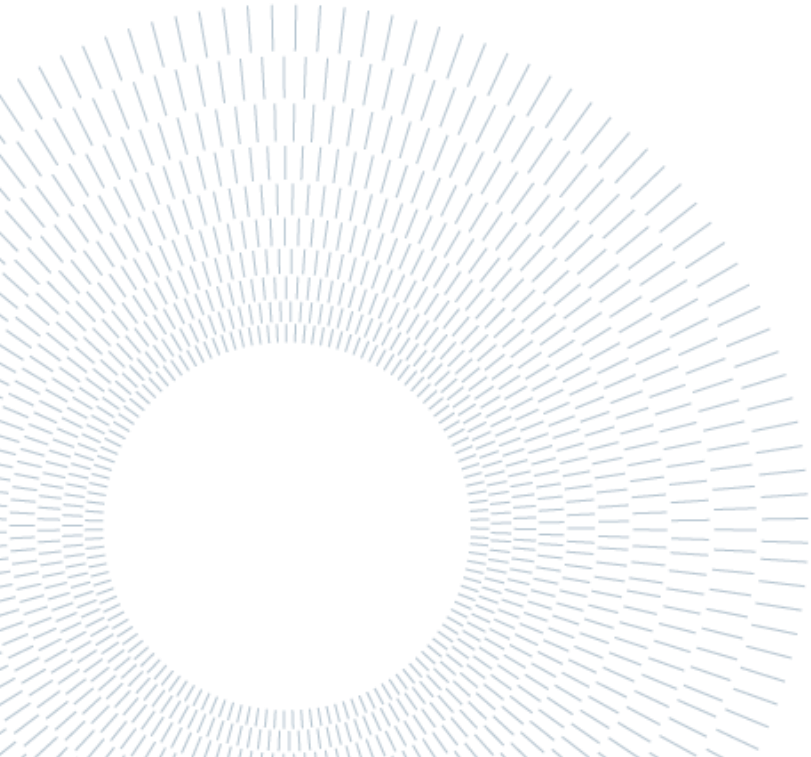

Contents

Introduction

Climate change and environmental concerns are now putting greater focus than ever on electrification and sustainability in all aspects of modern life. In this sense, the Sustainable Development Goals (Figure 0.1), defined by the United Nations, are an appeal for action by all countries in order to enhance prosperity while preserving the environment, within 2023 [1]. They are role model for achieving a better and further sustainable future for everyone, addressing the many problems and the global challenges that the world is now dealing with, particularly those related to climate change and environmental degradation.

Figure 0.1: The Sustainable Development Goals [1].

According to the most recent data, the world is moving closer, and slowly, to its sustainable energy goals. In 2019, renewable energy sources accounted for 17,7% of all final energy consumption, with an increase of 1,6 percentage points than in 2010.

Nevertheless, the cost of manufacturing and exporting solar photovoltaic modules, wind turbines, and biofuels has grown due to rising energy and transportation prices, adding uncertainty to a development trajectory that is already well behind the sustainability levels targeted by 2030. Therefore, a large mobilization of public and private capital and continued policy support for clean and renewable energy will be necessary to achieve energy and climate goals, particularly in developing countries.

These needs represent the starting point of the work of this thesis. Among all aspects of life, an important focus is pointed towards sustainable mobility and the transport sector, which is one of the major causes of emissions in the world.

Described in this work is a methodology for the design of an Electric Vehicle (EV) model and validation on a real-world vehicle system with detailed analysis of the results.

Firstly an introduction about sustainability is carried out, with an analysis on emissions and comparison between EVs and Internal Combustion Engine (ICE) vehicles on emissions, costs and market share, in reference to last year's trends and future predictions.

Furthermore, the EV model has been presented, with a focus on the most important parameters. The speed and altitude profiles and the choice of the vehicle are indeed essential for this analysis, since they are the inputs of the model, and their characteristics influence significatively all the aspects of road transportation. Thus, the model has been explained in detail, with both its dynamic and energetic blocks and their parameters. Moreover, the experimental campaign has been explained, focusing on the differences between the several tests.

In conclusion, the results of the model and of the experimental tests has been analyzed and compared, trying to motivate the reasons for possible similarities and differences, and giving the solutions.

1 General Overview

1.1. Emission Analysis

Human carbon dioxide and other GreenHouse Gases (GHGs) emissions are a primary driver of climate change and present currently one of the world's most important concerns and pressing challenges. This relationship between atmospheric greenhouse gas concentrations, especially CO_2, and global temperature rise appears to have existed throughout Earth's history [2], even though the involvement of human emissions in climate warming is still not unanimously recognized.

Therefore, in order to prevent catastrophic climate change and environment warming, people must act fast to slow down global greenhouse gas emissions, starting with the sectors with the highest contribution and from the emissions which might, theoretically, be completely cut down. Furthermore, it must be needed to first identify the sources of global gas emissions, with an important focus of transport sector, in order to better understand how emissions can be most effectively reduces and which contributions could be eliminated using contemporary technologies.

Every year, the globe emits around 50 billion tons of greenhouse gases, measured in carbon dioxide equivalents (CO2eq) [3]. It can be clearly seen in Figure 1.1 that most of these emissions are created by the energy sector, specifically by industry, commercial and residential buildings and transportation field.

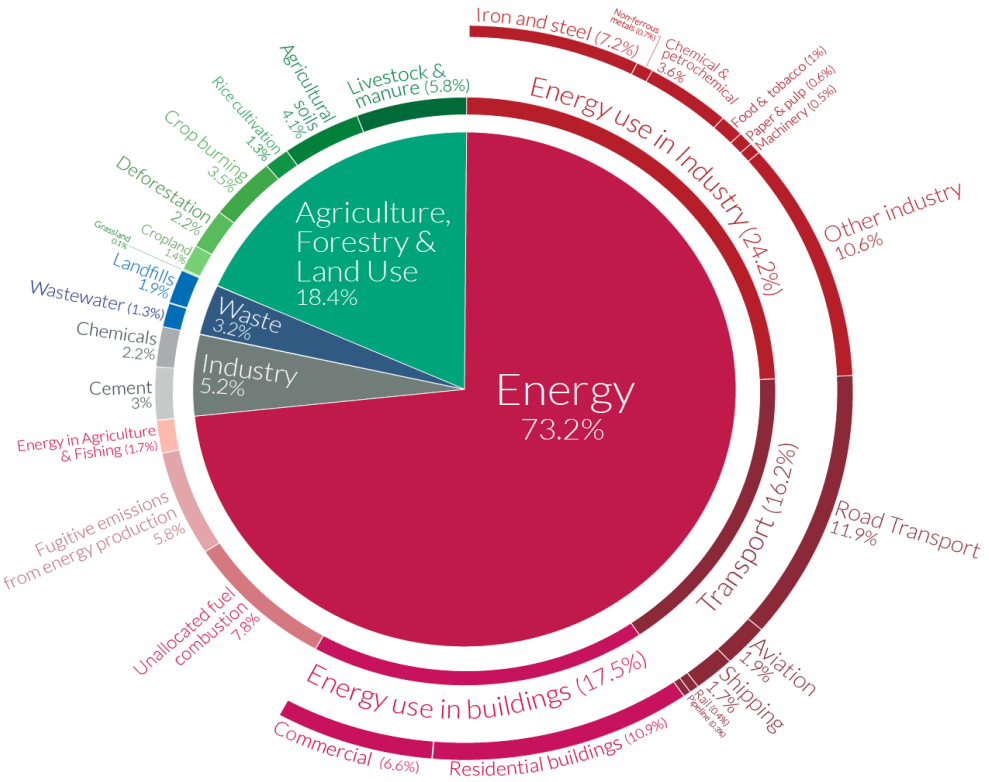

Figure 1.1: GHG emissions by sector [3].

Anyway, the trend in global emissions is not changing (Figure 1.2 (a)), due to the high and continuously increasing GHGs emissions of some of the biggest states in the world such as USA and China, Figure 1.2 (b). Even if a small reduction in emission has been observed between 2019 and 2020, this is mainly due to the COVID-19 pandemic; indeed, the trend of recent years shows that emissions still grow up [4].

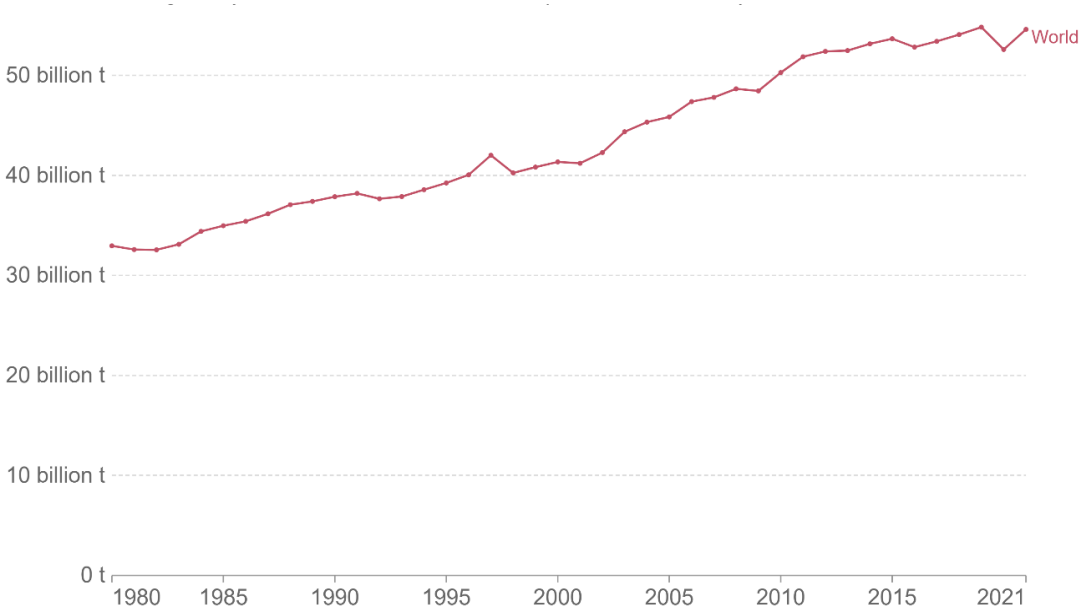

(a)

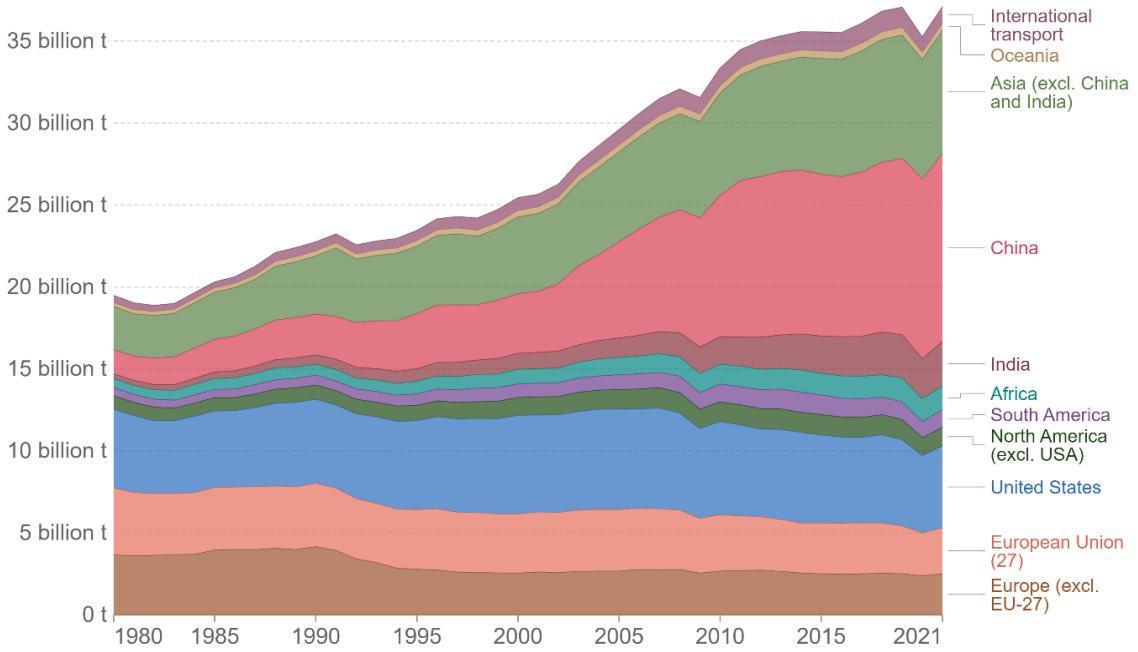

(b)

Figure 1.2: History of Greenhouse gas emissions [4]; (a) Global; (b) By world region.

Fortunately, a bit different is the situation in Europe [5]. The EU surpassed its 2020 greenhouse gas reduction target of 20%. According to official data reported by Member States in 2022, GHG emissions were 32% lower in 2020 than in 1990. This steep decline was mainly related to the COVID-19 pandemic, but anyway, emission levels have been below the 2020 target since 2018.

Although GHG emissions remained below pre-pandemic levels, preliminary data for 2021 show a post-pandemic increase. EU greenhouse gas emissions increased by 5% in 2021 compared to the previous year, owing mostly to the economic rebound experienced after COVID-19 limitations were abolished throughout Europe. Rising gas prices in the second half of 2021 were another factor contributing to the recent spike in emissions.

In Figure 1.3, also some projections about EU emissions are showed. In particular, looking ahead to the climate target for 2030, the EU's GHG emissions are predicted to continue dropping, resulting in a net emissions decrease of 41%.

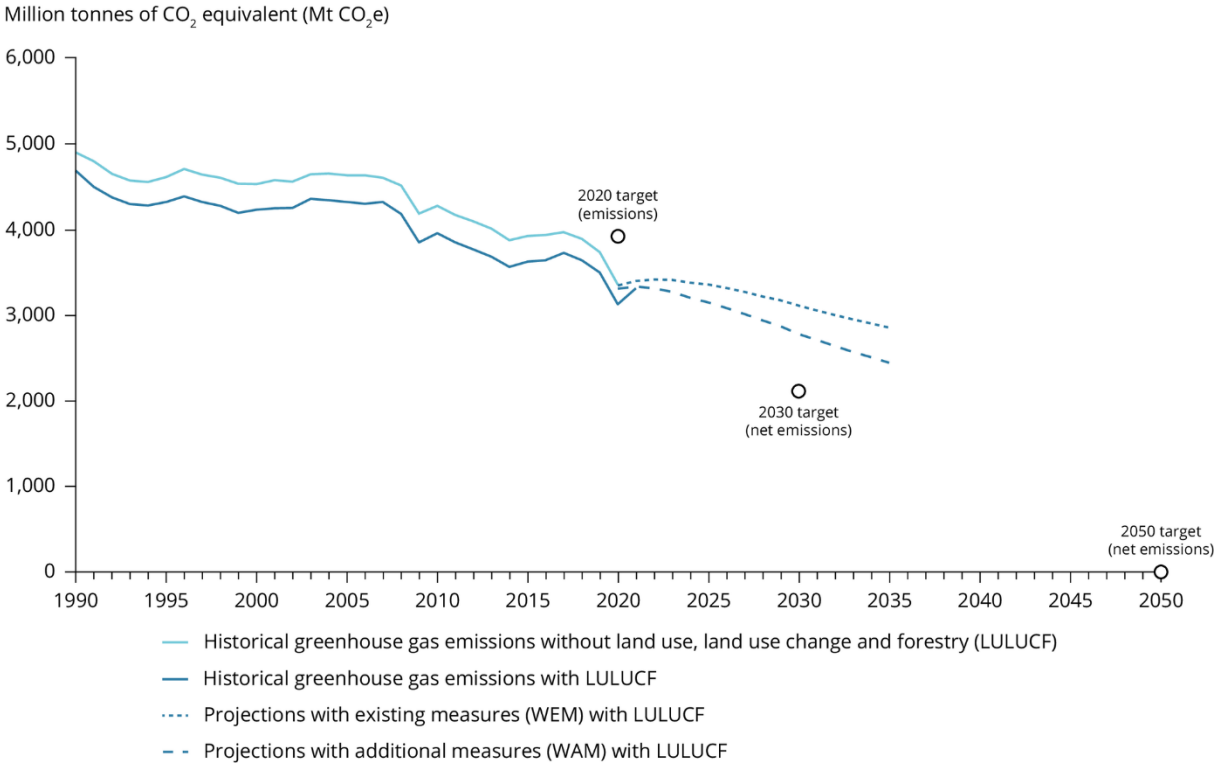

Figure 1.3: Historical trends and future projections of EU greenhouse gas emissions [5].

These GHG forecasts given by Member States in 2021 and 2022 have not yet included efforts to meet the net 55% objective established in the European Climate legislation for 2030.

In the longer term, the EU aims to be carbon neutral by 2050. This will necessitate emissions reductions that are more than twice as large as the average decrease achieved each year between 1990 and 2020. Thus, it is clear that further implementation of policy is fundamental.

1.1.1. Road Transportation emissions

As stated above, the transport sector is one of the major sources of greenhouse gases, accounting for approximately 16,2% of worldwide emissions. It's important to state that this value incorporates a small quantity of electricity (called "indirect emissions") along with all direct emissions from burning fossil fuels to power transport activities, but do not include emissions from the manufacturing of motor vehicles or other transport equipment, which are contained in other sectors [3].

Within the transportation area, road transport contributes the most (11,9%): this value includes emissions from the combustion of gasoline and diesel from all forms of road transport, comprising automobiles, trucks, lorries, motorbikes, and buses. In particular, passenger vehicles (cars, motorbikes, and buses) account for 60% of road transport emissions, with road freight (lorries and trucks) accounting for the remaining 40%.

As regards Europe transport emissions [6], in this case they similarly exhibit the same worldwide trend, showed in Figure 1.4.

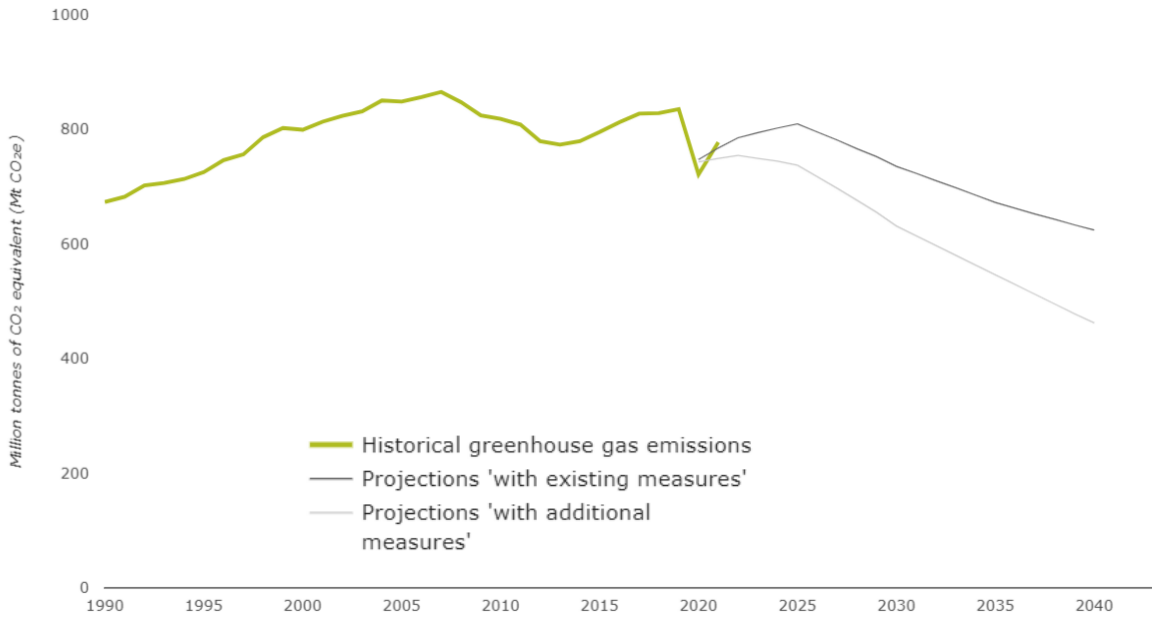

Figure 1.4: Greenhouse gas emissions from transport in Europe [6] .

The EU's domestic transport emissions rose regularly between 2013 and 2019 because of increase in passenger transport and inland freight volumes, which are closely interconnected to economic growth trends. The emissions then decreased by 13.6% during the pandemic, due to a severe reduction in transport activity. Anyway, the trend of the last years is returning again to pre-pandemic values, with an increase of 7,7% in 2021. Also in this case, the projections for transport emissions with existing and additional measures are similar to the EU emissions one, with a moderate increase in the first part and then a drop in the future.

Focusing on road transport, also in this case the trend is like the global one, with a steady increase in the 2010s years and then a reduction due to the pandemic, Figure 1.5. Similarly, the projections show the same trend.

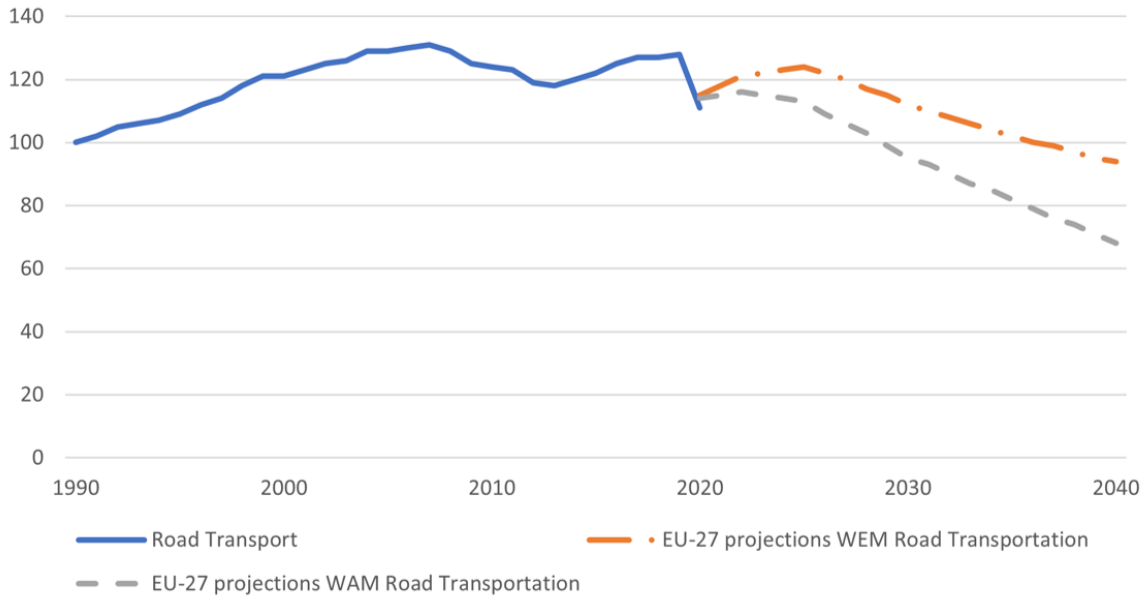

Figure 1.5: Greenhouse gas emissions from road transport in the EU and projections.

The road transport accounts for the highest proportion of all transportation emissions, producing 77% of all greenhouse gases in the EU in 2020. This is also a result of the emissions from ICE vehicles, which are widely utilized across the world and continue to be the primary mode of transportation for the most of the world's population. In any case, this value is likely to decline as road transport decarbonizes quicker than other forms of transportation. The reason is sustainable transportation and the increasing importance of hybrid and electric vehicles, which contribute significantly to the reduction of greenhouse gas emissions. This means that, if the whole road transport sector could be electrified and a transition to a fully decarbonized electricity mix would be possible, global emissions could be feasible reduced by the already stated value of 11,9%.

Anyway, it is evident from this background that a variety of processes and sectors contribute to global emissions. This means that there is no single or easy solution to deal with climate change. Concentrating on electricity, or transport, or food, or deforestation alone is not enough. Even within the energy sector – which accounts for almost three-quarters of emissions – there is no quick fix. Even though the electricity supply could be fully decarbonized, it would be also needed to electrify road transport and heating sectors. In addition, emissions from shipping and aviation, that are sectors in which low-carbon technologies are not available yet, would be still present.

To summarize, focusing only on the road transport, Figure 1.1 states that fully decarbonizing this sector could in theory reduce the emissions of about 12%, but it is also important how the energy has been produced. A decarbonization in the transport sector can be only together with a decarbonization in the energy field and production.

1.1.2. Comparison between EVs and ICE vehicles

The reasons of the importance of a decarbonization in the transport field and a strong transition towards green mobility have been already explained above. Hence, in this part, a comparison between the traditional ICE vehicles and the EVs has been made, with a focus on emissions. In particular, the starting point of this work of thesis is a previous case study, in which an EV and an ICE vehicle were compared on emissions and costs [7]. Even if the environmental background of the comparison was in Canada, the results are now considered and generalized, in order to decontextualize the case study.

Essentially, a fully EV has zero net emissions. This is partially true since the method of the production of electricity must be taken into account too. In the particular of the Canadian environment, CO_2 emissions were found to be at a mean value of 35 gCO_2-eq/kWh. These values are extremely low since most of the power in Canada is produced from hydropower. However, different is the situation in Europe, in which specific emission for generating power is between 300 and 400 gCO_2-eq/kWh [8], since the renewables still not represent the main energy source. In addition, battery-production-related emissions also must be taken into account, since they were found to represent a huge contribution (about 75 $kgCO_2$-eq/kWh [9]). Moreover, emissions produced/recovered from the recycling of the vehicle batteries cannot be considered yet, as they are extremely difficult to account for and the battery recycling technology is still very young.

Anyway, after all this background, the EV's carbon footprint over its lifetime is much way lower than that of traditional vehicles [10]. This is true even though the initial emissions associated with the fabrication of the electric car and battery pack are more than double the emissions for manufacturing the conventional vehicle. Thus, EVs already represent a big alternative and solution for the sustainability and the emissions, and considering the technological advancements, they will be more and more considered.

Furthermore, from the costs point of view, EVs will be in the long term cheaper than conventional vehicles, since the cost for travelling and maintenance costs are lower. Moreover, it is expected that EVs are going to be available at lower prices making them a far superior alternative also in terms of cost.

Precisely for the reasons stated above, in the transport sector there is a strong transition towards an increasingly green and sustainable mobility. In fact, great technological advancements have been made in electric vehicles in modern years, with an increasing focus on sustainability.

However, in these days, the introduction of EVs is more adapted and limited towards urban and suburban environments, but since the technology matures, battery capacity improves, and charging infrastructures are widely distributed, long-distance trips, such as truck travel or intercity, will become cheaper and easier than the options available nowadays [11], [12]. In the future, transportation will be powered by clean energy, making it more environmentally friendly and sustainable.

1.2. Market Analysis

The traditional ICE vehicles are still the most common vehicles used for road transportation. However, Electric Vehicles are becoming more popular, with several major automakers investing in the technology, for a variety of reason. They are far more ecologically beneficial than petrol or diesel cars, with zero emissions. Anyway, there are still some drawbacks to electric cars. They can be more expensive to purchase outright, and their range is frequently less than that of standard vehicles, even though this is improving more and more.

It is difficult to predict whether electric vehicles will totally replace regular vehicles. However, it appears that their popularity will only expand in the next years.

The combined annual sales of Battery Electric Vehicles (BEV) and Plug-in Hybrid Electric Vehicles (PHEV) tipped over the two-million-vehicle mark for the first time in 2019 [13], representing the 2,5% of the global market share. The global sales of EVs in 2019 increased fast, driven by the growth of EVs in Europe (+93 per cent). In Figure 1.6, the annual passenger-car sales in major regions are showed for the 2010s years, with an indication of the market share.

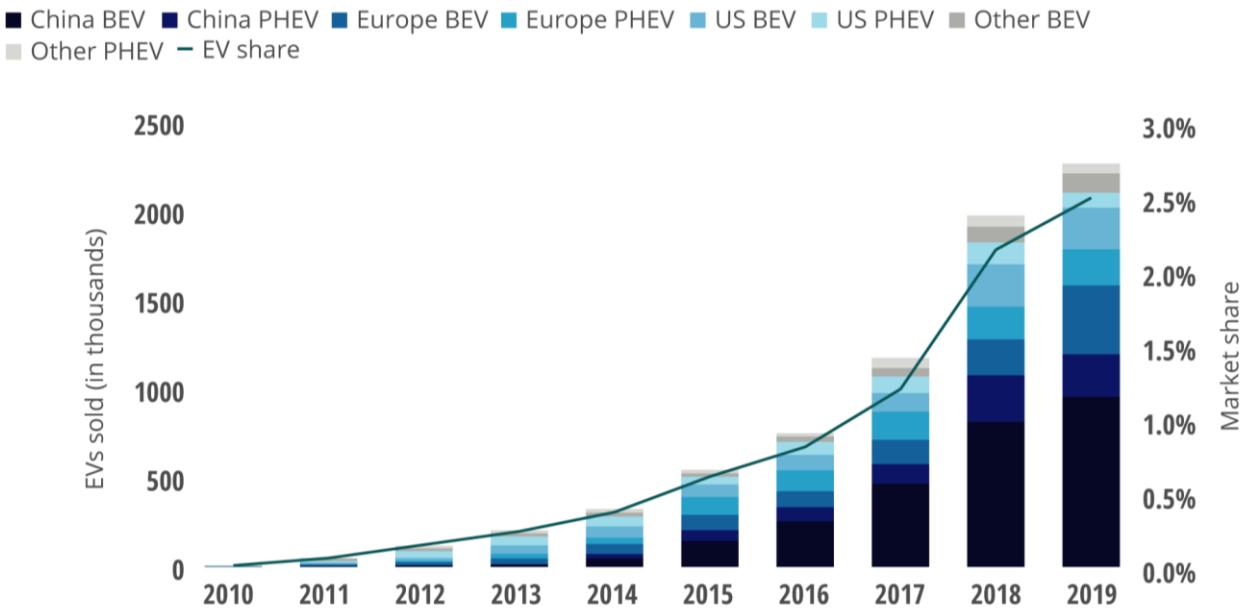

Figure 1.6: Annual passenger-car sales in major regions [13].

Of course, the situation is strongly dependent on the various regional markets. China dominates the EV market, accounting for half of all vehicle sales, followed by Europe and US. Unfortunately, the rest of the world is far behind in terms of EV sales for several reasons, including a lack of government commitment to EVs, insufficient or inappropriate charging infrastructure, EV availability, and cultural differences in mobility models.

After this decade of rapid growth, in 2020 the global electric car stock hit the 10 million mark, a 43% increase over 2019, and representing a 1% stock share [14]. In Figure 1.7, global electric passenger car stock between 2010 and 2020 are showed, with a classification of the different EVs.

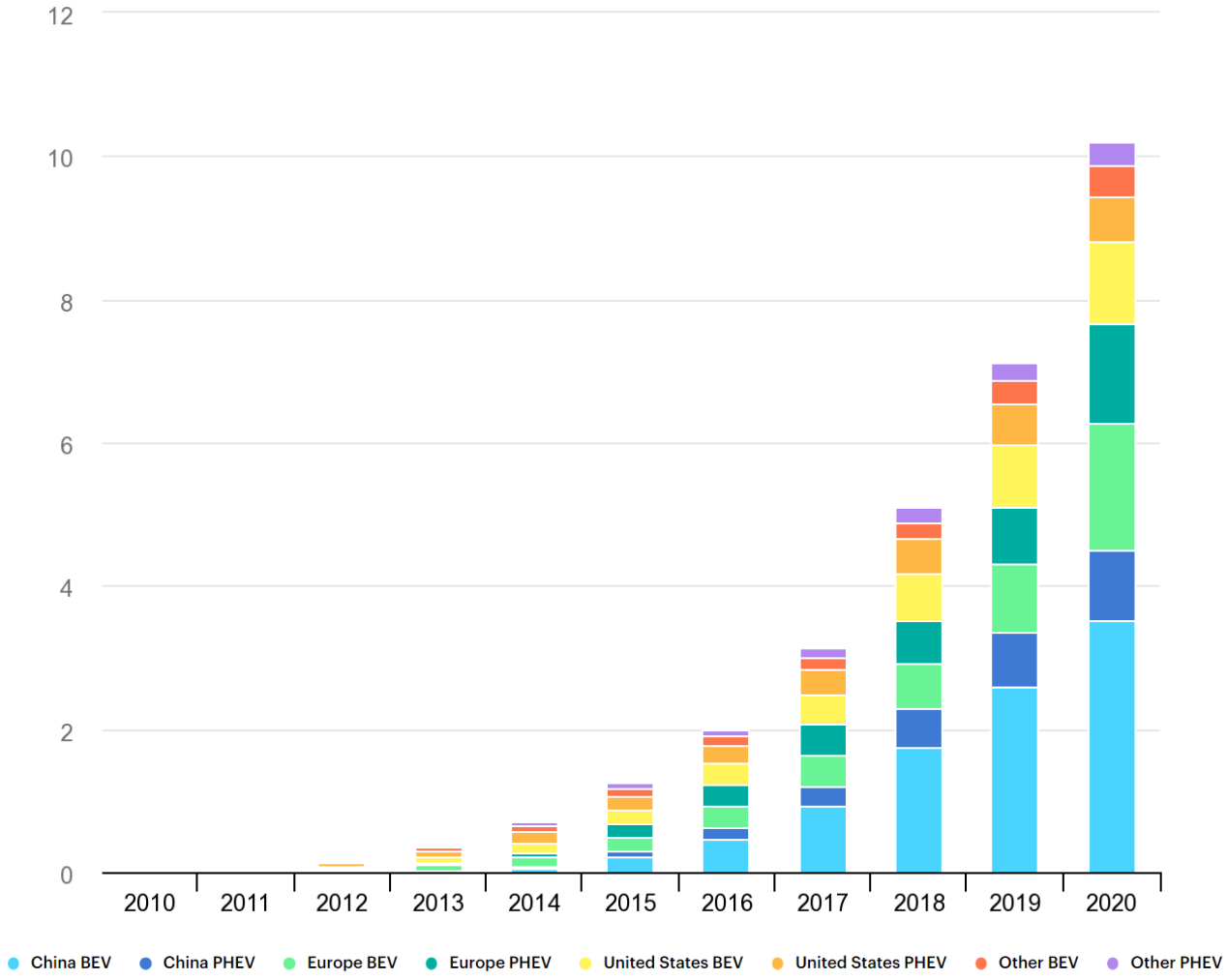

Figure 1.7: Global electric passenger car stock, 2010-2020 [14].

It is important to notice how, among all the EVs, BEVs represent the highest contribution. In 2020, BEVs accounted for two-thirds of new electric car registrations and two-thirds of the stock. The reason of this can be easily found out in the fact that BEVs represent a totally zero net emission transport mode, rather than the other hybrid vehicles. In addition to this, their range is increasing more and more, gaining the trust of customers.

In general, the success of EVs is being driven by a variety of factors. The key pillar is sustainable policy support. Moreover, public spending on subsidies and incentives is increasing year after year and a rising number of countries have pledged to phase out internal combustion engines or have aggressive car electrification goals for the future decades [15].

According to Figure 1.8, China still has the largest fleet, with 4,5 million electric vehicles, while Europe saw the highest yearly rise in 2020, reaching 3,2 million. After a small drop of the global market affected by the economic repercussions of the Covid-19 pandemic in the first part of 2020, about 3 million new electric cars were registered in the same year. Europe led the way for the first time, with 1,4 million new registrations. China came in second with 1,2 million registrations, while the United States recorded 295 000 new electric vehicles.

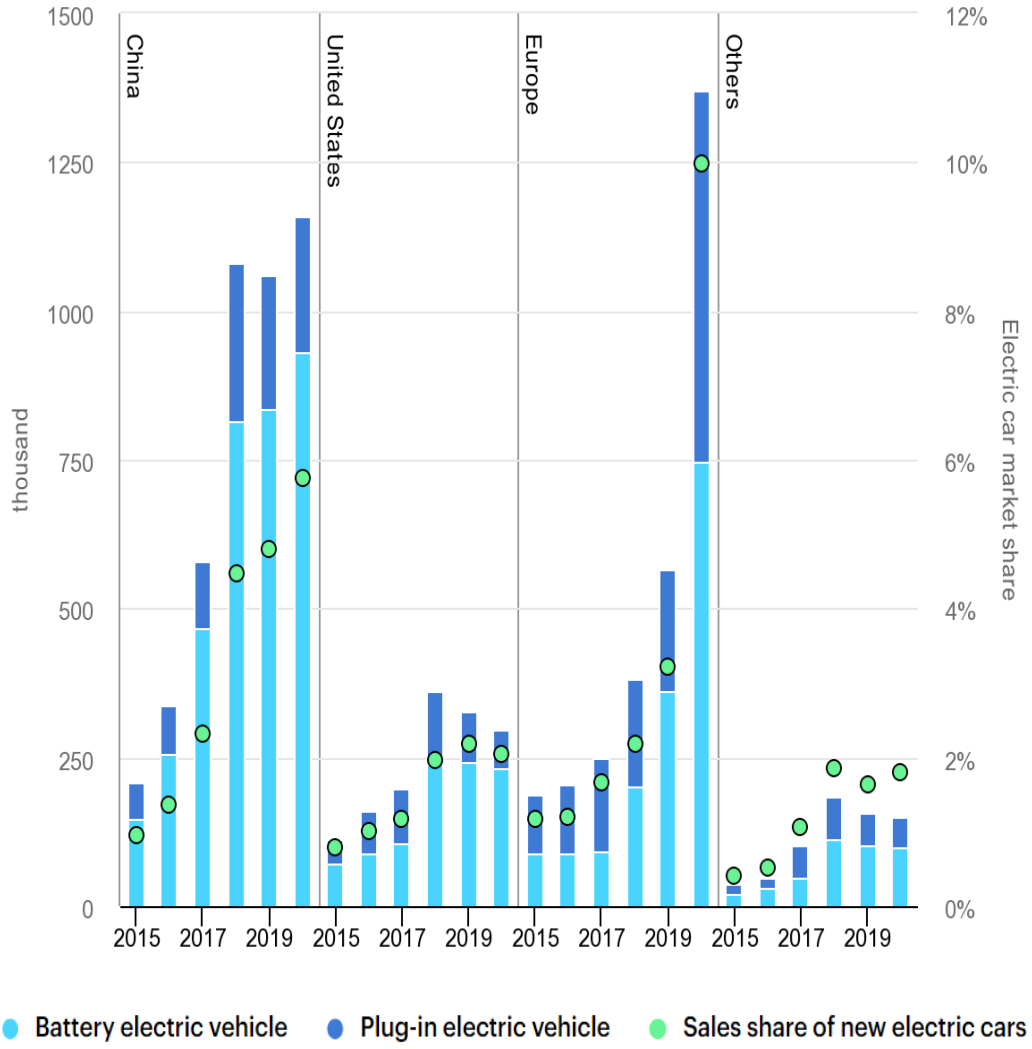

Figure 1.8: Global Electric car registrations and market share, 2015-2020 [14].

A variety of reasons contributed to a rise in electric vehicle registrations in 2020. Notably, on a total cost of ownership basis, electric vehicles are increasingly becoming more competitive in some nations. Several governments provided or extended economic incentives that insulated electric car sales from the car industry collapse.

An up-to-date prediction of the EV market has been developed for the next years, analyzing the most recent indicators [13], showed in Figure 1.9.

It is known that BEVs already outperform PHEVs globally, as stated above, and it has been predicted that by 2030, BEVs will likely account for 81% (25,3 million) of all new EVs sold. PHEVs sales, on the other hand, are predicted to reach 5,8 million by 2030. Furthermore, ICE vehicles growth will resume up to 2025 (81,7 million), followed by a drop in market penetration.

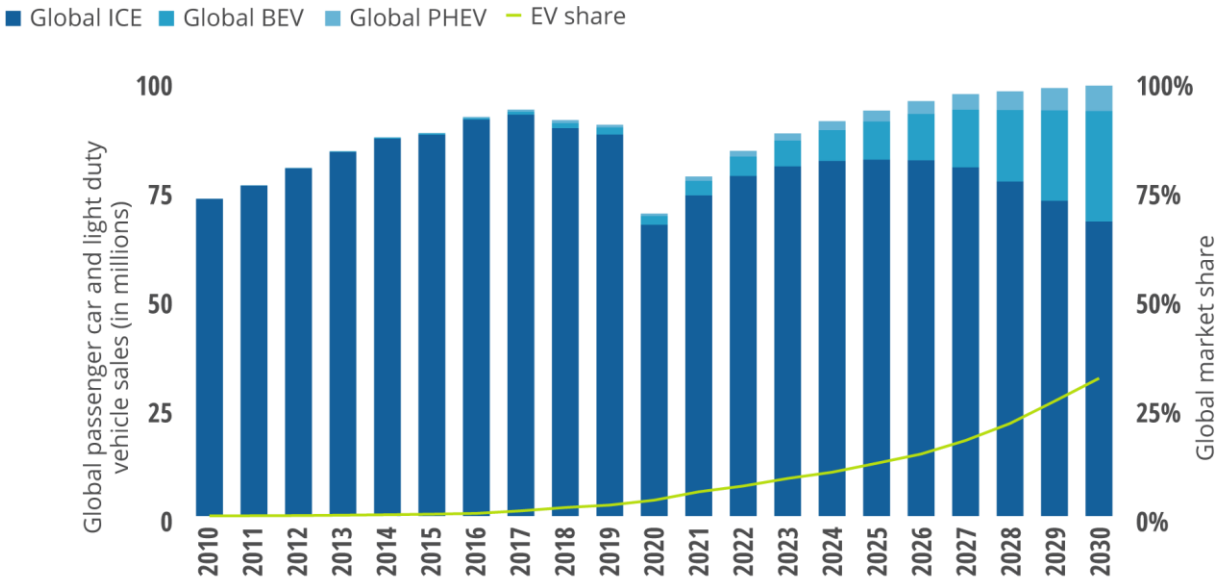

Figure 1.9: Prediction for annual passenger-car sales in major regions [13].

Total EVs sales will increase from 2,5 million in 2020 to 11,2 million in 2025, and then to 31,1 million by 2030. EVs would capture almost 32% of the entire market share for new car sales. Annual vehicles sales are unlikely to return to pre-COVID-19 levels until 2024. However, even if the slowing of ICE sales is expected to reduce the rate of recovery, EVs will continue to have a positive trajectory during the COVID-19 recovery period and may end up grabbing a disproportionate percentage of the market in the short term.

As it has been stated, EVs sales keep rising, but much more needs to be done in order to support charging infrastructure and heavy-duty vehicles. In particular, the International Energy Agency (IEA) found out some recommendations to accelerate the uptake of EVs worldwide [16]. As the electric car market matures, direct subsidies must be reduced and finally fade out. Stringent CO2 regulations have accelerated EV adoption in the most of leading EV markets and should be adopted by all governments wanting to promote the transition to sustainable mobility. Moreover, an important focus must be put towards the heavy-duty market (with electric buses and trucks) and towards the emerging and developing economies. Electrification of road transport in these countries should prioritize two and three-wheelers and urban buses, since they

are the most cost competitive vehicles. Price signals and the availability of charging infrastructure can further support the economic case for electrification.

Furthermore, it is necessary to expand EV infrastructure and smart grids. It is critical to incentivize and facilitate the installation of home chargers in existing parking places. Simultaneously, local governments should support the installation of chargers in existing structures. Coordination of grid extension and upgrading plans, including digital technologies to enable two-way communication and pricing between EVs and grids, is now required to guarantee that EVs can become a resource for grid stability, rather than a challenge.

2 Vehicle Model

The approach for designing and developing an EV model is described in detail in this section of the work. As explained in Chapter 1.1.2, this work follows a previous case study [7], in which this EV model was firstly developed. Afterwards, the model has been modified and corrected according to the literature, in order to give more accurate estimations of the outputs.

To summarize, the model employs telemetry from a real-time speed profile acquisition across a fixed route to accurately calculate the energy consumption required. The block diagram of the model is shown in Figure 2.1.

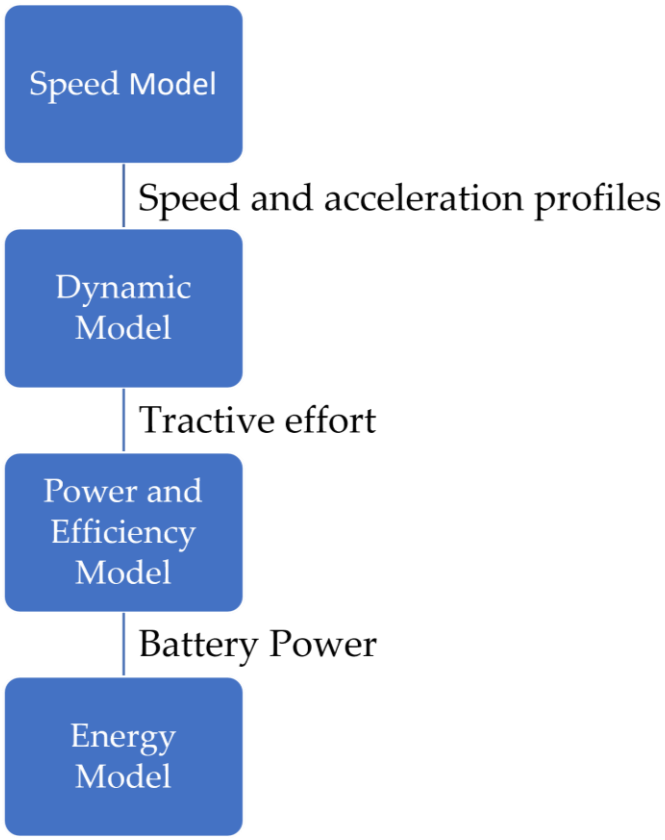

Figure 2.1: Block Diagram of the Model.

In order to simplify the explanation, the model has been broken into four blocks, which will be explored in detail below:

- The starting point of this model is the speed profile, which is used to calculate the acceleration of the vehicle.

- Furthermore, the acceleration profile is used to compute the dynamic behavior of the vehicle, and thus to calculate all the forces involved along the path. In this part, other essential inputs include the vehicle characteristics, which are combined with both acceleration and velocity in order to determine the resistance forces and the traction force.
- Once the tractive effort has been determined, the power of the battery must be calculated taking into account other quantities such as motor and transmission efficiencies.
- At the end, starting from the power of the battery, the energy consumption has been calculated. This represents the output of the model and hence the value that must be confirmed by the experimental tests in order for the model to be validated.

In order to simplify the description of the model, all the variables have been listed in Table 2.1.

Table 2.1: Variables used in the model.

Name	Symbol
Mass of the vehicle	$M_{Vehicle}$
Mass of the passenger	$M_{Passengers}$
Total Mass	M_{tot}
Equivalent Mass Coefficient	β
Equivalent Mass	m_{eq}
Rolling Resistance Force	F_{rr}
Rolling Friction Coefficient	f
Velocity of the Vehicle	v
Tyres Pressure	P_{Tyres}
Hill Climbing Force	F_{hc}
Slope of the Road	α
Aerodynamic Force	F_{ad}

Drag Coefficient	c_d
Frontal Area	S
Air Density	ρ
Inertia Force	$F_{Inertia}$
Acceleration of the Vehicle	a
Adhesion Force	$F_{Adhesion}$
Adhesion Coefficient	$c_{Adhesion}$
Tractive Effort	F_{te}
Instantaneous Power Flow	P_{te}
Positive Power	P_{pos}
Negative Power	P_{neg}
Motor Efficiency	μ_m
Transmission Efficiency	μ_g
Torque	T
Angular Speed	ω
Gear Ratio	G
Tyre Radius	r
Copper Losses Coefficient	k_c
Iron Losses Coefficient	k_i
Windage Losses Coefficient	k_ω
Constant Losses Coefficient	C
Tractive Power	P_{te}
Braking Power	$P_{braking}$

Power required by the motor	$P_{mot_{in}}$
Power of auxiliaries	$P_{auxiliaries}$
Power provided by the battery	$P_{battery}$
Instantaneous Energy profile	$E_{battery}$
Battery Capacity	$C_{battery}$

2.1. Speed Profile Model

The first part of the model deals with the definition of the speed profile and, from this, with the calculation of the acceleration of the vehicle. These are the two most important parameters used to calculate the vehicle dynamics, i.e., all the resistance forces which characterize the vehicle behaviour during the route.

As regard the velocity, since the goal of the model is to represent a true vehicle behavior through a fixed route, it has been decided to use a real speed profile acquisition. This profile of velocities represents the starting point of the model, which continues with the calculation of the acceleration profile. This could have been done in three different methodologies:

- The acceleration profile could be obtained directly from the experimental values acquisition;
- The acceleration profile could be calculated analytically making the derivative of the already obtained speed profile;
- Using Simulink software, the profile has been automatically computed starting from the speed profile. To calculate the acceleration, the "Drive Cycle Source" block implements Savitzky-Golay differentiation using a second-order polynomial with a three-sample point filter. [17]

It has been chosen to use Simulink model for the following reasons. As regards the real accelerations values, they are registered every time step of 0,05 seconds. Thus, it is inconvenient to use this method, since the other variables profiles are acquired every one second time step, and this could give some calculation and approximation mistakes. Moreover, using the real acceleration values could give additional mistakes caused by acquisition issues. The comparison between the two other methodologies is showed in Figure 2.2.

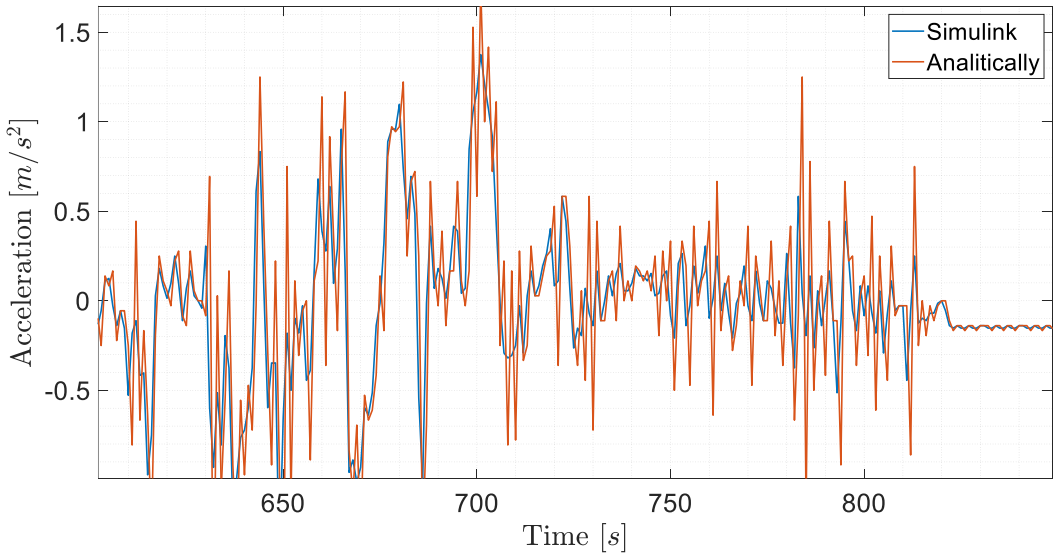

Figure 2.2: Comparison between Simulink acceleration and analytical acceleration profiles.

The trends of the two profiles are very similar, but it can be noticed that the analytical profile shows sharper peaks and a more frequent scattering, which can be explained by a not so precise acquisition. Instead, the Simulink acceleration profile presents a more smoothed variations and a lower peak, thanks to the differentiation used for the calculation. In general, since the latter seems to be a more correct acceleration profile, this was the method used in the model.

In Figure 2.3, the scheme used in Simulink is reported.

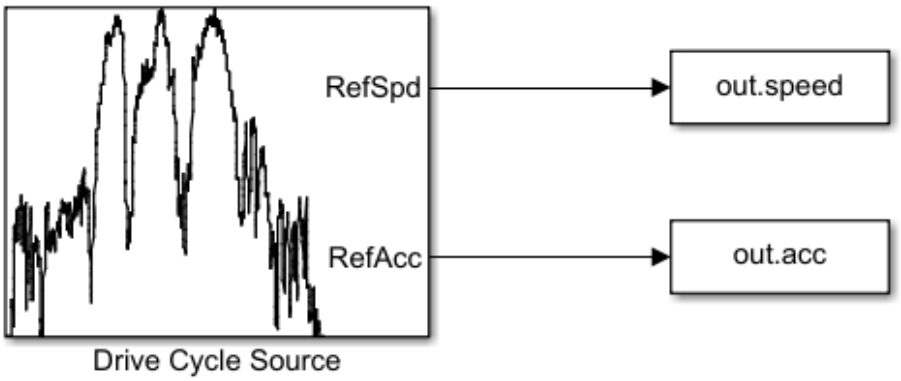

Figure 2.3: Speed and acceleration profile Model.

It is clear that the input is the real telemetry, which uses the "Drive Cycle Source" block to convert the output speed from km/h to m/s in order to simplify the future calculations. In addition, another output of this part is the acceleration profile, with values measured in m/s^2, which will be useful to calculate the forces during the route.

2.2. Dynamic Model

After obtained speed and acceleration profiles, resistance forces had to be calculated in order to compute the tractive effort, useful to calculate powers and energy of the battery. A typical dynamic model of the vehicle has been used, represented in Figure 2.4, which includes three resistance forces (rolling resistance F_{rr}, hill climbing F_{hc} and aerodynamic drag F_{ad}) plus the inertia term $F_{Inertia}$ [18]–[20].

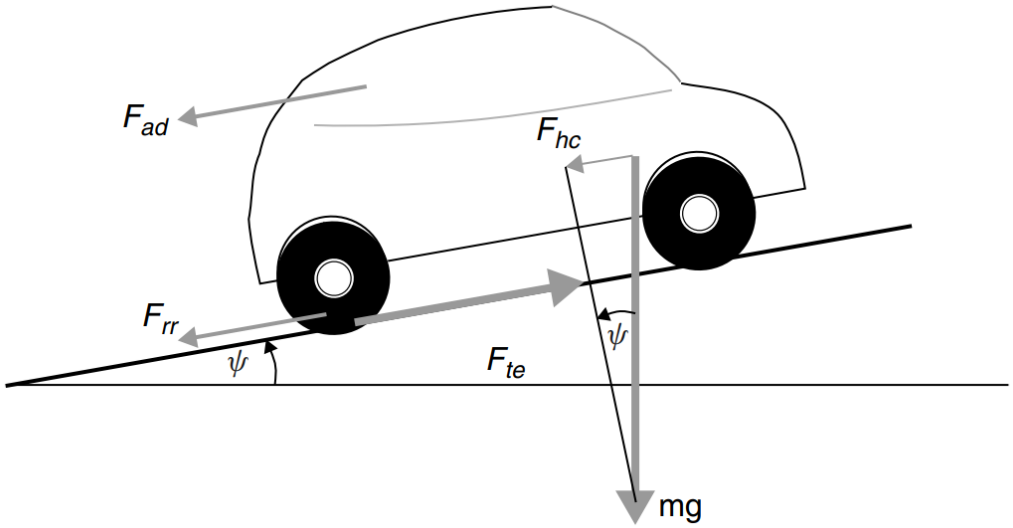

Figure 2.4: Free Body Diagram of the vehicle [18].

2.2.1. Rolling Resistance Force

The rolling resistance force is essentially caused by the friction of the tyre of the vehicle on the road, with a minor contribution of friction in gearing system and bearing. This force is approximately constant and it is basically proportional to vehicle weight [21], [22], according to $F_{rr} = f\ (M_{Vehicle}\ + M_{Passengers})\ g$

(2.1)$F_{rr} = f\ (M_{Vehicle}\ + M_{Passengers})\ g$ (2.1:

$$F_{rr} = f\ (M_{Vehicle}\ + M_{Passengers})\ g \quad (2.1)$$

Where f is the rolling friction coefficient. The main factors controlling this value are the type of tyre and its pressure (P_{Tires}), and it hardly depends on the vehicle speed v, according to the following equation $f = 0{,}005 + \frac{1}{P_{Tires}} * \left(0{,}01\ + 0{,}0095\ \left(\frac{v}{1000}\right)^2\right)$ (2.2) [23]:

$$f = 0{,}005 + \frac{1}{P_{Tires}} * \left(0{,}01\ + 0{,}0095\ \left(\frac{v}{1000}\right)^2\right) \quad (2.2)$$

In Table 2.2, some typical values are presented [24], [25], in which has been considered several road conditions.

Table 2.2: Values of rolling friction coefficient for different road conditions.

Road Surface	f
Concrete or Asphalt	0,013
Small Gravel Ground	0,02
Macadamized Road	0,025
Soil Road	0,1-0,35

2.2.2. Aerodynamic Drag Force

The aerodynamic drag force is produced by the friction of the vehicle moving through the air. It is a function of the shape and the dimensions of frontal area and of the speed of the vehicle, according to $F_{ad} = \frac{1}{2} C_d S \rho v^2$ (2.3):

$$F_{ad} = \frac{1}{2} C_d S \rho v^2 \quad (2.3)$$

where ρ is the density of the air, S is the frontal area, and v is the velocity of the vehicle. C_d is a constant called the drag coefficient. This value can be reduced by good vehicle design. There is greater opportunity for reducing C_d in electric vehicles because they do not require air inlets at the front and thus, there is more flexibility in the location of the major components. This means that a normal value for a common electric car is 0,35, significantly lower than a conventional one, and some electric vehicles can reach much lower values. Several aerodynamic drag coefficient for different type of vehicles are reported in Table 2.3 [24], [25].

Table 2.3: Values of drag coefficient for different type of vehicle.

Vehicle Type	C_d
Cabriole	0,5-0,7
Car	0,3-0,4
Bus	0,6-0,7
Truck	0,8-1,5

Optimal Design	0,2-0,3

2.2.3. Hill Climbing Force

This force represents the one needed to drive the vehicle up a slope. To simplify, the hill climbing force is the component of the vehicle weight that acts along the slope, according to $F_{hc} = \left(M_{Vehicle} + M_{Passengers}\right) g \sin(\alpha)$ (2.4):

$$F_{hc} = \left(M_{Vehicle} + M_{Passengers}\right) g \sin(\alpha) \quad (2.4)$$

Where α is the slope of the road. This coefficient has been calculated starting from the altitude and the speed profiles over the time, in particular it is important to notice that the value of the speed in a time step of 1 second is also the value of the distance travelled in the same period of time. Thus, α has been calculated using the following equation $\alpha = \text{atan}\left(\frac{Altitude_{i+1} - Altitude_i}{Speed}\right)$ (2.5):

$$\alpha = \text{atan}\left(\frac{Altitude_{i+1} - Altitude_i}{Speed}\right) \quad (2.5)$$

It is important to notice that this force could be either positive or negative depending on if the vehicle is climbing or vice versa. Moreover, it represents one of the biggest contribution to the resistance force, in particular when the slope of the road is significantly high [24].

2.2.4. Inertia Force

If the vehicle is accelerating or slowing down, its velocity is changing, and so another force is needed in additions to the ones showed in **Errore. L'origine riferimento non è stata trovata.**. This force will provide the linear acceleration of the vehicle, and it is given by the well-known equation derived from Newton's second law $F_{Inertia} = m_{eq} * a$ (2.6):

$$F_{Inertia} = m_{eq} * a \quad (2.6)$$

Where a is the acceleration and m_{eq} is the equivalent mass of the vehicle. Indeed, some considerations must be done. For a more accurate value of the force needed to accelerate the vehicle, also the contribution of the rotational acceleration of the parts must be considered, in addition to the linear one. Since the calculation of the inertia terms for the motor and the drivetrain of the vehicle is not so easy to compute, the contribution of the rotating acceleration has been taken into account considering a coefficient β and an equivalent mass, which is calculated using the following equation $m_{eq} = (1 + \beta) * M_{tot}$ (2.7):

$$m_{eq} = (1 + \beta) * M_{tot} \quad (2.7)$$

Also in this case, it is important to notice that the inertia term could be either positive or negative, depending on if the vehicle is accelerating or braking. In particular, this latter case represents one of the most important advantages of the EVs, which can use the regenerative braking to recover some of this energy when the vehicle is slowing down, until a certain value of speed.

Furthermore, slip condition has been considered and verified using the following equation $F_{Adhesion} = c_{Adhesion}\ (M_{Vehicle} + M_{Passengers})\ g\ \epsilon$ (2.8):

$$F_{Adhesion} = c_{Adhesion}\ (M_{Vehicle} + M_{Passengers})\ g\ \epsilon \tag{2.8}$$

Where g represents the acceleration of gravity, $M_{Vehicle}$ and $M_{Passengers}$ are the masses respectively of the vehicle and of the passengers; ϵ is the fraction of wheels that transfer the force, and this value depends on the following conditions:

- during acceleration is 0,5;
- while during braking it is 1.

Moreover, $c_{Adhesion}$ is the adhesion coefficient. It depends on the speed of the vehicle according to this experimental formula $c_{Adhesion} = 0{,}64 + 0{,}26\ e^{-0{,}08\ v}$ (2.9) [26]:

$$c_{Adhesion} = 0{,}64 + 0{,}26\ e^{-0{,}08\ v} \tag{2.9}$$

Anyway, in this specific case, it was obvious that no slip condition occurred (meaning that the adhesive force is always lower that the tractive effort), because accelerations and decelerations were far below their maximum value, being these taken in a real-drive condition.

Finally, the total tractive effort F_{te} can be calculated summing all the forces, as follows $F_{te} = F_{hc} + F_{Inertia} + F_{rr} + F_{ad}$ (2.10):

$$F_{te} = F_{hc} + F_{Inertia} + F_{rr} + F_{ad} \tag{2.10}$$

2.3. Efficiency and Power Model

Once computed the total tractive force, the instantaneous power flow P_{te}, measured in kW, required by the vehicle can be calculated $P_{te} = F_{te} * v$ (2.11):

$$P_{te} = F_{te} * v \tag{2.11}$$

These values of the power profile can be either positive, P_{pos}, or negative, P_{neg}, when the vehicle is reducing its velocity. At this point, the advantage of the electric vehicles appears: during the slow down, the regenerative braking allows to recover energy to the battery; this energy in a conventional vehicle would be lost. It is important to notice that not all the energy can be recovered: the efficiency of the regenerative braking, $\eta_{reg.braking}$, also plays its role, and thus having a higher value allows to recover more energy. Some of the newest electric vehicles have different options for regenerative braking, taking into account that the more the vehicle is recovering energy, the more it is self-braking, affecting the driving.

In Figure 2.5, the power block of the model is showed.

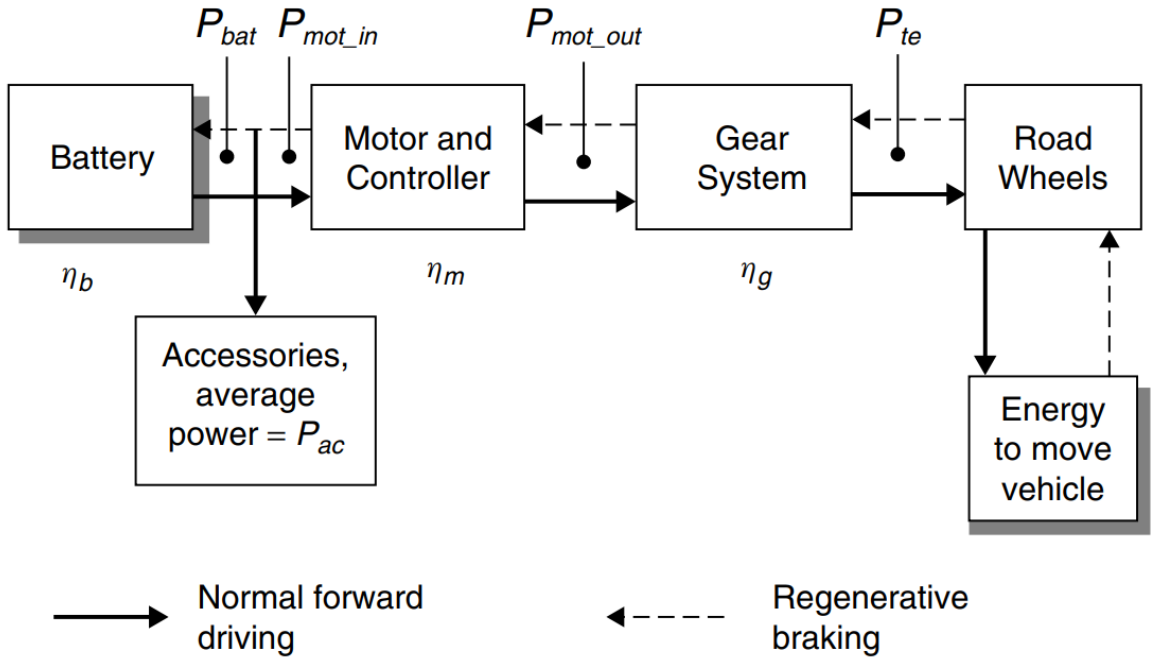

Figure 2.5: Power Model Block [18].

Moreover, to pass from the power required by vehicle to the one provided by the battery, the efficiencies of the motor η_m and of the gear system η_g must be considered, as showed in **Errore. L'origine riferimento non è stata trovata.**. While the gear system efficiency η_g is usually very high (considering inverter and transmission this efficiency can be around 0,95-0,99 [27]), a different evaluation must be done for the motor

efficiency, because this is generally lower and it affects much more the performances of the vehicle.

The motor efficiency has quite similar values for traction and braking. Hence, in this model they are considered with the same value η_m. Moreover, usually the value of efficiency ranges from 0,7 up to 0,95 and thus a typical mean value of 0,85 can be accepted, despite the fact that the precise number cannot be determined.

Anyway, another approach has been also used in this model. Since the efficiency is a function of motor speed and torque, it has been chosen to estimate the efficiency starting from the Losses Coefficients, as reported in the equation $\eta_m = \frac{T*\omega}{T*\omega+k_c*T^2+k_i*\omega+k_\omega*\omega^3+C}$ (2.12) for an electric motor [28]:

$$\eta_m = \frac{T*\omega}{T*\omega+k_c*T^2+k_i*\omega+k_\omega*\omega^3+C} \quad (2.12)$$

Where T is the torque and ω is the motor angular speed, whose equations are respectively $\omega = v * \frac{G}{r}$ (2.13) and $T = F_{te} * \frac{r}{G}$ (2.14):

$$\omega = v * \frac{G}{r} \quad (2.13)$$

$$T = F_{te} * \frac{r}{G} \quad (2.14)$$

Where r is the tyre radius and G is is the gear ratio of the system connecting the motor to the axle.

As regards the motor losses coefficients: k_c is the copper losses coefficient, k_i is the iron losses coefficient, k_ω is the windage losses coefficient and C represent the constant losses that apply at any speed. In Table 2.4, some typical values for a motor that is likely to be used in electric vehicles are reported [28]:

Table 2.4: Typical values of loss coefficient for an electric motor.

Loss coefficient	Value	Unit
$\boldsymbol{k_c}$	0,12	$\frac{\text{s}}{\text{kg m}^2}$
$\boldsymbol{k_i}$	0,01	J
$\boldsymbol{k_\omega}$	$5 * 10^{-6}$	kg m^2

C	600	W

Another alternative could be to use the Efficiency Map of the specific motor of the vehicle used in the validation of the model, in order to have the most precise value of the efficiency. However, it must be considered that if neither the efficiency map nor the losses coefficients are known, using a value of efficiency of 0,85 does not represent a not so wrong estimation.

At the end, the formulas will be $P_{mot_{in}} = P_{tractive} + P_{braking}$ (2.15), $P_{tractive} = \frac{P_{pos}}{\eta_g * \eta_m}$ (2.16) and $P_{braking} = P_{neg} * \eta_g * \eta_m * \eta_{reg.braking}$ (2.17) :

$$P_{mot_{in}} = P_{tractive} + P_{braking} \quad (2.15)$$

Where:

$$P_{tractive} = \frac{P_{pos}}{\eta_g * \eta_m} \quad (2.16)$$

$$P_{braking} = P_{neg} * \eta_g * \eta_m * \eta_{reg.braking} \quad (2.17)$$

Once obtained the power required by the motor, the power of auxiliaries ($P_{auxiliaries}$) must be added in order to calculate the amount of power that the battery ($P_{battery}$) must provide to the vehicle during the route $P_{battery} = P_{mot_{in}} + P_{auxiliaries}$ (2.18):

$$P_{battery} = P_{mot_{in}} + P_{auxiliaries} \quad (2.18)$$

This power can significantly vary depending on the conditions of travelling, starting from low values if no auxiliaries are used, up to strongly influence the autonomy of the electric vehicle if air conditioning is in function [18], [29], as it can be clearly seen in Figure 2.6 and Table 2.5.

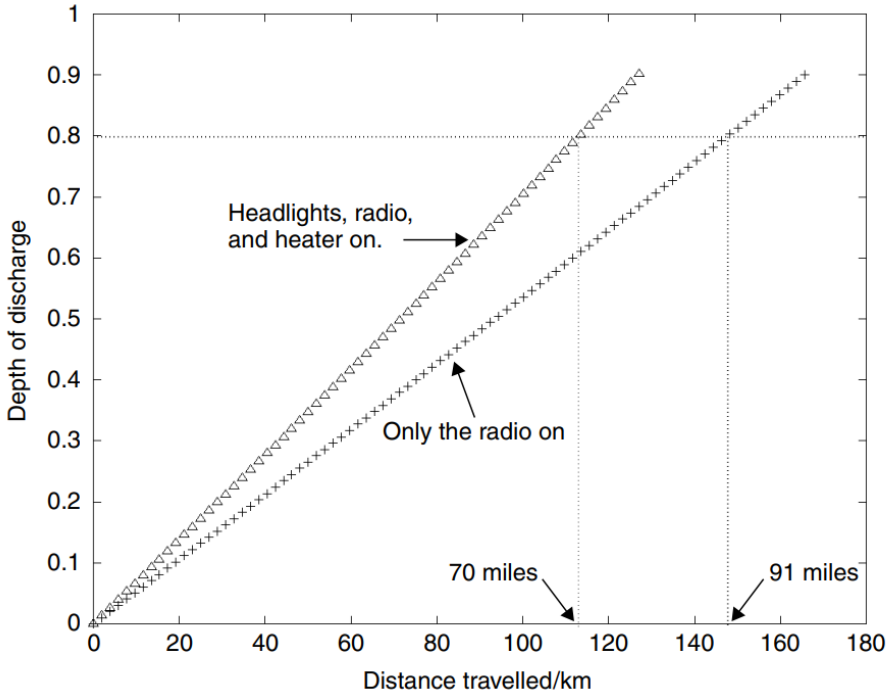

Figure 2.6: Effect of auxiliary system on the vehicle range.

Table 2.5: Energy consumption of different auxiliaries.

Auxiliary System	**Part of the traction battery energy**
Climate control: cooling heating	 Up to 30% Up to 35%
Power steering	Up to 5%
Braking system	Up to 5%
Other (lights, media, locks, etc.)	Up to 5%

Since the climate control represents the biggest contribution to the power of auxiliary, a focus is pointed towards this and some values of energy consumption are given in Table 2.6.

Table 2.6: Values of energy consumption of cooling system.

External air temperature, °C	**Internal temperature, °C**	**Needed power, kW**
43	21	1,5 -2

43	25	1
43	29	0,5

2.4. Energy Model

As regards the computation of the energy consumption, and thus the last step of the model, the aim is to calculate the State Of Charge (SOC) of the vehicle needed to travel the fixed route. The calculation of the SOC is a complex task depending on several conditions, among these there are the battery type and the application in which the battery is used. Anyway, since battery charge and discharge implicate complex physical processes and chemical reactions, it is not so obvious to estimate the SOC precisely under different operation conditions and much research work and developments are still done in the present days to improve SOC estimation accuracy. [30]

Coulomb counting is a well-known method for estimating the state of charge, and it is regarded as accurate if the battery capacity and the beginning state of charge are known. However, the Coulomb counting approach, and also other SOC estimation methods, are based on measure very accurately several quantities, such as the coulombs and current flowing in and out of the battery stack and the individual cell voltage and temperature under all operating conditions [31]. Coulomb counting, on the other hand, is prone to inaccuracies from a variety of sources, and the magnitude of these errors has not been explored in the literature.

For the reasons stated above, these methods are not taken into account in this model, given also that the instantaneous values of current and voltage are not very accurately measurable during the experimental tests. Thus, for the determination of the SOC, a "macroscopic" approach has been used, considering only the power that the battery must provide during the route, and not the contribution of the quantities already mentioned above. Once obtained an instantaneous power profile of the battery ($P_{battery}$), also the instantaneous energy profile can be calculated, considering that each value is obtained for a time step of 1 second, with the relation $E_{battery} = \frac{P_{battery}}{3600}$ (2.19):

$$E_{battery} = \frac{P_{battery}}{3600} \tag{2.19}$$

Making the cumulative sum of these instantaneous values, the energy consumption can be calculated, where of course the last value represents exactly the energy spent in order to travel the route chosen $EnergyConsumption = \sum E_{battery}$ (2.20):

$$EnergyConsumption = \sum E_{battery} \tag{2.20}$$

From this information, the SOC can be calculated, knowing also the starting SOC of the vehicle and the capacity of the battery $C_{battery}$, according to the equation $SOC = SOC_{start} - \frac{EnergyConsumption}{C_{battery}}$ (2.21):

$$SOC = SOC_{start} - \frac{EnergyConsumption}{C_{battery}} \quad (2.21)$$

3 Experimental Parameters

In this part of the work, the model parameters are presented, dividing them into three areas that are the route, the choice of the electric vehicle and the power of auxiliaries. Indeed, the validation of the EV model has been done on a real-world vehicle and the detailed analysis of the results will be presented in the next chapter.

In the first part of the this section, the experimental campaign for the validation of the model is presented and described in detail, focusing on the main differences of the several tests, the common conditions and the particular cases.

The analysed route consists in about 31 km distance journey between the two cities of Trepuzzi and Lecce, in the south of Puglia, Italy. The travel consists in a round trip between these two cities in order to simulate a real journey that a worker does every day. In particular, the path of the travel was a mix between different driving conditions, indeed both high-speeds and city roads are present, with also some climbs and descends. This was chosen to take into account all the aspects that can be present in a common daily travel, in order to better simulate a real life-like travel example. Thus, in the first part of the chapter, altitude and speed profile are analysed in detail, in order to understand the main characteristics of the route focusing on two main sub-environments:

- City road, with a limited maximum speed, full of fast stops and accelerations and with an elevation more or less constant.
- Extra-urban road, that is a way faster street, with an important difference in elevation.

The vehicle chosen for the validation of the model is a Renault Twingo E-Tech Electric [32]. This vehicle represents the perfect city car: small but comfortable, useful in urban conditions because it can partially recover kinetic energy with regenerative braking and in addition it is an emission-free vehicle, even if the way of production of electricity must be taken into account too, as stated above. Anyway, due to its low battery capacity (22 kWh), range is limited at only 160 km, calculated in a mixed WLTP cycle (Worldwide harmonized Light vehicles Test Procedure), even if it is well-known fact that the real autonomy is lower. For this latter reason, the Renault Twingo model is not one of the best-selling EV in Europe.

In the context of this thesis, the low range of the Renault Twingo is a great drawback, since charging infrastructures in Salento territory are still in development and they are

not so widespread [33]. However, it must be stated that the autonomy of this vehicle is enough to drive the typical number of kilometers that a worker usually do every day. In addition, even if the vehicle does not support type 3 fast charge, the battery can be fully recharged in one night, starting from less than 11 hours at 2,3 kW to about one hour at 22 kW.

In the last part, some other meaningful parameters are presented. Among these, an important focus is pointed towards the power of the auxiliaries, which can be significantly different between every travel, depending on the condition of the day.

3.1 Experimental Campaign

As explained in the last chapter, the validation of the vehicle model requires the acquisition of the real speed and altitude profiles of the car, which are two of the main inputs of the model. The acquisition of data has been made for the same fixed route, repeated several times. In this way, different conditions, such as time of the day, weather, traffic, have characterized the data acquired and thus the results obtained, to have the most realistic value and to consider all the possibilities of the real world.

In order to validate the model, an experimental campaign has been executed, consisted in fifty experimental tests in a real-drive conditions. In particular, these were divided into two groups of twenty-five each, depending on the driver's behavior on the road:

- The first driver, D1, represents a slow driver, with a maximum speed limited and eco-driving behaviour, in order to take advantage of the energy recovery, helping to reduce unnecessary kilowatt consumption and bringing the motor closer to its maximum energy efficiency level.
- The characteristics of the second driver, D2, instead, are quite the opposite: fast maximum speed and not limited by the eco-driving, rapid accelerations and slow down.

In **Errore. L'origine riferimento non è stata trovata.** and **Errore. L'origine riferimento non è stata trovata.**3.2, the main characteristics of the tests are reported.

The two groups of measurements are significantly different for several reasons, but they have also some similarities:

- The weight of the passengers was set at a value of 60 kg for D1 and 100 kg for D2, which represent the mean weight of the two drivers that conducted the tests.
- The distance travelled is more or less the same; this is because the route is fixed, as stated above. Moreover, some tolerances between these values can be noted: even if the route is always the same, some other variables (such as traffic, parking and roads blocked) play their role. Anyway, the differences between distance are very low and in addition some of the output, such as the specific energy consumption, are independent from the distance travelled.
- For the D1, the data is acquired always divided into two travels, instead the travel of the D2 is more or less always done in one time. Thus, for the D1 tests, the conditions, in particular temperature, weather, and power of auxiliaries, could change between the outward and the return journeys, especially when the acquisitions are done few hours apart. The opposite situation is valid for D2, with constant conditions in one single measurement test.

Table 3.1: D1 Experimental Tests.

D1								
N	**Day**	**Time (o/r)**	**Max Speed [km/h]**	**Time [s] over 90 km/h**	**Time [s] over 100 km/h**	**Mean Speed [km/h]**	**Duration [mm:ss]**	**Distance [km]**
1	27-feb	07:27/13:14	107,2	217	33	49,2	37:48	31,13
2	28-feb	10:57/12:44	98,5	138	0	46,8	39:33	30,85
3	01-mar	07:31/11:29	104,0	294	61	48,5	38:08	30,82
4	02-mar	07:31/13:11	95,8	67	0	44,7	41:12	30,72
5	03-mar	07:36/14:07	104,6	207	15	48,8	37:32	30,55
6	06-mar	07:16/12:03	105,8	195	69	47,6	38:54	30,85
7	07-mar	10:58/11:55	105,3	195	64	46,7	39:19	30,62
8	09-mar	07:36/12:19	104,0	159	21	48,8	37:49	30,78
9	25-mar	08:51/10:16	107,8	396	128	50,4	36:36	30,79
10	27-mar	07:47/13:11	106	216	46	53,5	34:38	30,89
11	28-mar	10:49/13:26	106,5	326	146	48,0	38:31	30,85
12	29-mar	07:32/12:33	106,1	248	94	50,4	36:41	30,84
13	13-apr	07:33/13:16	103,8	179	22	44,6	41:37	30,92
14	14-apr	07:33/13:11	97,5	61	0	46,8	39:31	30,83
15	17-apr	07:26/14:10	106,4	246	49	50,2	37:03	31,01
16	18-apr	10:46/13:21	106,3	198	37	48,6	38:11	30,93
17	19-apr	07:35/19:13	104,9	134	71	49,6	37:06	30,71
18	21-apr	07:32/12:20	102	141	23	48,43	38:15	30,89
19	26-apr	08:14/11:38	100,2	173	1	47,7	38:41	30,78

20	05-may	07:22/13:09	107,5	151	51	45,7	40:27	30,84
21	08-may	17:29/19:36	97,3	148	0	49,7	37:04	30,72
22	11-may	07:30/13:08	108,7	136	30	49,9	37:21	31,09
23	12-may	07:26/13:08	98,1	74	0	48,4	38:17	30,87
24	23-may	09:50/16:28	96,9	127	0	47,6	38:43	30,74
25	26-may	07:22/11:43	103,1	185	14	50,2	37:06	31,05

Table 3.2: D2 Experimental Tests.

D2								
N	**Day**	**Time (o/r)**	**Max Speed [km/h]**	**Time [s] over 110 km/h**	**Time [s] over 120 km/h**	**Mean Speed [km/h]**	**Duration [mm:ss]**	**Distance [km]**
1	01-mar	16:45	111,9	5	0	55,1	33:44	30,99
2	04-mar	13:18	124,8	96	28	55,4	36:04	31,05
3	07-apr	14:56	127,8	130	64	56,7	32:51	31,08
4	09-apr	17:00	137	226	92	59,4	31:15	30,95
5	12-apr	20:29	127,5	171	70	57,5	32:30	31,02
6	13-apr	17:21	128	160	66	54,2	34:23	31,13
7	14-apr	15:02	128,2	58	32	59,5	31:16	31,01
8	15-apr	15:54	134,0	193	69	63,1	29:29	31,01
9	16-apr	14:53	136,6	208	114	62,2	29:54	31,02
10	16-apr	15:26	136,8	186	120	62,6	29:45	31,05
11	17-apr	14:31/19:45	133,2	152	64	57,3	31:27	30,05
12	17-apr	20:13/00:31	131,2	235	67	60,5	30:43	30,99
13	18-apr	13:51	133,4	209	79	54,9	33:50	30,97

14	19-apr	20:19	127	179	64	55,3	33:42	31,09
15	19-apr	22:17	130,5	191	45	61,5	30:17	31,04
16	20-apr	20:17	123,3	223	47	61,9	30:00	31,01
17	21-apr	14:13	130,6	151	66	60,9	30:42	31,16
18	21-apr	16:48	128,7	140	68	50,8	36:41	31,1
19	22-apr	12:39	137,6	218	137	56,71	32:31	30,75
20	23-apr	12:04	129,1	156	52	53,88	35:49	32,18
21	24-apr	13:47	131,3	232	116	61,3	30:44	31,41
22	26-apr	14:20	127,8	122	30	57,3	32:37	31,14
23	29-may	13:54	108,5	0	0	54,3	33:59	30,82
24	30-may	13:37	132,9	161	79	56	33:08	30,93
25	01-jun	17:13	133,6	197	88	55,7	33:03	30,69

- The hours of the acquisitions are more or less the same for the driver 1 one (D1), starting in the early morning and coming back at the end of the morning. This could perfectly represent the typical condition of a worker, who travels the same road at nearly the same hours. As it will be notice afterwards, this condition is more affected by the weather, and thus the power of auxiliaries, rather than the traffic, since this one tends to be constant for near all the acquisitions with very similar speed profiles.
- Instead, for the second driver (D2), it is different. The acquisitions vary in all the hours of the day, and for this reason, it is clear that in this case also the traffic conditions and the speed profile play a significant role.
- The D1 velocities are always low, with a maximum value lower that 110 km/h and a mean average value of 48 km/h. Instead, the D2 speeds are much higher, with maximum speed values over 130 km/h and a significantly higher average speed, which makes the duration of the travel to significantly drop of about 5 minutes. However, for the duration of the travel there is not a unique value, and it can change a lot between the experimental tests; thus, it must be stated that the average speed do not represent a universal parameter because it can depend on the presence of more stops and other causalities. For this reason, also the time for which the vehicle runs at high speed must be considered and not

only the average and maximum speed, in order to have the most complete analysis of the results. A comparison between these two speed profiles is showed in **Errore. L'origine riferimento non è stata trovata.**.

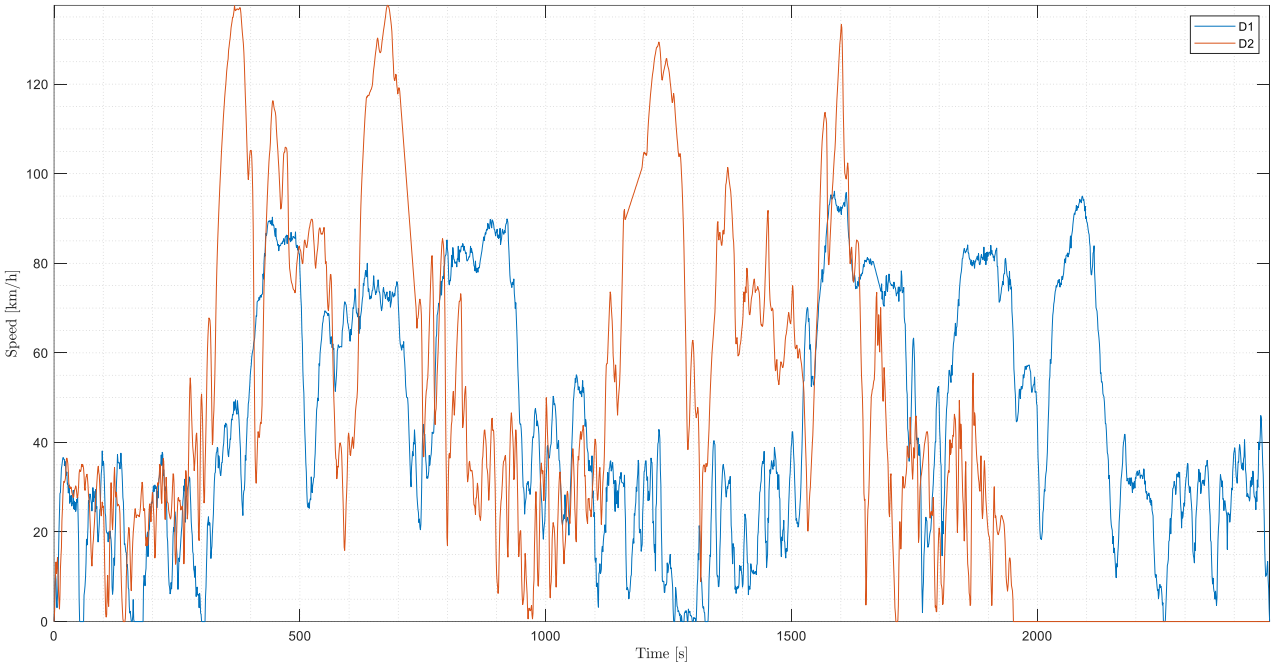

Figure 3.1: Comparison between D1 and D2 speed profiles.

From the comparison, it is quite clear as the D1 would represent a slow driver, instead the D2 would represent a faster behaviour on the road. It can be noticed that this difference of velocities is not for the whole travel, but only in the extra-urban environments. Indeed, in the city conditions the two profiles are quite similar, with speeds under 40 km/h and frequent stops and accelerations. Thus, it can be already stated that the differences in the results, and especially in the energy consumption, will be principally due to the difference of behaviour in the extra-urban conditions. For these reasons, the results for the two groups of tests will be analysed separately.

3.1. Route

The analyzed route consisted in an about 31 km round trip between the cities of Trepuzzi (Le), from via Calvario 58C – A, and Lecce, to Istituto Presta-Columella - B, as showed in Figure 3.2 [34]. The choice of this route was due to simulate a typical journey that a worker may do daily.

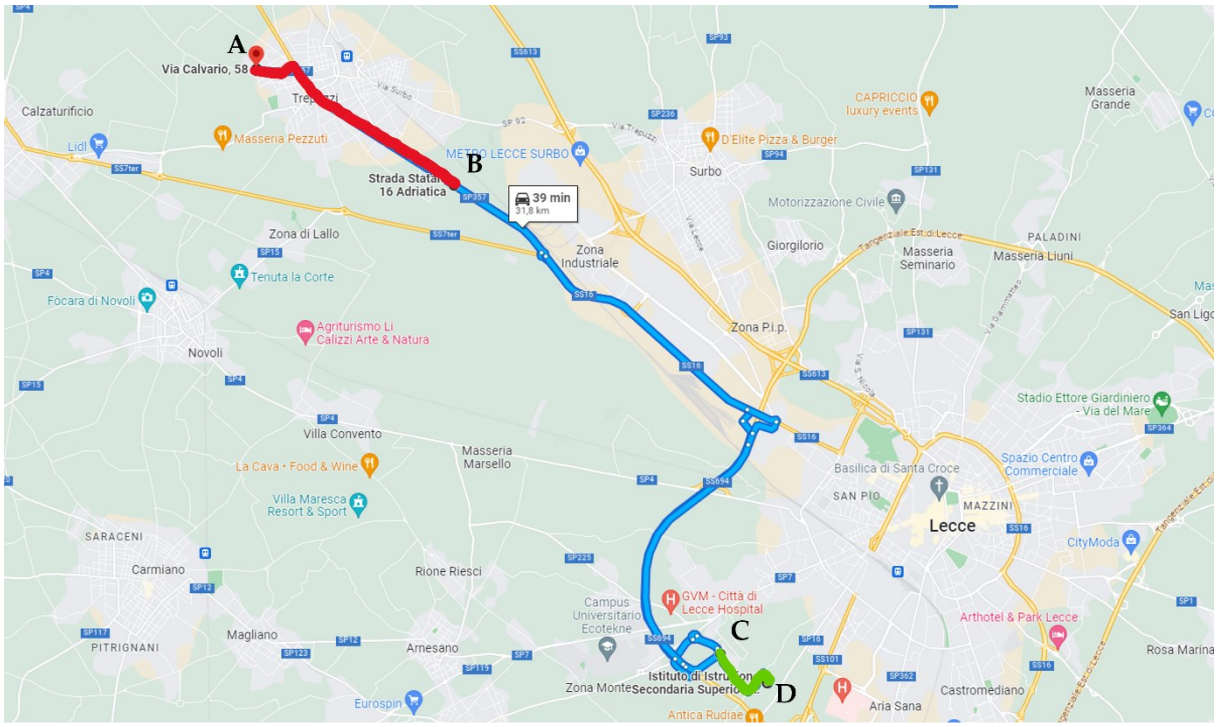

Figure 3.2: Google Maps visualization of the travel [34].

The route can be divided into three zones (**Errore. L'origine riferimento non è stata trovata.**.3):

- A 2,2 km country-side road, near the Istituto Presta-Columella, that is also a slow street due to characteristics of the road and the presence of pedestrians and other vehicles (Figure 3.3.3 - A).
- A 7,2 km urban road, in the small city of Trepuzzi, with all the characteristics of a city road: limited maximum speed, full of stops and fast accelerations due to the congestion and the traffic-lights, and with an elevation more or less constant (Figure 3.3.3 - B).
- An extra-urban road in between them, which represents the biggest contribution to the travel (about 21,5 km). This is a way faster street, with an important difference in elevation, but it can be seen that some roundabouts or junctions are present, which make the vehicle speed slow down (Figure 3.3.3 - C).

Figure 3.3: Photos of the road, (A) country-side; (B) City; (C) Extra-urban road.

Table 3.3: Characteristics of the travel.

Type of Road	Distance [km]	Colour	
Urban	7,2	Red	A-B
Extra-urban	21,6	Blue	B-C
Country-side	2,2	Green	C-D
Total	**31**		

The speed and the altitude profiles has been obtained using "TrackAddict"[35], a data acquisition app which uses GPS to capture and analyze video and telemetry data, such as velocity, acceleration and altitude profiles, useful to calculate respectively inertia and slope forces.

A critical point of this route is the presence of a 1 km long tunnel, Figure 3.4. During the travel of the tunnel, a lack of GPS signal could happen, giving wrong acquisition of data. It is important to highlight that this problem could happen only for few seconds over the whole duration of the travel, in particular only for about 80 over 1800 seconds for D1 and 120 over 2200 seconds for D2, and these represent only the 5% of the travel. However, the solutions for this problem will be given later in this chapter.

Figure 3.4: Google Maps visualization and photo of the tunnel [34].

3.1.1. Speed Profile

As stated above, the speed profile chosen is a real acquisition of the speed of the vehicle. This solution has been selected for different reasons:

- The use of a real vehicle telemetry simulates better the driver's style and behavior on the road, rather than using the standard Driving Cycles. In this way, a more accurate results can be obtained, for example the energy consumption and the autonomy. In fact, it is a well-known fact that these cycles, such as the WLTP, the one used in Europe nowadays, underestimate the autonomy of the vehicles, and also the emission for conventional ones.
- Using a real telemetry, the speed profile can also change from time to time, and so also the State of Charge output vary. Instead, the use of the same Drive Cycle for each experimental test will give always the same results, and this is clearly a mistake.

The speed profile of D2 is showed in Figure 3.5. The three different zones are clear and visible: urban, in the first and last part of the travel; extra-urban, characterized by speeds above 60 km/h; and country side in the middle of the travel, where the velocities return to lower values.

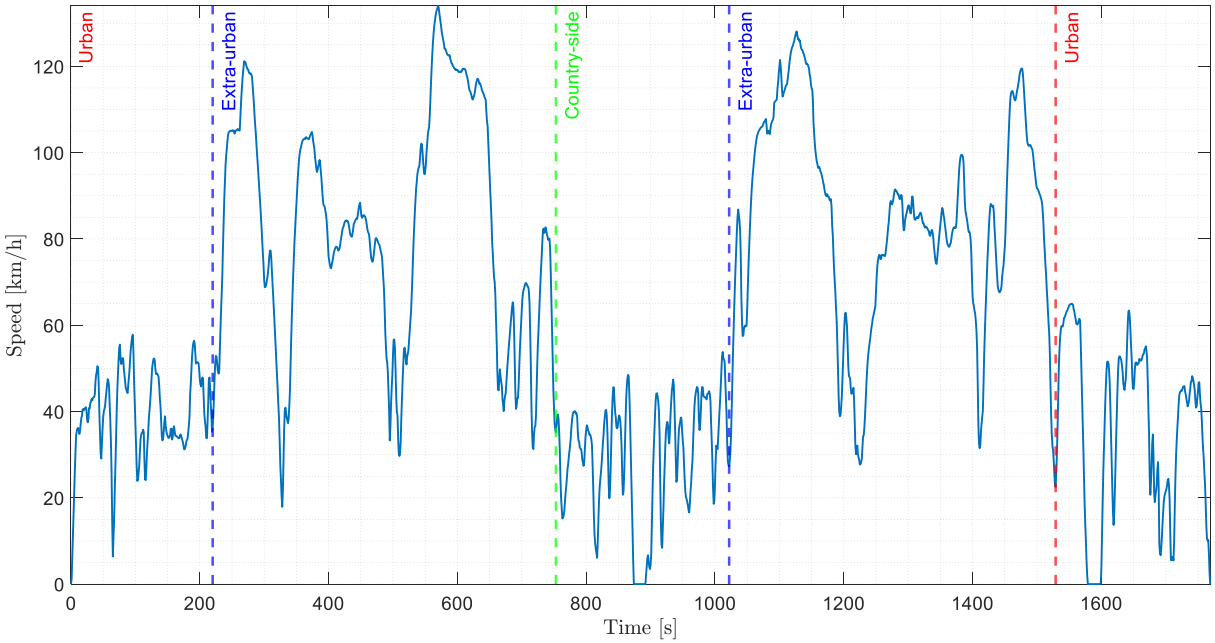

Figure 3.5: D2 Speed Profile.

Moreover, it can be noted that urban and country-side environments are both characterized by low or limited speed and common stops and fast accelerations, which make them far different from the extra-urban road. Thus, in order to simplify the analysis, these two zones are considered together and combined, as showed in **Errore. L'origine riferimento non è stata trovata.**. Same logic applies for D1.

Table 3.4: Characteristics of the road in which urban and country-side conditions are combined together.

Type of Road	Distance [km]
Urban	9,4
Extra-urban	21,6
Total	**31**

Furthermore, the comparison between the Speed profile of D2 and the WLTP cycle is showed in Figure 3.6: Comparison between D2 speed profile and WLTP cycle Class 3.and their principal characteristics are showed in **Errore. L'origine riferimento non è stata trovata.**:

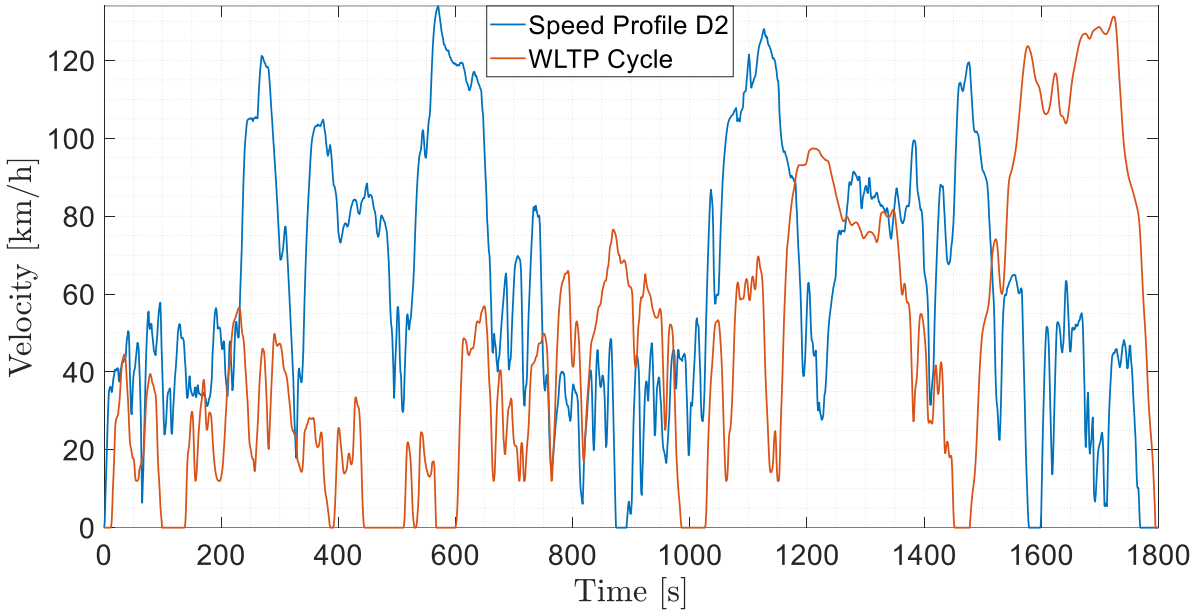

Figure 3.6: Comparison between D2 speed profile and WLTP cycle Class 3.

Table 3.5: Characteristics of D2 speed profile and WLTP cycle.

	Speed Profile Cycle	WLTP Cycle
	D2	Class 3
Max Speed [km/h]	134	131,3
Average Speed [km/h]	63,1	53,5
Distance [km]	31	23,26

Duration [mm:ss]	29:29	30:00

As regards the duration and the maximum speed, the values are very similar between the two cycles, but since the distance of WLTP cycle is much lower, also the average speed is lower. Anyway, most of the results, such as the specific energy consumption, are independent from the distance, thus using the real telemetry is more correct, because it simulates better the driver's style on the road, as explained above.

Same logic applies also for D1 Speed profile, but with some differences. This time, the WLTP Class 2 has been taken as a reference, due to the lower velocities with respect to the case before. The comparison between the Speed profile of D1 and the WLTP Class 2 cycle is showed in Figure 3.7: Comparison between D1 Speed Profile and WLTP cycle Class 2. and their principal characteristics are showed in **Errore. L'origine riferimento non è stata trovata.**:

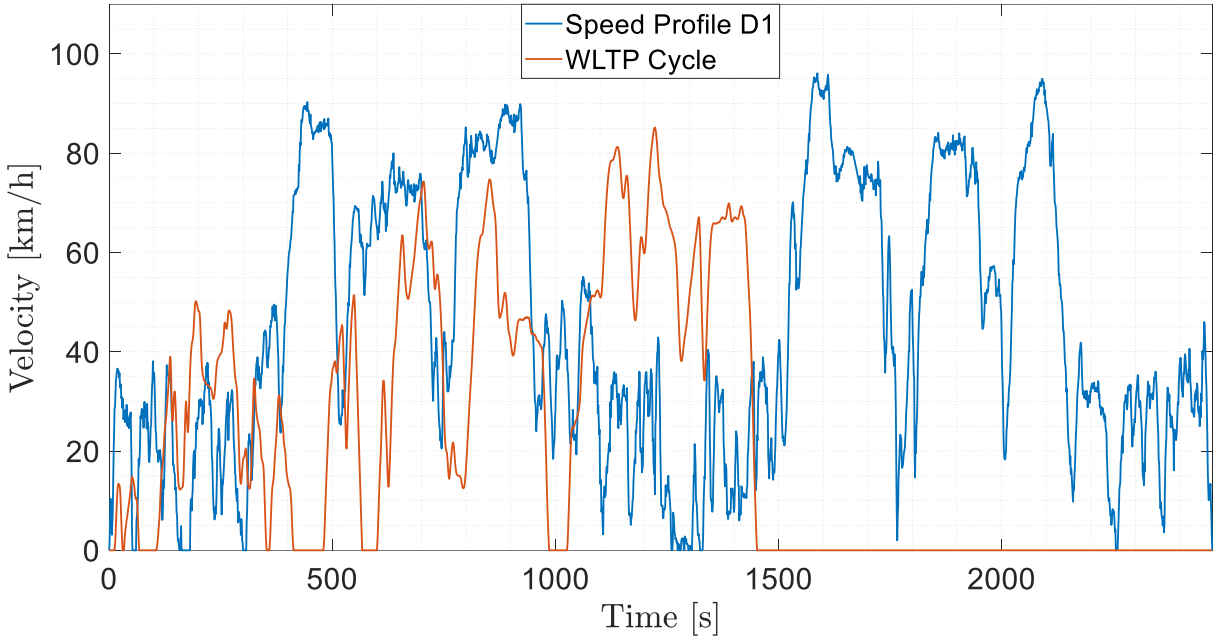

Figure 3.7: Comparison between D1 Speed Profile and WLTP cycle Class 2.

Table 3.6: Characteristics of the D1 Speed Profile and WLTP cycle.

	Speed Profile Cycle	**WLTP Cycle**
	D1	**Class 2**
Max Speed [km/h]	96,1	85,2
Average Speed [km/h]	44,9	42,4
Distance [km]	31	14,66

Duration [mm:ss]	41:12	24:37

In this case, it can be noticed that the average speeds between the two profile are quite similar. The distance is still not comparable, but again the results will be independent on it. For the reasons stated above, the use of the real speed profile is a way more correct choice, rather than using the Drive Cycles.

As regards the lack of GPS in the tunnel, a Speed Profile in which this happens is reported in Figure 3.8.

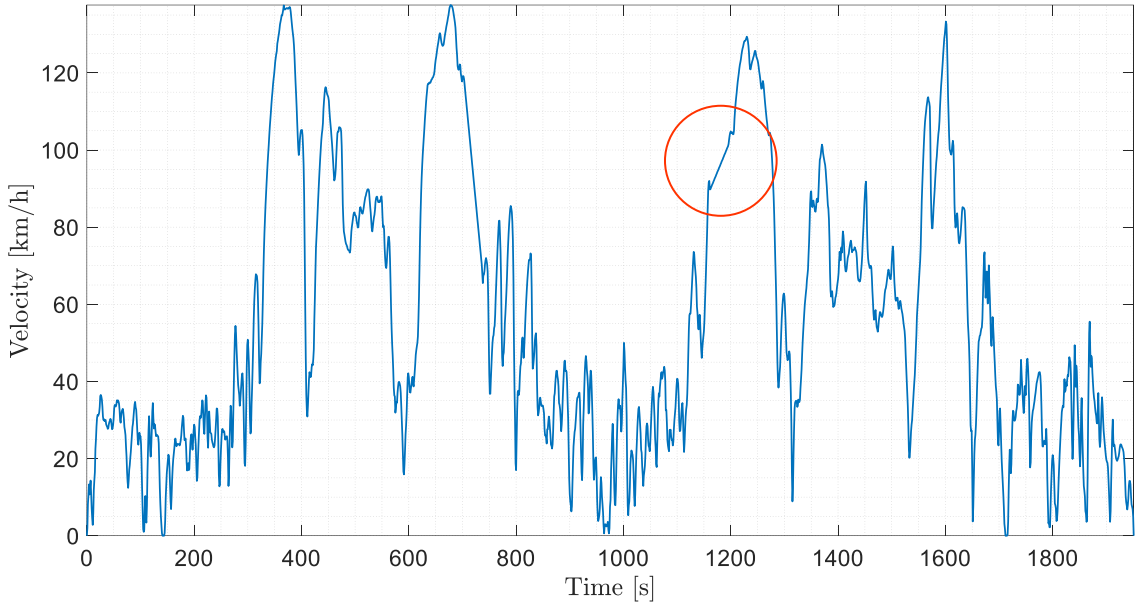

Figure 3.8: D2 Speed profile. In the highlighted region, the lack of GPS signal can be observed.

In particular, it can be noticed in the highligthed zone how the app solves this problem: it just takes the last value before the lack of signal and the first value after the signal comes back, then it makes a linear interpolation, giving as a result the wrong approximation showed in Figure 3.8. Thus, the profile has been corrected and reconstructed considering also the real velocity on the street, in order to have the more life-like speed profile of the vehicle, Figure 3.9. It is also important to state again that the lack of signal happens only for 32 seconds over the whole duration of the travel, as it can be clearly seen on Figure 3.8, thus the mistake given by the wrong approximation is quite minimum.

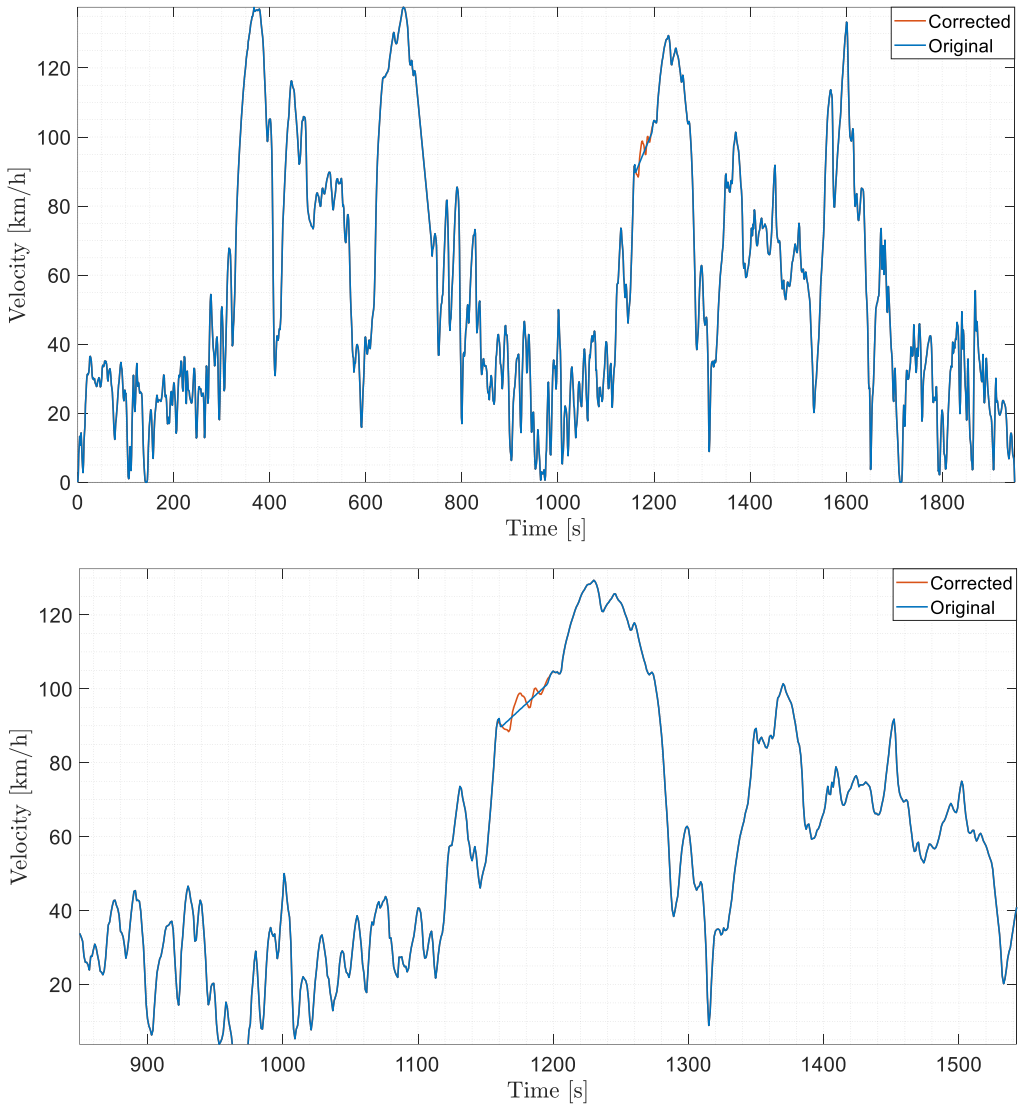

Figure 3.9: Comparison between the original speed profile and the corrected speed profile, with a zoom on the different region.

In Figure 3.8, an example of the problem of the tunnel is given. However, it must be highlighted that this problem did not happen in all the tests. A real speed profile, without any correction, has been already given in Figure 3.5.

3.1.2. Altitude Profile

In order to calculate the slope force, an altitude profile has been acquired, using "TrackAddict". The altitude profile is showed in Figure 3.10, in which an indication of the speed is given, with the aim of consider the elevation in the zones previously described.

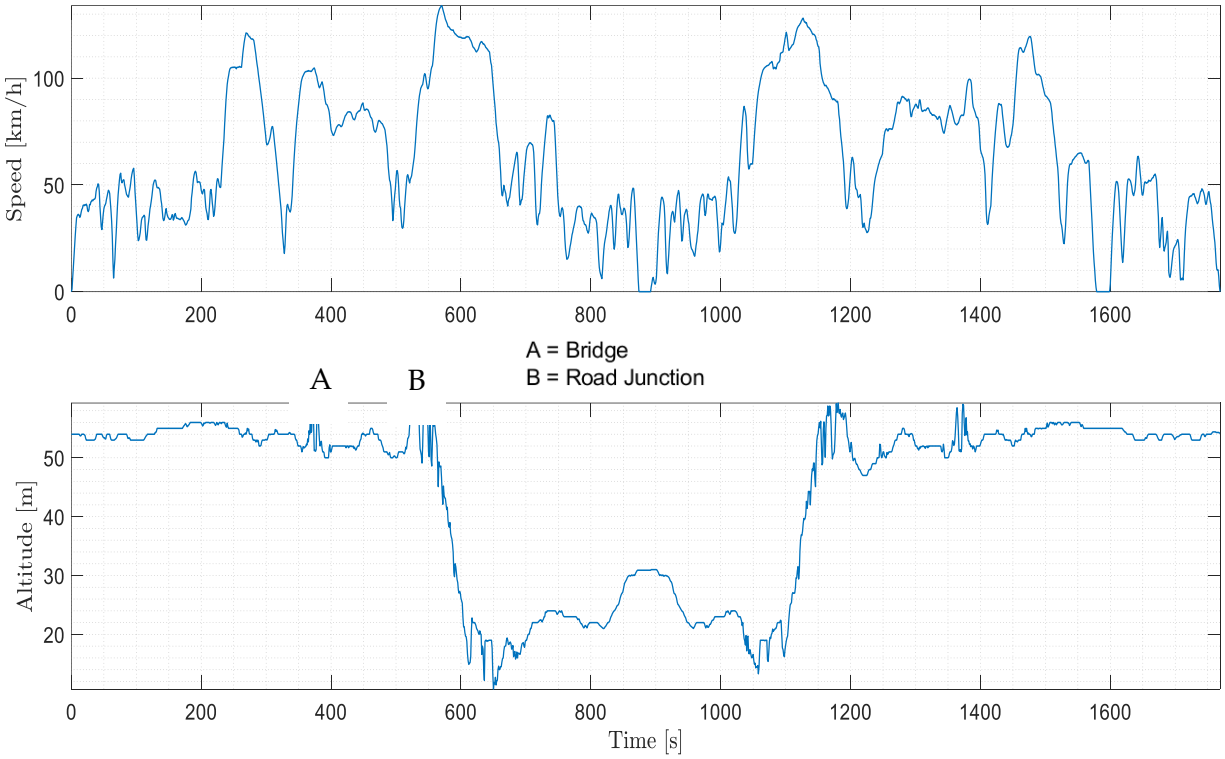

Figure 3.10: Altitude Profile with Speed Profile reference.

From the graph, it can be clearly seen how the elevation is quite constant in the urban zone. Furthermore, in the first part of the extra-urban road, the altitude remains more or less constant, with some exceptions: in this part of the travel, indeed, a bridge, Figure 3.11 (a), and a road junction to enter the high-speed road are present, Figure 3.11 (b). In the second part of the extra-urban road, a massive reduction in elevation can be noted, which will be recovered in the last part of the travel, i.e. the country-side. The opposite is valid for the return journey.

(a)

(b)

Figure 3.11: Photo of the road; (a) Bridge; (b) Road junction.

It is also important to notice the errors in the acquisition of the values and thus the profile presents some scattering. For this reason, a comparison with Google Earth altitude profile is showed in Figure 3.12.

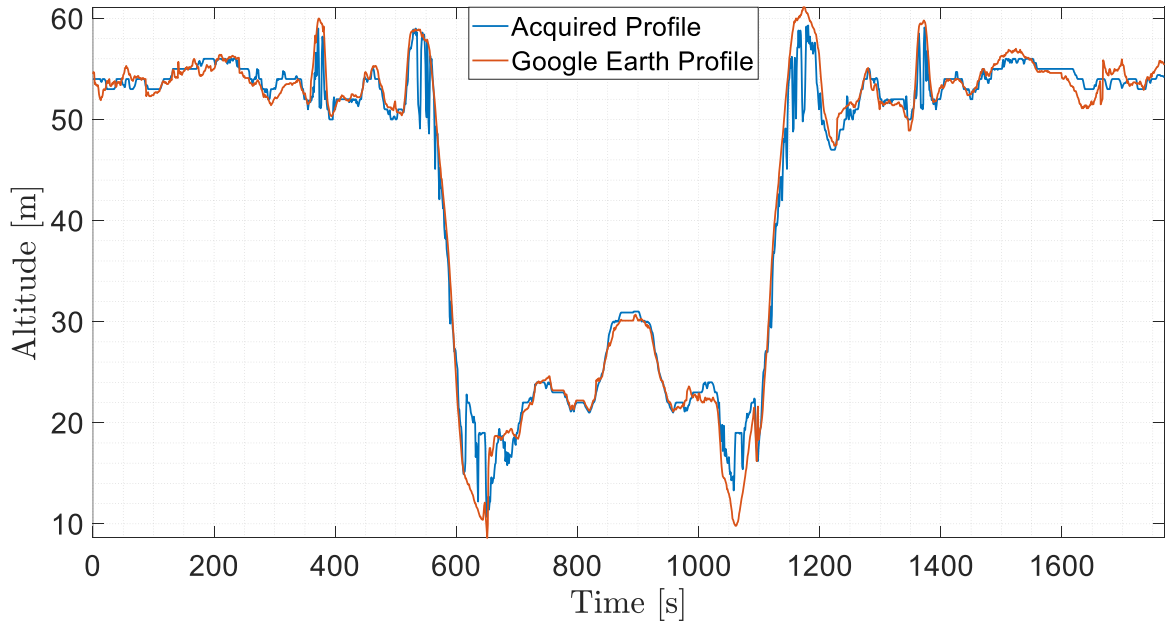

Figure 3.12: Comparison between the acquired altitude profile and Google Earth profile.

It can be notice how the two profiles present the same general trend, in particular the bridge and the road junction can be clearly distinguish. Some small mistakes in the elevation values are present, due to the GPS signal accuracy. The big difference between the two profiles is the computation of the altitude of the tunnel; of course, the Google earth one is more correct, because it takes into account the real elevation of the street, rather than the altitude of the tunnel. Furthermore, the Google Earth profile show small or no scattering, unlike of the profile acquired. For the reason explained above, the latter in the model has been modified and corrected using the former as a reference, in order to avoid or minimize the measurement errors, which could give wrong values of the slope force.

3.2. Vehicle and Characteristics

The vehicle chosen for this work is a Renault Twingo E-Tech Electric. The choice of vehicle determined numerous parameters that were then used in the calculations [32], [36], [37]. The parameters set for the case study are:

- The mass of the vehicle was at over 1133 kg without the passengers. Unconventionally, the main contribution for this value is not given by the 165 kg battery, as usually is for EV. Thus, since the battery has small capacity and small mass, the value of the weight is quite low for a city car, helping to save more energy. For example, the weight of the conventional Renault Twingo model is 1330 kg.
- The equivalent mass was fixed at 104% of the original mass, to consider the inertial effects of the wheels, of the motor and of the drivetrain. This equivalent mass is essential for the calculation of the inertial forces produced during the acceleration and deceleration of the car, as stated in chapter 2.2.4. In order to have a first estimation of the added inertia given by the rotating parts of the vehicle, a preliminary computation on the inertial effects of the wheels (tires and rims) was performed, using the following equations

$$\begin{cases} J_{rim} = \frac{1}{2} * M_{rim} * (R_{rim})^2, \\ J_{tyre} = \frac{1}{2} * M_{tyre} * \left(R_{tyre}\right)^2, \\ J_{tot} = 2 * \left(J_{tyre} + J_{rim}\right), \\ M_{rot} = \frac{J_{tot}}{\left(w_{tyre}\right)^2}. \end{cases} \quad (3.1):$$

$$\begin{cases} J_{rim} = \frac{1}{2} * M_{rim} * (R_{rim})^2, \\ J_{tyre} = \frac{1}{2} * M_{tyre} * \left(R_{tyre}\right)^2, \\ J_{tot} = 2 * \left(J_{tyre} + J_{rim}\right), \\ M_{rot} = \frac{J_{tot}}{\left(w_{tyre}\right)^2}. \end{cases} \quad (3.1)$$

and it was found to be around 4% of the inertia of the vehicle. The parameters used for the calculations are listed in Table 3.7.

This calculation is only a starting point for determining the equivalent mass coefficient, in order to consider also the moments of inertia of the motor and the

transmission, that are much lower and difficult to be computed, the typical value of 4% has been used [38].

Table 3.7: Parameters for the first computation of Equivalent Mass Coefficient.

			Front	**Rear**	**Total**
Tyre Type			185/50R16 81H	205/45R16 83H	
Rim Type			6Jx16 ET50	7Jx16 ET37	
Tyre Mass	M_{tyre}	kg	7	7	
Rim Mass	M_{rim}	kg	7	7	
Rim Diameter	D_{tyre}	in	16	16	
		m	0,392	0,392	
Rim Radius	R_{rim}	m	0,196	0,196	
Tyre Width	w_{tyre}	m	0,185	0,205	
Tyre Diameter	D_{tyre}	m	0,577	0,577	
Tyre Radius	R_{tyre}	m	0,289	0,288	
Tyre moment of inertia	J_{tyre}	kg m^2	0,291	0,291	
Rim Moment of inertia	J_{rim}	kg m^2	0,134	0,134	
Total Moment of inertia	J_{tot}	kg m^2	0,426	0,425	
Rotational Mass for one wheel	M_{rot}	kg	12,44	10,12	
Rotational Mass for both wheels	$M_{rot,2}$	kg	24,88	20,24	**45,12**
Vehicle Mass	M	kg			**1133**

Equivalent Mass Coefficient	β	%			**3,98**

- Aerodynamic drag coefficient is 0,32, which is not a very low value for a vehicle [39], but is significantly lower than the other conventional city cars. This is mainly due to the fact that the vehicle does not require air inlets at the front, hence, there is more flexibility in the location of the major components. This is instead necessary for Internal Combustion Engines (ICE) powered vehicles because the engine needs air to work; thus, they can be eliminated in electric vehicles. The frontal area of the vehicle is set to 2,11 m^2. This is a low-medium value for a vehicle, due to its limited dimensions, reported in Figure 3.13.

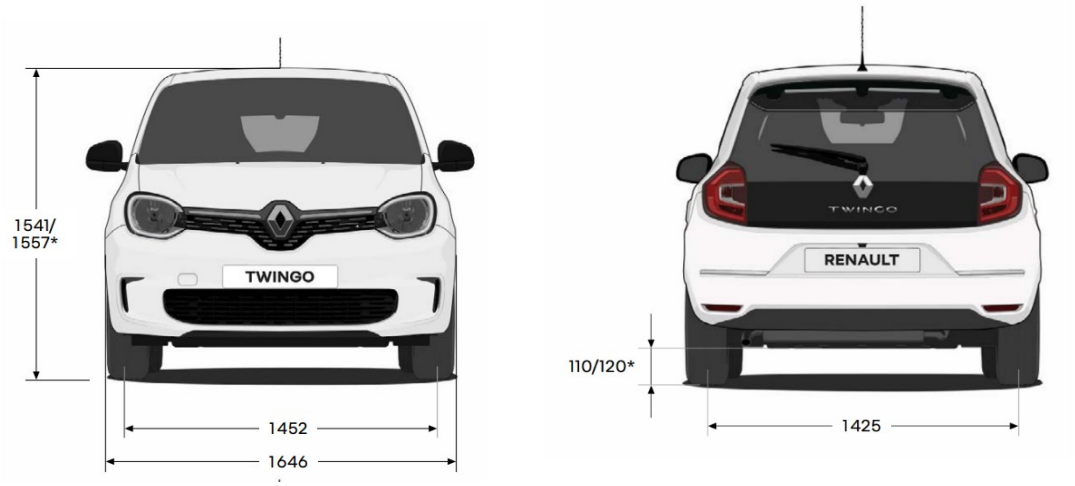

Figure 3.13: Dimensions of the Renault Twingo Model.

Furthermore, the density of air does of course vary with altitude, temperature, and humidity, which vary a lot between all the tests. Anyway, a value of 1,25 kg/m^{-3} is a reasonable value to use in most cases. These details are useful in order to calculate the drag force acting on the vehicle.

- In order to calculate the rolling resistance force, the formula $f = 0{,}005 + \frac{1}{P_{Tires}} * \left(0{,}01 + 0{,}0095 \left(\frac{v}{1000}\right)^2\right)$ (2.2) for the rolling coefficient f described in chapter 2.2.1 has been used. The pressure of the tires was set at 2,5 bar.
- The slope force has been computing using the altitude profile acquired during the tests, as explained in chapter 2.2.3.
- Slip condition has been checked using $FAdhesion = c_{Adhesion} (M_{Vehicle} + M_{Passengers})\, g\, \epsilon$ (2.8), even though no slip occurred during the experimental tests.

- Renault Twingo model powertrain is a wound rotor synchronous motor. This technology renders very high energy efficiency up to high speeds, offering an increase of the range of several kilometers [40]. Traction and braking efficiencies are usually very similar and are a function of the velocity and torque, ranging from 0,8 up to 0,95. Unfortunately, the map of the electric motor was not found for the specific vehicle, and so also the values of the efficiencies. Thus, two different methods were used:

a) For D1, since the vehicle travels with eco-driving behavior, the electric motor works almost always in the optimal point, i.e. the best efficiency region. Thus, the typical value of 0,85 has been chosen, in order to consider both motor efficiency (around 0,8-0,97 depending on the operating point) and transmission efficiency (around 0,95-0,99);
b) A different case is valid for D2. From the speed profiles, it can be seen that there are some regions in which the vehicle travels at its maximum speed available and, as a consequence, the efficiency of the motor will not be optimal. Thus, in this case, the loss coefficient method, explained in last chapter, was used, which gives as a result a slightly lower value of efficiency. As regards the transmission, it is a single-speed automatic transmission, like the most of EVs. The efficiency is very high and it can vary between 0,95 and 0,99, hence a standard value of 0,97 was considered [27]. In Table 3.8: , the values of the loss coefficients and the quantities used for the calculations are reported.

Table 3.8: Parameters for the calculation of the motor efficiency with Loss coefficients model.

		Value	**Unit**
Simple Fixed Gear Ratio	G	9,7:1	
Tyre Radius	r	0,289	m
Copper Losses Coefficient	k_c	0,12	$\frac{\text{s}}{\text{kg m}^2}$
Iron Losses Coefficient	k_i	0,01	J
Windage Losses Coefficient	k_ω	$5 * 10^{-6}$	kg m^2
Constant Losses	C	600	W

- Regenerative braking efficiency was set at 0,85. Similarly to the other efficiencies, it was not possible to find an official value from the manufacturer. However, it must be considered that Renault Twingo has at disposal three modes of regenerative braking: B1, the softest one, B2, that is the standard one,

and B3, the hardest. It has been chosen to use the B2, because it is the one selected by default and it provides the optimal value of deceleration [41]. Moreover, regenerative braking has been allowed only above 12 km/h, as showed in Figure 3.14.

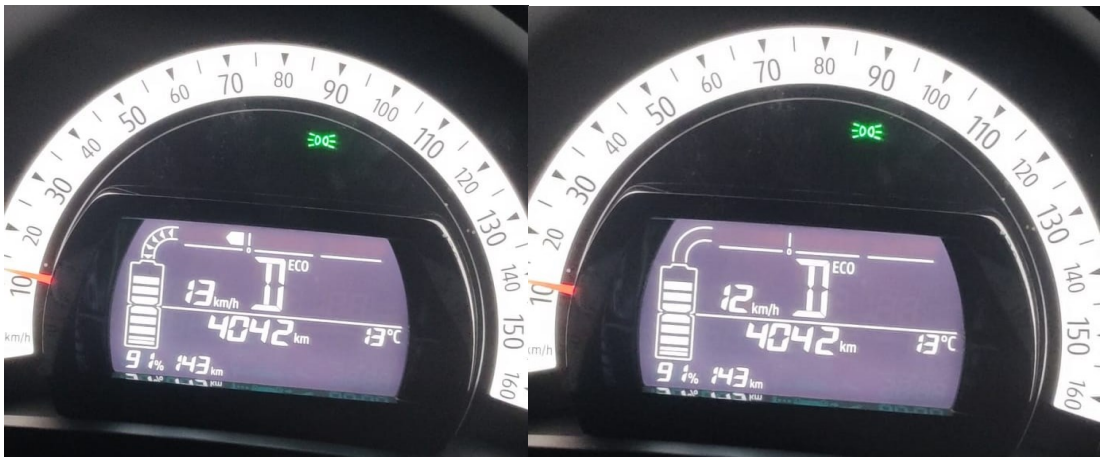

Figure 3.14: Photos of vehicle dashboard during Regenerative braking

It can be clearly seen that for a speed value of 13 km/h (or higher), the regenerative braking is in function, showed by the arrows which indicate the flux of energy towards the battery. For lower values, no regenerative braking is applied.

- The battery capacity is 22 kWh, which is a low-medium value for modern e-cars, which also explains the not so long range that this vehicle possess [42], as already stated above. However, even if this is a brand-new EV and the State Of Health (SOH) is 0%, the net available capacity is assumed a bit lower at 21,5 kWh.

3.3. Auxiliaries Power

The other important parameter in the simulation is the power of auxiliaries, which can be significantly different from time to time, depending if air cooling, lights and other utilities are switched on or off. For this reason, there cannot be a unique value for this power, but instead it can change according to the conditions of the travel. In Table 3.9, several values have been reported, according to the typical values founded in literature [27]:

Table 3.9: Values of Auxiliaries power.

Auxiliary Component	Power [W]	Operation mode
Air-Conditioner	500	Continuous
Audio	35	Continuous
Driving Control	150	Continuous
Energy Management System	150	Continuous
Head and Tail Lamps	120	Continuous
Parking, Turn and interior lamps	50	Intermittent
Horn	10	Intermittent
Power Steering	400	Continuous
Power Windows	80	Intermittent
Window Defroster	250	Continuous
Wipers	40	Continuous

However, it is important to notice that these values are only a starting point, since it can happen that some auxiliaries (such as air-conditioner or wipers) are switched on only for a limited period of time and not for the whole duration of the travel. Hence, the power of auxiliaries has been classified depending on the condition of the travel, on the base of the different experimental simulations. To simplify the model, this power has been generally classified into three classes, which represent the energy consumption of the auxiliaries during the tests. The classes and their energy value are listed in Table 3.10.

Table 3.10: Auxiliaries Power conditions used in the model.

Auxiliary Power Condition	Energy Consumption [W]
Poor	100
Moderate	500
High	900

Anyway, it must be stated that also these classes are not fixed for all the tests, but there can be some travels in which the value of the energy consumption is slightly different, but this do not represent a so wrong approximation. The effects of the different values of the power of auxiliaries will be investigated and analyzed later in the work.

4 Results

In this last chapter of this work of thesis, the results as been reported, divided them into experimental and model results, and analyzed, with an important focus towards the parameters which mostly influenced the tests and the simulations and their outputs.

Firstly, the results of the different tests have been analyzed, dividing them into the two groups already seen above: D1 and D2. The reasons behind this classification have been explained again and indagated more.

Furthermore, the model results have been analyzed and compared with the experimental ones. Similarities and differences have been explored, trying to give a meaning and a solution to the critical point of this comparison. In particular, the phenomenon of the full SOC has been explained.

Moreover, another important parameter has been considered. More comparison has been made, considering the importance of the power of auxiliaries: in order to give a deeper meaning to the results, a comparison on the basis of the same energy consumption has been made, focusing on the different cases and conditions happened in the tests.

In the last part of the chapter, a further analysis has been made, trying to compare D1 and D2. Indeed, it has been stated many times how the two speed profiles cannot be compared, due to the meaninglessness of their comparison. However, a reason of analysis has been found on the type of the road, and thus on the conditions of the travel. The divergences and the similarities between the two speed profiles has been explored, focusing on the environments which characterized the travel. Indeed, as stated in the previous chapter, the speed profiles of D1 and D2 in urban conditions are similar, hence they can give similar results. Opposite condition is valid for the extra-urban road, in which the two velocities differ a lot between each other, and so will be the results.

4.1. Experimental Results

In this section, the experimental results are reported. In particular, for every experimental test, two photos of the vehicle dashboard have been captured, one before and the other after the travel, Figure 4.1. In this way, it has been possible to find out the indication of the State of Charge of the vehicle, and so the value of energy consumption for the route.

Figure 4.1: Photos of vehicle dashboard before and after D2 travel.

As regards D2, most of the time two photos were enough to exactly represent the SOC before and after the route, because this was travelled in a single journey. Moreover, it can be seen that, as well as the SOC, the pictures consent to monitor some other useful quantities like the temperature, which can be an indication if the heating or the cooling is activated or not, the distance travelled and the range of the vehicle. It is important to notice how the difference in distance between the two photos is 31 km, which is exactly the length of the route.

Instead, different situation is valid for D1, because sometimes it happens that between the going and the return a few km are travelled, and thus they must not be included in the energy consumption of the route. For this reason, this time four photos are needed, one for each step of the travel, Figure 4.2. Anyway, also in this case, it can be noticed that the kilometers travelled are about 31.

Figure 4.2. Photos of the vehicle dashboard before, during and after D1 travel.

After capturing the photos with the indication of the energy consumption of the travel, the experimental results were collected and analyzed. In particular, in the previous chapter, the experimental tests for D1 and D2 have been compared, focusing on the differences between the values, especially the speed profiles. In Table 4.1, a further comparison of the average values of the experimental tests has been done, with addition of the difference between the starting and the ending value of SOC of the travel.

Table 4.1: Average quantities of D1 and D2 travels.

Average Values	D1	D2
Maximum Speed	103,4	129,3
Mean Speed	49,6	58,8
Duration	38:15	32:20
Distance	30,84	31,03
SOC Difference	**15,72**	**21,06**

The only value that is the same between the two groups of tests is of course the distance travelled, since the route is fixed, with some minor deviations. Instead, maximum and mean speeds are much bigger in D2 (especially the maximum speed, which is higher

of about 25 km/h), which makes the duration of the travel significantly lower. From this further comparison, it is much clearer how the two groups cannot be compared, since the difference in speed behavior is reflected in energy consumption difference. In particular, the difference in SOC is about 5,4%.

For all the reason stated above, in the next sections, the results will be analysed separately.

4.1.1. D1 experimental Results

In Table 4.2, the results of D1 experimental tests are reported, with also an indication of the average quantities.

Table 4.2. D1 Experimental Results.

N	Auxiliaries Power	Max Speed [km/h]	Mean Speed [km/h]	Starting SOC	SOC 1	SOC 2	Final SOC	SOC Difference
1	moderate	107,2	50,9	100	94	94	86	14
2	moderate	98,5	48,1	72	64	61	52	17
3	high	104,0	49,8	64	54	54	44	20
4	poor	95,8	46,1	48	40	39	31	16
5	moderate	104,6	49,7	43	34	35	26	18
6	moderate	105,8	48,2	100	96	96	87	13
7	moderate	105,3	47,6	88	80	80	71	17
8	moderate	104,0	49,8	49	40	41	33	17
9	moderate	107,8	52,7	100	94	91	83	14
10	poor	106	53,7	82	74	74	65	17
11	high	106,5	49,9	100	93	93	83	17
12	moderate	106,1	51,3	100	95	93	84	14
13	moderate	103,8	46,3	67	57	57	49	18
14	poor	97,5	47,2	80	72	72	64	16
15	poor	106,4	51,3	100	97	96	87	12
16	moderate	106,3	49,4	78	70	71	62	17
17	poor	104,9	50,1	100	97	94	85	12
18	poor	102	49,1	100	97	97	89	11

19	poor	100,2	50,0	100	97	95	86	12
20	high	107,5	47,5	65	57	57	47	18
21	moderate	97,3	50,0	50	42	42	33	17
22	high	108,7	50,4	56	47	47	38	18
23	poor	98,1	50,5	79	72	72	64	15
24	moderate	96,9	49,4	74	67	66	57	16
25	moderate	103,1	51,2	77	70	68	58	17
Average Values		**103,3**	**49,6**					**15,72**

Furthermore, the outputs of the tests were reported in a diagram, Figure 4.3, in order to find out the possible correlation between the energy consumption (expressed as SOC difference between the initial and the final values) and the mean speed. A linear trend and an indication about the power of auxiliaries are also given, in particular, green points represent poor auxiliary power, yellow moderate and red high value.

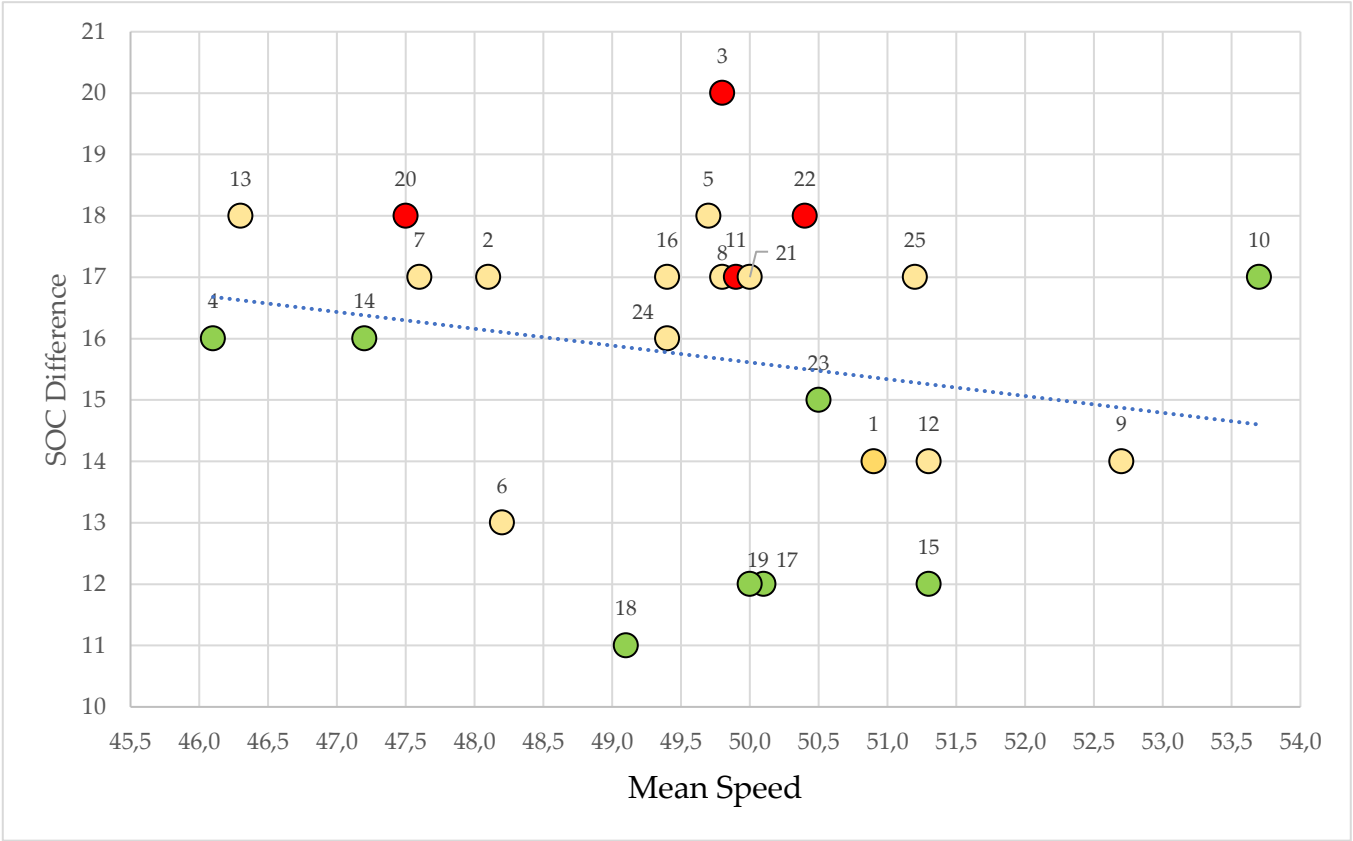

Figure 4.3. D1 experimental results: SOC difference vs Mean speed

At a first impression, the diagram seems to show no relation between the mean speed and the SOC difference. Indeed, the trend is quite the opposite: when the mean speed is higher, also the energy consumption should be higher, and vice versa. Anyway, as already stated above, the mean speed does not represent the only parameter on which the SOC difference depends; also the maximum speed, the time at maximum speed and the power of auxiliaries play their role. In particular, this can be better explained having a look to the experimental tests characterized by a similar value of mean speed. It is clear that, in the case of tests 22 and 23, which have a difference of 3% in energy consumption, what makes this difference is the power of auxiliaries and a faster behaviour on the road.

Furthermore, considering for instance the points 13 and 22 on the diagram, they represent two experimental tests which have the same SOC. This could seem a bit unusual, since both mean speed and power of auxiliaries are higher in test 22. However, this could be easily explained by the fact that during the test 22, the vehicle has spent more time at high speed than test 13, even if the mean speed is lower.

To summarize, for D1 group, it can be concluded that, for low velocities, the mean speed gives a smaller contribution to the output than the power of auxiliaries and the time at high speed: the energy consumption is affected more by these two parameters rather than the mean speeds, since they are quite low. In support of this conclusion, there is also the fact that all the tests characterized by a low value of the power of the auxiliaries are at the bottom of the diagram, and thus they have a low SOC consumption. Exceptions to this are the test number 10, which however is characterized by a very high mean speed, and test 11, which, even if is characterized by a high level of power of auxiliaries, has an average output value, for a reason that will be explored later.

4.1.2. D2 Experimental Results

The results of D2 experimental tests are reported in Table 4.3, with also an indication of the average quantities.

Table 4.3. D2 Experimental Results.

N	Auxiliaries Power	Max Speed [km/h]	Mean Speed [km/h]	Starting SOC	SOC 1	SOC 2	Final SOC	SOC Difference
1	poor	111,9	56,5	42			23	19
2	high	124,8	55,4	69			47	22
3	high	127,8	58,8	100			80,5	19,5
4	high	137	60	83			60	23
5	high	127,5	58	59			37	22
6	moderate	128	55,4	68			47	21
7	poor	128,2	60,4	74			54	20
8	poor	134,0	64,5	76			55	21
9	high	136,6	63,1	100			79,5	20,5
10	poor	136,8	63,7	79,5			57	22,5
11	high	133,2	59,5	86	76	70	58	22
12	high	131,2	63,1	58	46	42	28	26
13	poor	133,4	55,6	62			40	22
14	moderate	127	56,3	85			64	21
15	moderate	130,5	62,2	64			41	23
16	high	123,3	62,2	82			58,5	23,5
17	high	130,6	61,4	96			75	21

18	poor	128,7	51,8	84			66	18
19	moderate	137,6	57	100			80	20
20	poor	129,1	54,2	93			73	20
21	poor	131,3	62,3	72			50	22
22	high	127,8	58,9	98			78,5	19,5
23	poor	108,5	55,3	86			69	17
24	poor	132,9	58,3	74			53	21
25	poor	133,6	57,3	45			25	20
Average Values		**129,3**	**58,8**					**21,06**

Moreover, the outputs of the tests were reported in a diagram, Figure 4.4, in order to find out the possible correlation between the energy consumption (expressed as SOC difference between the initial and the final values) and the mean speed. An indication about the power of auxiliaries and a linear trend are also given.

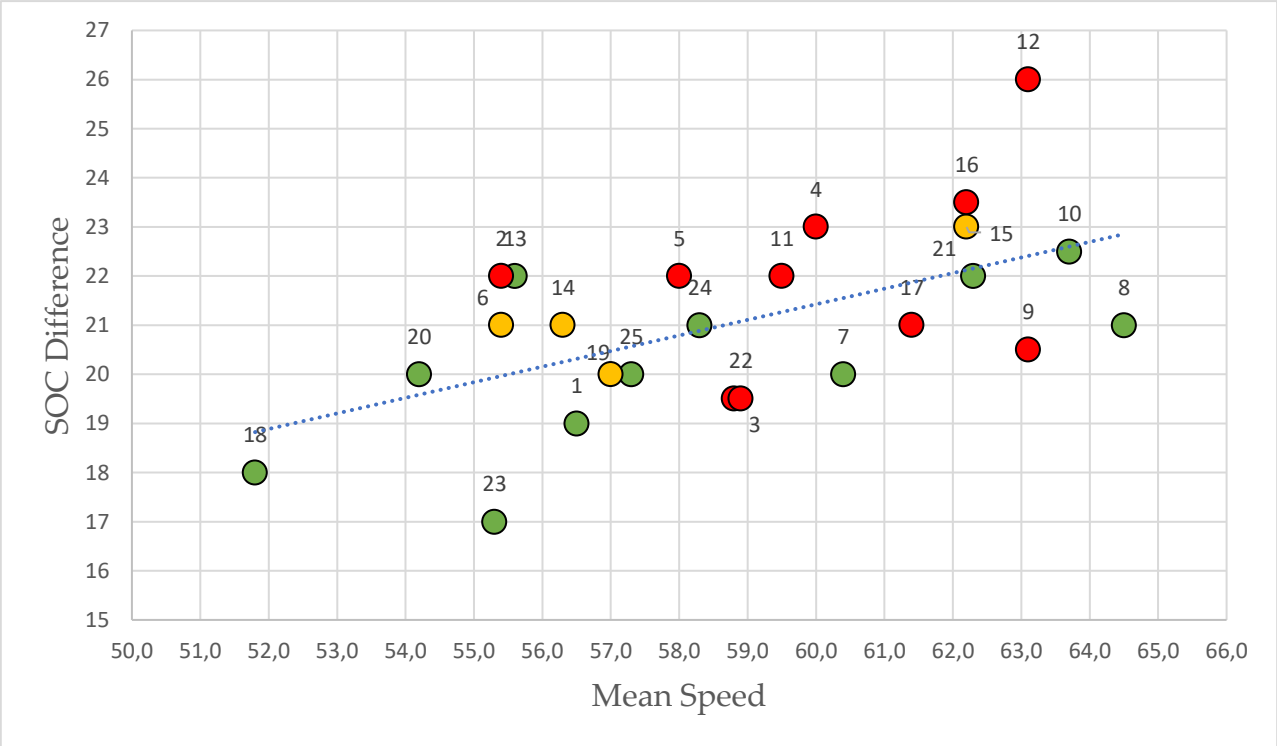

Figure 4.4. D2 Experimental Results: SOC difference vs Mean speed.

In this case, instead, a correlation between the mean speed and the difference in SOC can be found: when the speed is higher, so it is the energy consumption. Anyway, also this time, the output of the test still depend on the other quantities (power of auxiliaries and maximum speed), even if with a minor contribution. In particular, considering simulations 21 and 5, they have the same SOC output. This is because the higher mean speed of test 21 is recovered by a higher auxiliary power of test 5.

To conclude, the D2 group results are affected more by the average speed during the travel, which is very high, rather than the power of auxiliaries. This is the opposite of the D1 group. This can also be explained by the fact that, for high velocities, the duration of the travel is lower, and so the energy of the auxiliaries is also lower; instead, they have much more influence when the velocities are small, since the duration of the travel is higher, and so is the energy consumption of the auxiliaries. However, the contribution of the power of the auxiliary system will be better explored later.

4.2. Model Results and Comparison

In this section, the results of the model are reported and compared to the experimental ones, with also a reference of average outputs, Table 4.4 and Table 4.5.

Table 4.4. Comparison between experimental and model D1 results.

D1			
N	**Experimental SOC Difference**	**Model SOC Difference**	**Error**
1	14	17,34	3,34
2	17	16,63	-0,37
3	20	18,84	-1,16
4	16	15,19	-0,81
5	18	17,28	-0,72
6	13	16,24	3,24
7	17	17,06	0,06
8	17	16,27	-0,73
9	14	18,36	4,36
10	17	16,26	-0,74
11	17	20,31	3,31
12	14	17,59	3,59
13	18	17,28	-0,72
14	16	15,15	-0,85
15	12	16,39	4,39
16	17	16,87	-0,13
17	12	15,76	3,76
18	11	15,47	4,47

19	12	15,73	3,73
20	18	18,38	0,38
21	17	16,54	-0,46
22	18	18,34	0,34
23	15	15,37	0,37
24	16	16,3	0,3
25	17	17,04	0,04
	15,72	**16,87**	**1,16**

Table 4.5. Comparison between experimental and model D2 results.

D2			
N	**Experimental SOC Difference**	**Model SOC Difference**	**Error**
1	19	18,64	-0,36
2	22	22,08	0,08
3	19,5	23,35	3,85
4	23	23,61	0,61
5	22	22,34	0,34
6	21	21,35	0,35
7	20	20,42	0,42
8	21	21,49	0,49
9	20,5	23,96	3,46
10	22,5	22,19	-0,31
11	22	21,82	-0,18
12	26	24,64	-1,36

13	22	21,92	-0,08
14	21	20,82	-0,18
15	23	23,03	0,03
16	23,5	23,71	0,21
17	21	23,32	2,32
18	18	19,82	1,82
19	20	23,53	3,53
20	20	20,85	0,85
21	22	22,56	0,56
22	19,5	22,44	2,94
23	17	17,91	0,91
24	21	21,41	0,41
25	20	21,17	1,17
	21,06	**21,9352**	**0,88**

In order to simplify the comparison and to visualize better the critical points, these results have been put in a diagram, Figure 4.5 and Figure 4.6, highlighting the error between the two values of SOC difference.

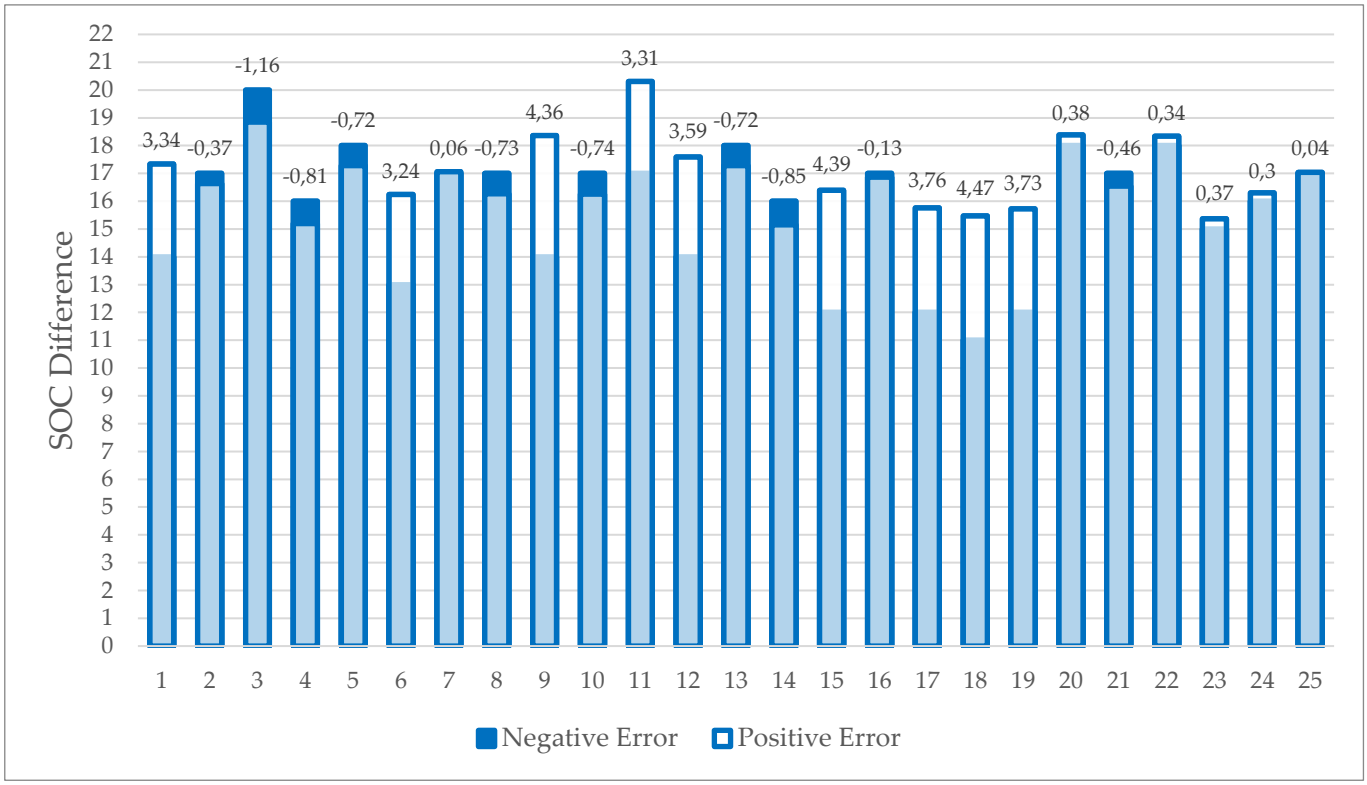

Figure 4.5: D1 Experimental and Model SOC Comparison.

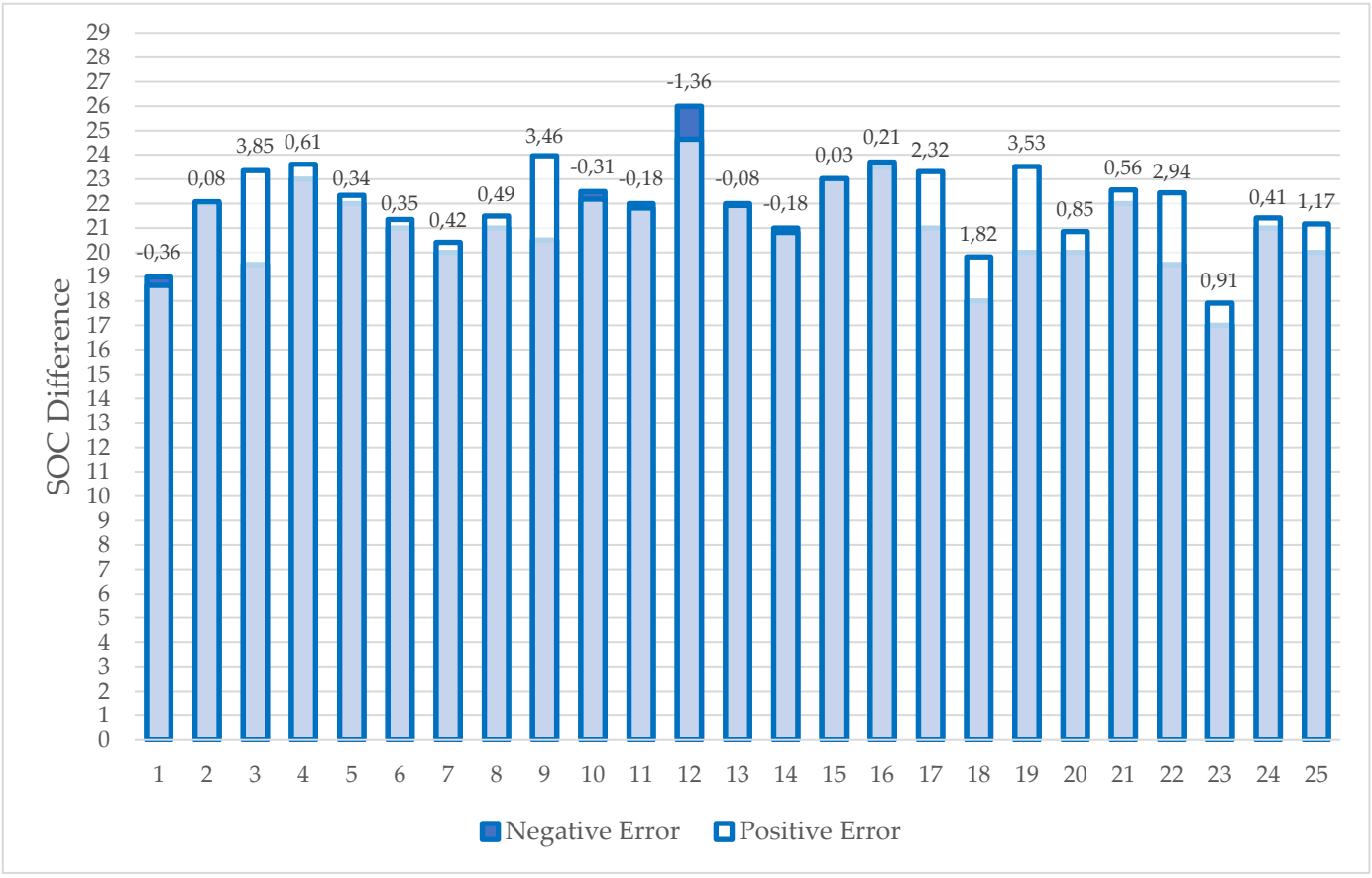

Figure 4.6: D2 Experimental and Model SOC Comparison.

In general, the experimental output and the model ones are quite similar for most of the tests. Anyway, some outbounds are present for both groups (highlighted in Table 4.4 and Table 4.5), which make the error increase a lot. In these cases, the model highly overestimate the output and the error between the two SOC differences is nearly always bigger than 3, with a maximum value of 4,47 for D1 and 3,85 for D2. These results cannot be accepted or justified by acquisition mistakes, even considering the approximations done in the model. In addition, considering the experimental SOC difference of these tests of D1 (11-12%) and considering that the useful capacity of the battery is 21,5 kWh, a value of 8,32 kWh/100km of specific energy consumption is obtained. This value is clearly wrong, since neither it does not match the other tests or it is not minimally close to the value given by Renault (around 14 kWh/100km in eco-driving).

This phenomenon seems to happen when the battery capacity of the vehicle is full charged, or particularly high, see Table 4.2 and Table 4.3. The technology of the battery of the Renault Twingo Model is a lithium-ion battery [32]. In literature, the effect of the SOC on the discharged energy has been found and analysed [43], [44]. It depends on the decrease of the Open-Circuit Voltage (OCV). In Figure 4.7, the OCV curve of a lithium-ion battery is showed.

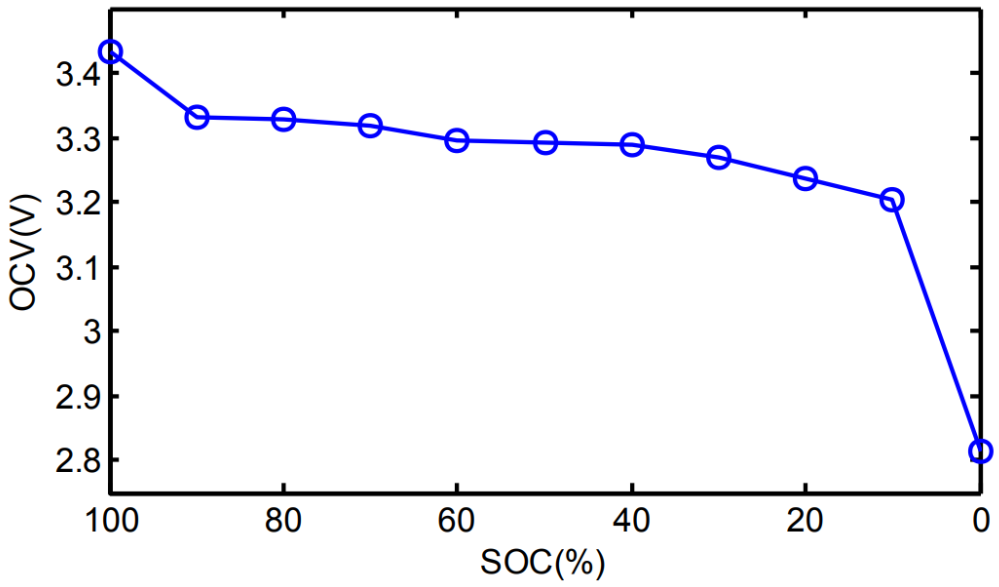

Figure 4.7: OCV curve of a lithium-ion battery [43].

It can be seen that when the SOC of the battery is higher than 90%, the OCV is also higher than the nominal values, and so will be the energy discharged. For decreasing values of SOC, the open-circuit voltage slightly decreases. This means that, since the battery energy is the product of the OCV and the capacity, for the same interval of the SOC, the discharged energy of the battery is not a constant, and in particular it will be much higher for values of SOC between 90% and 100%. In Figure 4.8, the different values of the discharged energy depending on the SOC are showed.

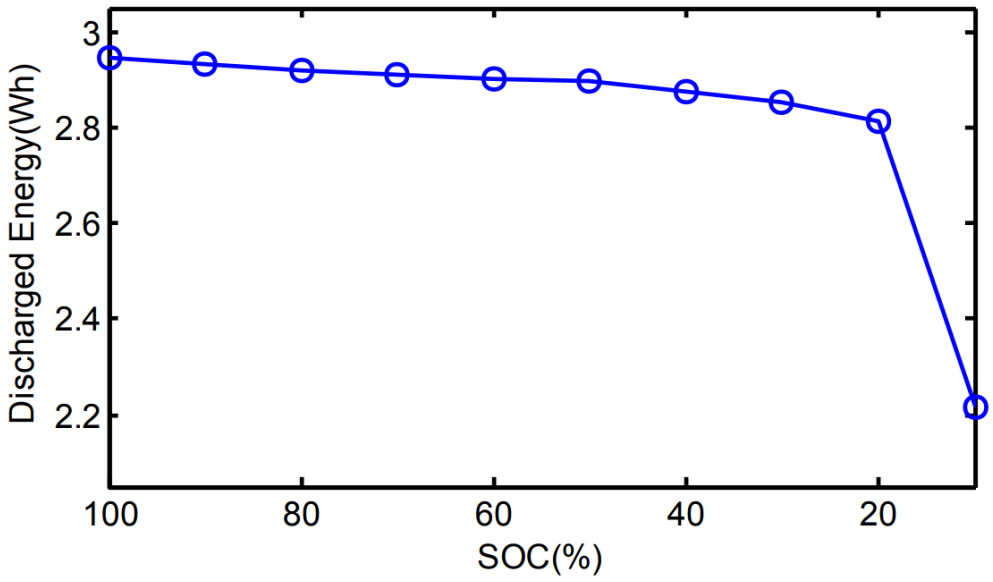

Figure 4.8: Values of the discharged energy depending on the SOC [43].

The discharged energy of the battery varies depending on the state of charge. Since a battery system is usually composed of hundreds or thousands of cells (for example, in the case of Renault Twingo, it is composed by 8 modules of 96 cells), these differences in discharged energy will be larger in actual operation.

4.2.1. Full SOC Correction

For the reasons explained above, the energy block of the model has been changed and corrected taking into account the effect of the full charged battery. It must be considered that the lowest value of SOC during the test was 23%. Since the SOC never was below the 20%, the correction has been made only in the 90%-100% interval, which is the one where the difference in discharged energy is bigger.

In particular, to consider the full-charged-battery effect, the energy consumption in the 90%-100% SOC interval has been decreased by a correction factor of 1,5, thus in order to simulate the bigger energy that the battery can provide in this interval.

In Figure 4.9, this correction is visualized and the two cases, before and after, are compared. The simulation D2-19 has been taken as reference.

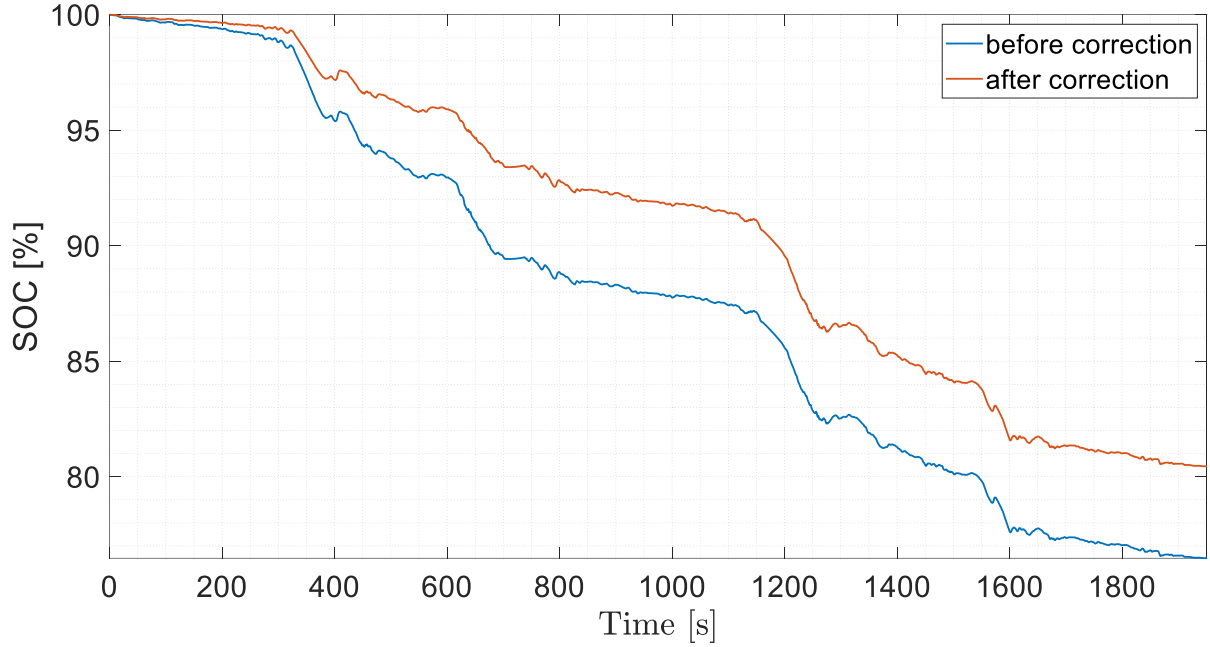

Figure 4.9: SOC profile comparison between before and after the correction.

It can be clearly seen how the energy consumption is reduced until the SOC becomes 90%; after this point, the two profile have the same consumption and thus their distance remains constant.

4.2.2. D1 Model Results

Starting from the D1 group, the model results are shown and compared to the experimental ones in Figure 4.10. To simplify the visualization of the error, the results have been compared in Figure 4.11.

Table 4.6: D1 experimental and model results comparison after the full-charged-battery correction.

N	Experimental SOC Difference	Model SOC Difference	Error
1	14	13,14	-0,86
2	17	16,63	-0,37
3	20	18,84	-1,16
4	16	15,19	-0,81
5	18	17,28	-0,72
6	13	12,19	-0,81
7	17	17,06	0,06
8	17	16,27	-0,73
9	14	14,17	0,17
10	17	16,26	-0,74
11	17	16,23	-0,77
12	14	13,19	-0,81
13	18	17,28	-0,72
14	16	15,15	-0,85
15	12	12,03	0,03
16	17	16,87	-0,13
17	12	11,44	-0,56
18	11	11,13	0,13

19	12	11,42	-0,58
20	18	18,38	0,38
21	17	16,54	-0,46
22	18	18,34	0,34
23	15	15,37	0,37
24	16	16,3	0,3
25	17	17,04	0,04
	15,72	**15,35**	**-0,37**

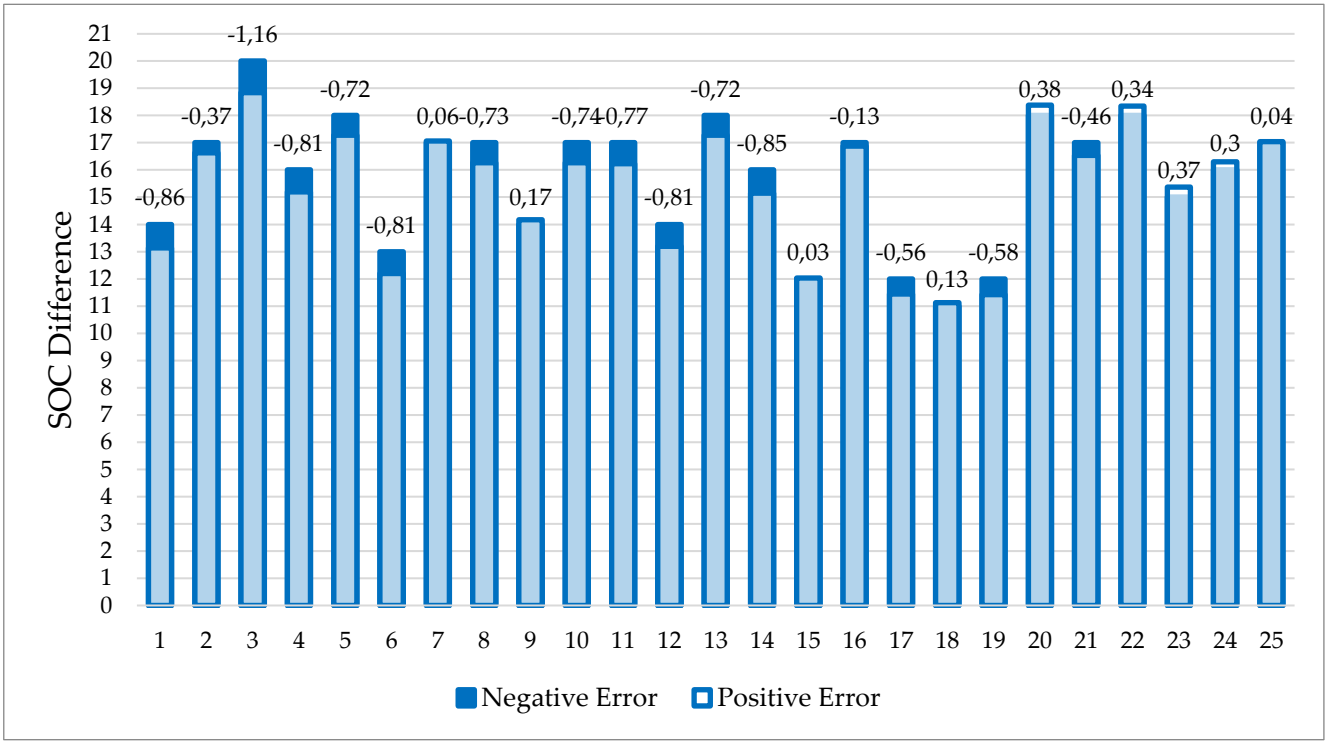

Figure 4.10: D1 Experimental and Model SOC Comparison after the correction.

In this case, all the simulations match the output of the test, since the error is almost always lower than 1%, with the only exception of simulation 3. This represents a particular case, because the value of the SOC measured is much higher than the others, thus, a higher value of power of auxiliaries should be considered in order to better represent the real conditions of the test.

In general, for D1 group, the model seems to underestimate a bit the experimental results, with an acceptable value of average error of -0,37%.

4.2.3. D2 Model Results

In Table 4.7 and Figure 4.11, D2 model results are shown and compared to the experimental ones.

Table 4.7: D2 experimental and model results comparison after the full-charged-battery correction.

N	Experimental SOC Difference	Model SOC Difference	Error
1	19	18,64	-0,36
2	22	22,08	0,08
3	19,5	19,3	-0,2
4	23	23,61	0,61
5	22	22,34	0,34
6	21	21,35	0,35
7	20	20,42	0,42
8	21	21,49	0,49
9	20,5	20,11	-0,39
10	22,5	22,19	-0,31
11	22	21,82	-0,18
12	26	24,64	-1,36
13	22	21,92	-0,08
14	21	20,82	-0,18
15	23	23,03	0,03
16	23,5	23,71	0,21
17	21	20,98	-0,02
18	18	19,82	1,82
19	20	19,55	-0,45

20	20	20,85	0,85
21	22	22,56	0,56
22	19,5	19,25	-0,25
23	17	17,91	0,91
24	21	21,41	0,41
25	20	21,17	1,17
	21,06	**21,24**	**0,18**

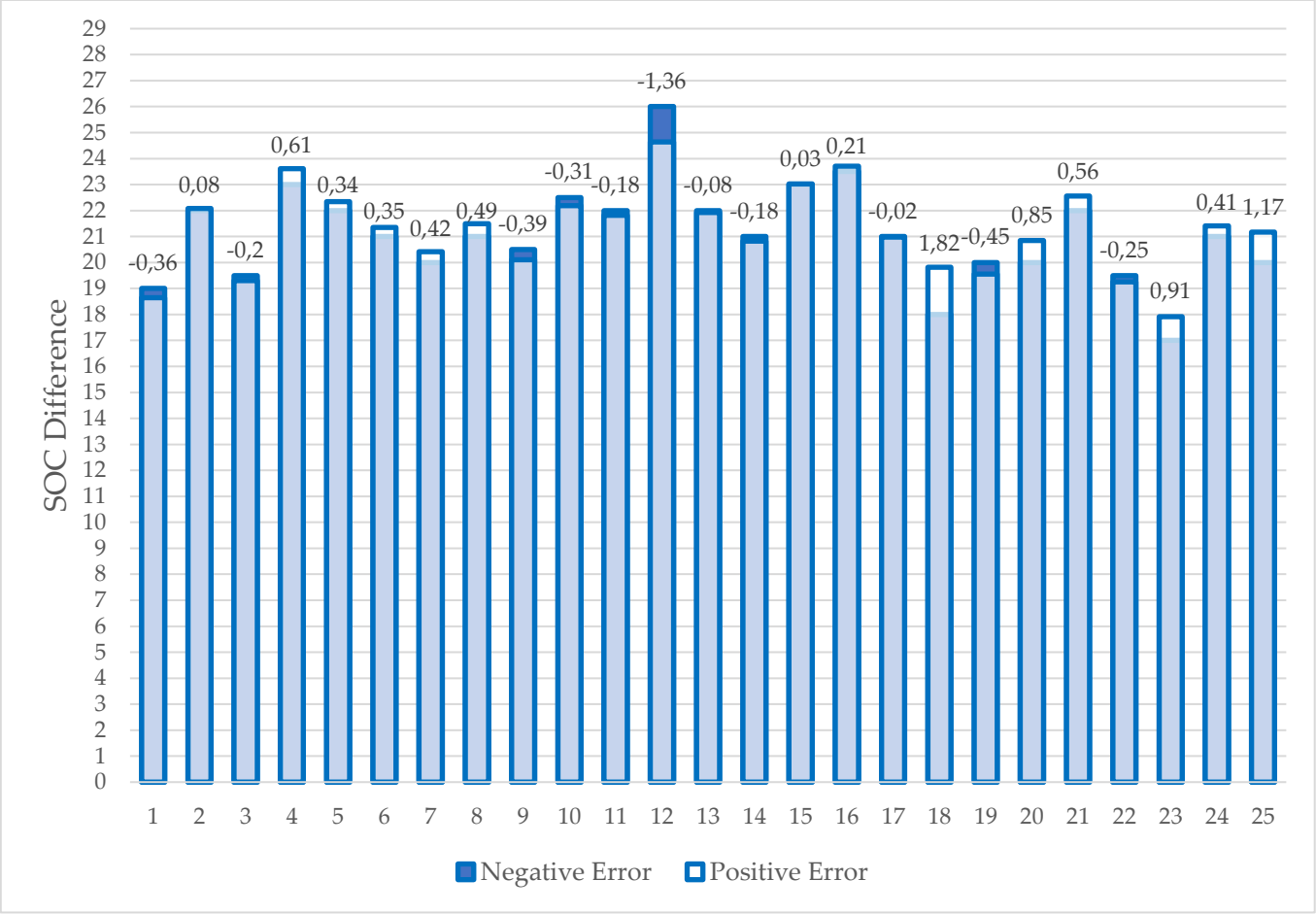

Figure 4.11: D2 Experimental and Model SOC Comparison after the correction.

In the case of D2 group, the model seems to better estimate the experimental result, with a value of average error of 0,18%. However, also this time, some particular cases are present. Starting from test 12, the model underestimated the SOC difference. This

is surely due to the power of auxiliaries, which should be much higher to better represent the conditions of the test, like in the case of D1-3 test. In Figure 4.12, an acquisition of the test is showed. It can be notice that lights, wipers and air conditioning have been switched on for the whole duration of the travel, this explains the higher level of auxiliaries power consumption.

Figure 4.12: Photo of the road during the test 12.

As regards simulation 18, a precise motivation cannot be found. Anyway, it must be considered that the SOC sensor of the vehicle, visualized on the dashboard, has a sensitivity of 1%, thus, the measured values of SOC have a tolerance of ±0,5%. This fact is showed in Figure 4.13, where it can be seen how for the same number of kilometres, two different values of SOC are indicated. The photos have been taken a few seconds apart.

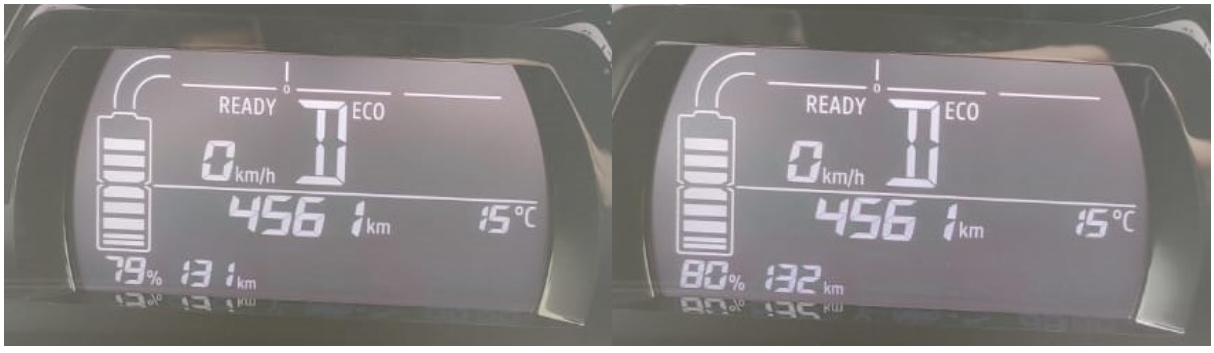

Figure 4.13: Photos of the vehicle dashboard.

4.3. Comparison for same power of auxiliaries

It has been already stated as the power of auxiliaries represents one of the biggest contribution to the energy consumption, especially for D1 group of tests. In this section, this parameter will be more explored, starting from a general comparison case.

The simulation D2-09 has been taken as a reference, and in Figure 4.14 the cumulative energy consumptions of the route for the three different values of auxiliary power are showed.

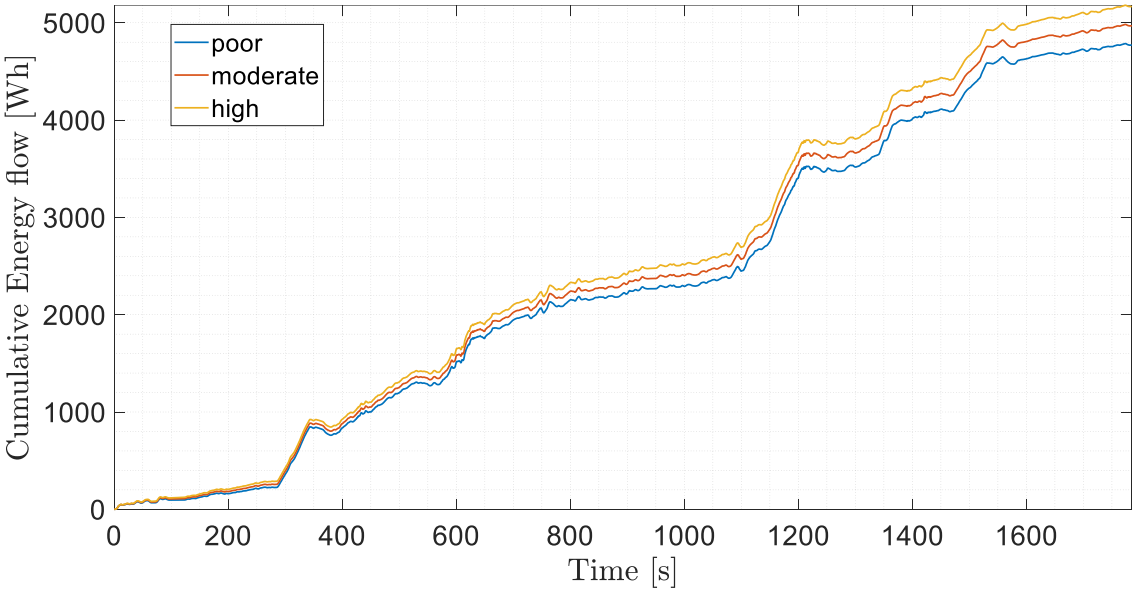

Figure 4.14: Effect of the power of auxiliaries on cumulative energy consumption.

It can be seen how higher the power of auxiliaries is, higher is also the energy consumption, resulting in an increase of SOC difference between the beginning and the end of 1-2%. Of course, in this case, since the distance travelled is fixed, the auxiliaries power increases the energy consumption. However, in actual life operation, increasing the energy consumption of the auxiliaries, the range of the vehicle will decrease.

4.3.1. D1 Results comparison

The model results have been ordinated according to the value of the power of auxiliaries and listed in Table 4.8.

Table 4.8: D1 results sorted by Auxiliaries power values.

N	Auxiliaries Power	Experimental SOC Difference	Model SOC Difference	Starting SOC
18	poor	11	11,13	100
19	poor	12	11,42	100
17	poor	12	11,44	100
15	poor	12	12,03	100
14	poor	16	15,15	80
4	poor	16	15,19	48
23	poor	15	15,37	79
10	poor	17	16,26	82
6	moderate	13	12,19	100
1	moderate	14	13,14	100
12	moderate	14	13,19	100
9	moderate	14	14,17	100
8	moderate	16	16,3	74
24	moderate	17	16,27	49
21	moderate	17	16,54	50
2	moderate	17	16,63	72
16	moderate	17	16,87	78
25	moderate	17	17,04	77
7	moderate	17	17,06	88

5	moderate	18	17,28	43
13	moderate	18	17,28	67
11	high	17	16,23	100
22	high	18	18,34	56
20	high	18	18,38	65
3	high	20	18,84	64

To make a further analysis, a pair of simulations with the same auxiliaries power consumption have been compared, in order to find out supplementary critical issues of the model. It must be stated that the simulations which have a starting SOC value higher than 90% were not considered. The comparison between simulations 5 e 8 is reported in Figure 4.15. These simulations both have a moderate value of auxiliaries power consumption, but different speed profile characteristics, reported in Table 4.9, and so a different energy consumption output.

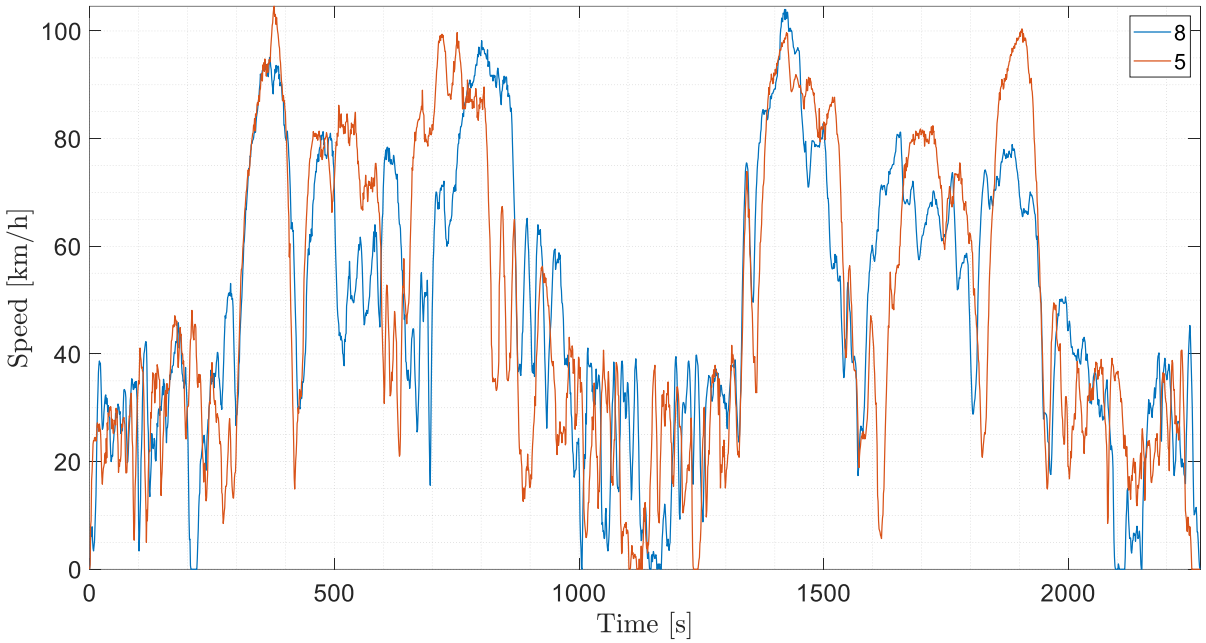

Figure 4.15: Comparison between simulation 8 and simulation 5 speed profiles.

Table 4.9: Characteristics of simulation 5 and 8 speed profiles.

N	Max Speed [km/h]	Time [s] over 90 km/h	Time [s] over 100 km/h	Mean Speed [km/h]	Duration [mm:ss]

5	104,6	207	15	48,8	37:32
8	104,0	159	21	48,8	37:49

As can be seen from the Figure 4.16, their speed profile is much different. Of course, in the urban condition, the speed are quite similar, but in some of the extra-urban sections, the mean speed and also the maximum speed of the simulation 5 are higher. This difference in speed profile is reflected on both experimental and model output, which increases respectively of 2% and almost 1%.

Another comparison can be made between two simulations that have a different power of auxiliaries output, but without considering this last parameter. This time the simulation chosen were the 3 e 10 ones, whose speed profiles and characteristics are reported respectively in Figure 4.17 and Table 4.10. As can be seen, the two speed profiles have similar trends.

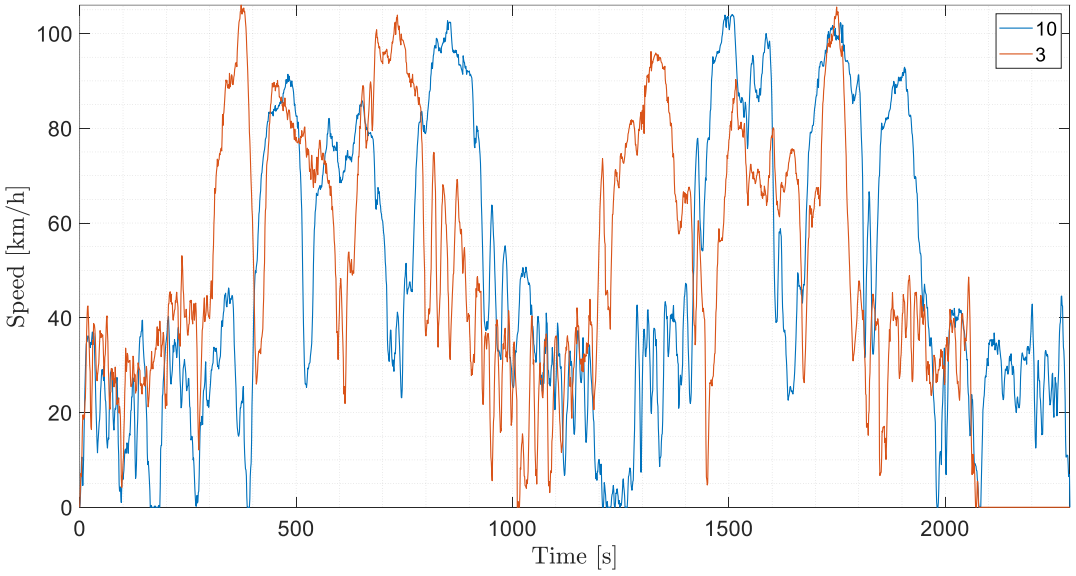

Figure 4.16: Comparison between simulation 10 and simulation 3 speed profiles.

Table 4.10: Characteristics of simulation 3 and 10 speed profiles.

N	Max Speed [km/h]	Time [s] over 90 km/h	Time [s] over 100 km/h	Mean Speed [km/h]	Duration [mm:ss]
3	104,0	294	61	48,5	38:08
10	106	216	46	53,5	34:38

In Figure 4.17, the result of the simulations is showed, expressed as SOC. It can be clearly seen that, with the same auxiliaries power, the two simulations present the same SOC trend, with a final value of SOC difference of 16,47 for 3 and 16,26 for simulation 10. The two SOC profile are shifted because they are instantaneous profiles, and so they depends also on the speed profile.

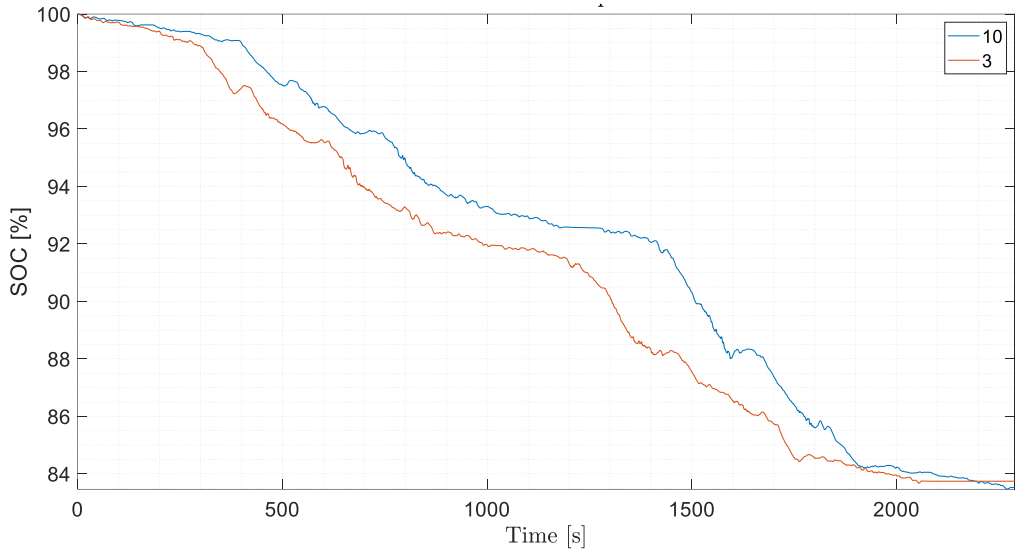

Figure 4.17: Comparison between simulation 10 and simulation 3 SOC profiles.

4.3.2. D2

Even for D2 group, the model results have been ordinated according to the value of the power of auxiliaries and listed in Table 4.11.

Table 4.11: D2 results sorted by Auxiliaries power values.

N	Auxiliaries Power	Experimental SOC Difference	Model SOC Difference	Starting SOC
23	poor	17	17,91	86
18	poor	18	19,82	84
1	poor	19	18,64	42
7	poor	20	20,42	74
20	poor	20	20,85	93
25	poor	20	21,17	45
8	poor	21	21,49	76
24	poor	21	21,41	74
13	poor	22	21,92	62
21	poor	22	22,56	72
10	poor	22,5	22,19	79,5
19	moderate	20	19,55	100
6	moderate	21	21,35	68
14	moderate	21	20,82	85
15	moderate	23	23,03	64
3	high	19,5	19,3	100
22	high	19,5	19,25	98
9	high	20,5	20,11	100
17	high	21	20,98	96

2	high	22	22,08	69
5	high	22	22,34	59
11	high	22	21,82	86
4	high	23	23,61	83
16	high	23,5	23,71	82
12	high	26	24,64	58

Again, the same logic as before is applied for the following comparison. Simulations 23 and 21, which have same poor power of auxiliaries, but different characteristics of speed profile, were compared. In Figure 4.18, the comparison between simulation 8 and simulation 5 speed profiles is showed, and their characteristics are reported in Table 4.12.

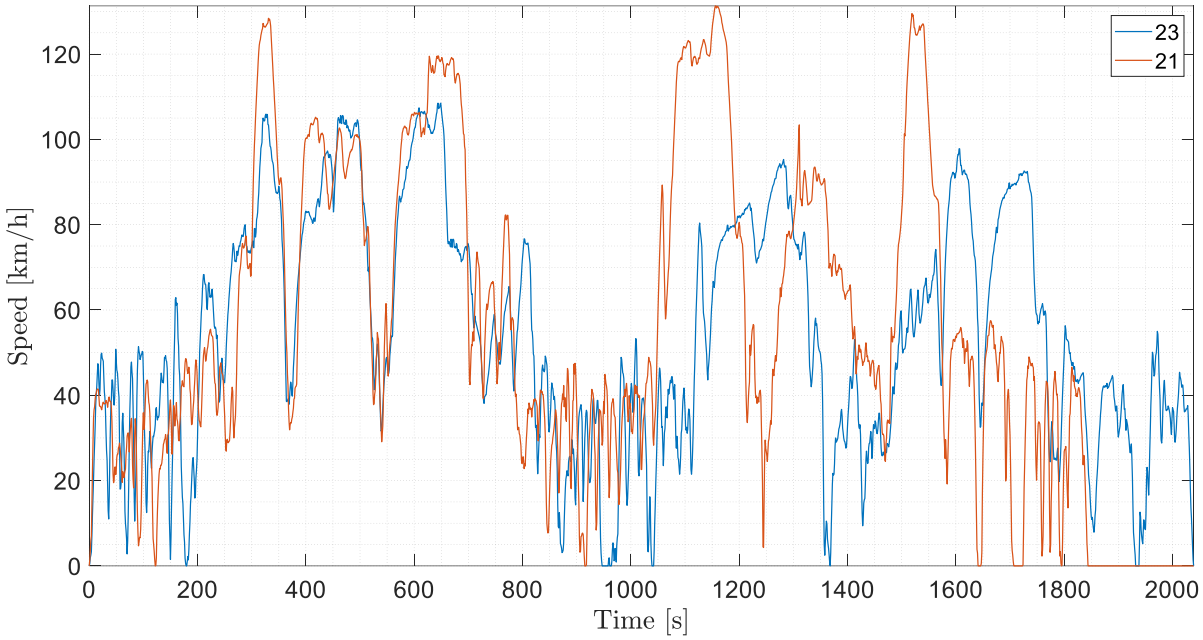

Figure 4.18: Comparison between simulation 23 and simulation 21 speed profiles.

Table 4.12: Characteristics of simulation 21 and 23 speed profiles.

N	Max Speed [km/h]	Time [s] over 110 km/h	Time [s] over 120 km/h	Mean Speed [km/h]	Duration [mm:ss]
21	131,3	232	116	61,3	30:44
23	108,5	0	0	54,3	33:59

It can be clearly noticed that the speed profile of simulation 21 is much way higher, in all the extra-urban sectors, with a difference of mean and maximum speed of respectively 7 and 23 km/h. Also in this case, it is clear that the difference in velocities is the main reason for the difference in SOC, 5% and about 4,5% respectively for the experimental tests and the simulation, since the auxiliaries power consumption is the same.

Furthermore, the particular case of test number 12 was also compared. It has been already said how in this case the auxiliaries power consumption was much higher than the others. Thus, this simulation was compared with simulation 8, which has similar speed profile characteristics, showed in Figure 4.19 and in Table 4.13.

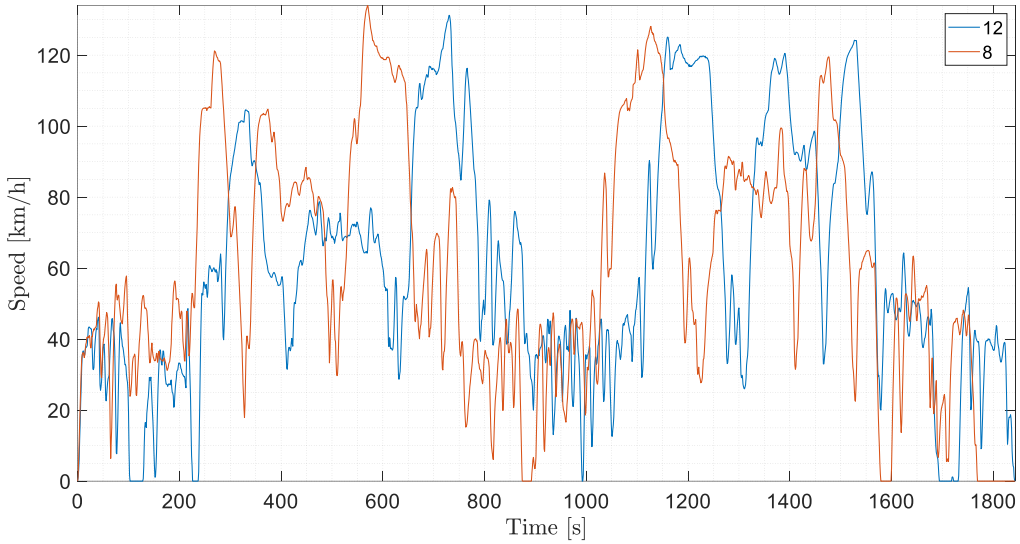

Figure 4.19: Comparison between simulation 12 and simulation 8 speed profiles.

Table 4.13: Characteristics of simulation 8 and 12 speed profiles.

N	Max Speed [km/h]	Time [s] over 110 km/h	Time [s] over 120 km/h	Mean Speed [km/h]	Duration [mm:ss]
8	134,0	193	69	64,5	29:29
12	131,2	235	67	63,1	30:43

In Figure 4.20, the result of the simulations is showed, expressed as SOC. It can be clearly seen that, with the same auxiliaries power, the two simulations present the same SOC trend, with a final value of SOC difference of 16,47 for 8 and 16,26 for simulation 12.

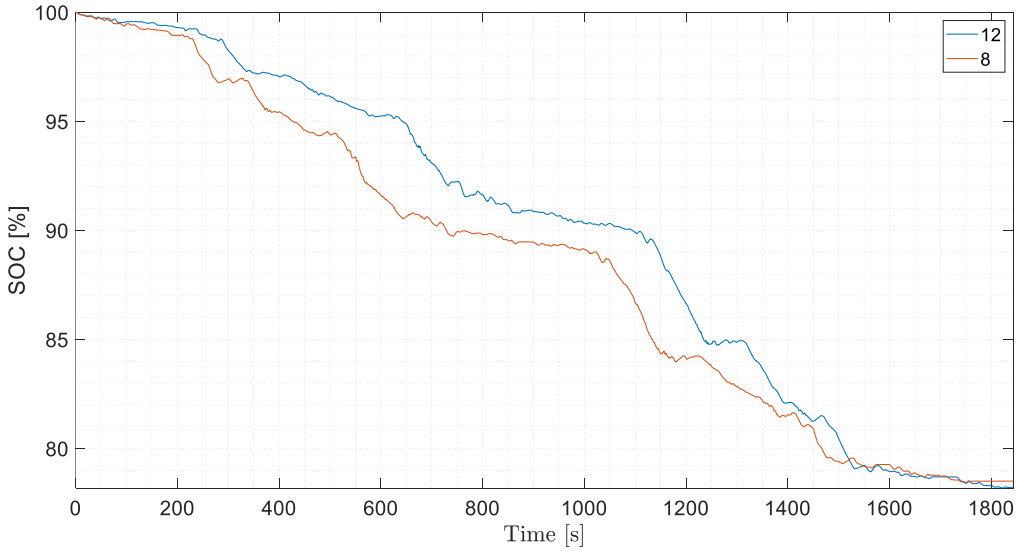

Figure 4.20: Comparison between simulation 12 and simulation 8 SOC profiles.

4.4. Comparison according to the type of Road

In the previous sections of this work of thesis, it has been more times stated how the two groups of tests cannot be compared due to the huge difference in velocities. However, now, this difference in speed profile becomes a starting point for a further comparison.

The comparison between the two SOC profiles is showed in Figure 4.21.

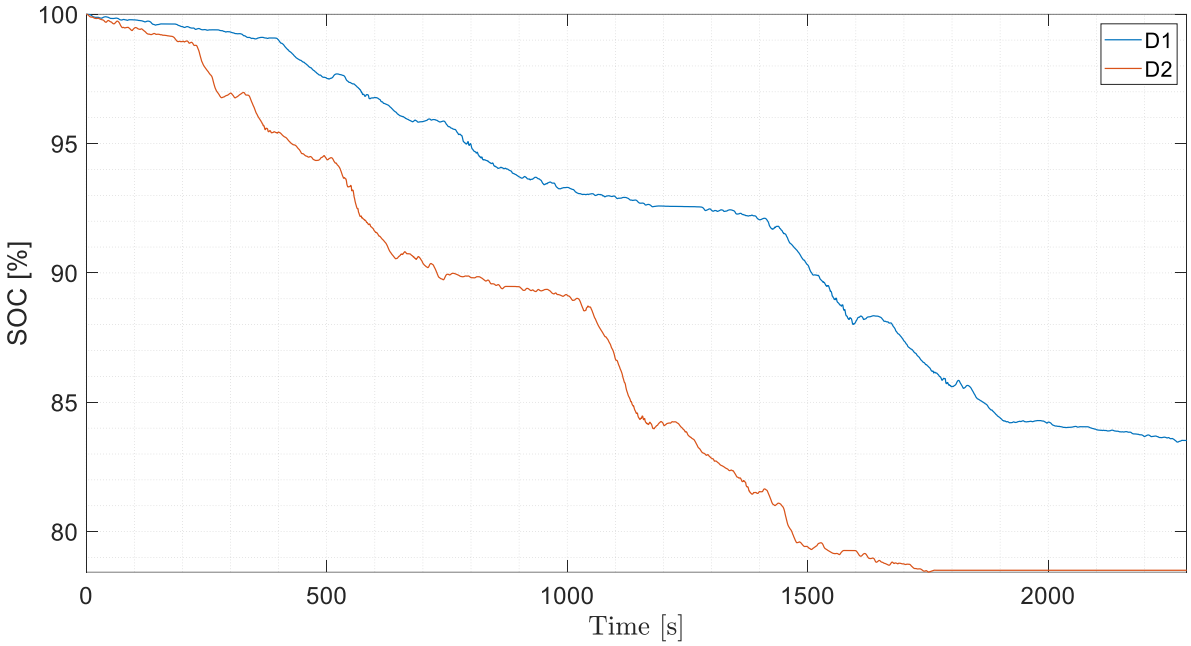

Figure 4.21: Comparison between D1 and D2 SOC profiles.

The two SOC profiles present some similarities. It can be clearly seen that in the city sections, the SOC profile is not so steep, instead, it dramatically drops in the extra-urban zones. However, the decreasing in SOC is much faster in D2, principally caused by the higher velocities, as it will be explored later.

Furthermore, the route has been divided into the same two parts already mentioned (urban and extra-urban) also in the simulations, in order to have the model results for the two conditions and to explore similarities and differences of the two groups. The comparison has been made for two sections of the speed profile, with the same moderate power of auxiliaries level, because the goal was to determine how the type of road effects the energy consumption.

In Table 4.14, the average values of the characteristics of the two road conditions for the two groups of tests are showed.

Table 4.14: Average characteristics of the two sections of road for D1 and D2.

	CITY		EXTRA-URBAN	
Average Quantities	**D1**	**D2**	**D1**	**D2**
Maximum Speed [km/h]	47,5	57,7	101,1	127,3
Mean Speed [km/h]	24,8	32,0	69,4	78,9

4.4.1. Urban

It has been already stated how the D1 and D2 speed profiles are very similar in urban environment. This is because they both suffers from the typical features of the city conditions: congestion, traffic lights, pedestrian and more. For this reason, typically the speed profiles, showed in Figure 4.22, present a limited maximum speed and frequent stop and acceleration. From the figure, it can be clearly seen that the two maximum speeds are very similar, instead D1 presents a mean speed quite lower than D2, but still comparable.

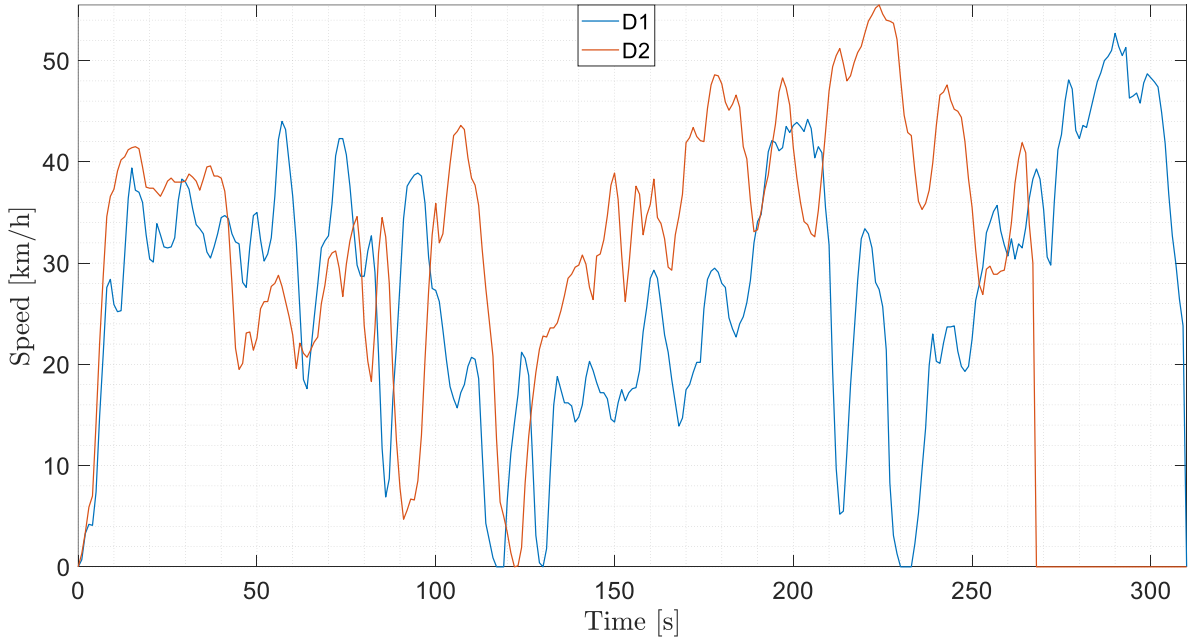

Figure 4.22: Comparison between D1 and D2 urban speed profiles.

In order to find out the energy consumption for this section of the route, a simulation has been made, considering as a reference the first city section of the speed profiles for D1 and D2, Figure 4.22. It is also important to state that the comparison has been made for the same value of power of auxiliaries.

The features and results of the simulations with an indication of the average values are reported in Table 4.15.

Table 4.15: Urban results for D1 and D2.

	D1			D2		
N	**Maximum Speed [km/h]**	**Mean Speed [km/h]**	**Specific Energy Consumption [kWh/100km]**	**Maximum Speed [km/h]**	**Mean Speed [km/h]**	**Specific Energy Consumption [kWh/100km]**

1	52,2	23,2	11,85	49,4	28,3	10,03
2	38,3	10,8	10,76	51,1	29,4	12,18
3	46,3	22,4	11,09	56,8	29,8	11,37
4	49,5	22,1	12,10	43,3	28,5	10,73
5	48,1	27,8	10,73	59,4	29,6	12,04
6	44,9	25,7	11,40	49,3	22,6	13,03
7	42,8	25,6	10,10	58	35,8	10,05
8	45,8	27,7	10,53	57,8	39,2	11,42
9	53,4	24,7	11,17	68,1	45,4	11,35
10	53,1	30,9	10,32	53,7	31	11,18
11	56,8	24,9	12,01	49,8	30,3	10,94
12	54,3	26,8	10,90	48,6	24,9	12,86
13	49,8	22,6	12,74	60,1	30,6	11,20
14	42,9	29,5	10,36	58,6	27,9	13,24
15	51,9	26,8	11,99	68	40,1	12,54
16	43,6	22,9	11,83	65,2	42,8	12,40
17	44	28,4	10,37	67,4	38,4	12,39
18	46,3	26,2	10,80	47,6	26,5	12,78
19	46,7	19,4	13,02	67,8	26,4	13,82
20	48,5	21,9	12,75	59,3	29,3	14,00
21	52,7	27,3	12,17	55,5	32,9	11,57
22	51,8	28,9	12,49	62,4	32,7	12,67
23	43	27,4	10,90	68,3	35	15,28

24	39,6	20,7	11,40	63,5	32,8	14,08
25	41,5	25,27	10,95	53,1	30,8	11,68
	47,5	**24,8**	**11,39**	**57,7**	**32,0**	**12,19**

The results show that a comparison between the two groups is meaningful in urban conditions. As stated above, the main reason is that the speed profiles are quite similar: the average mean speeds are 24,8 km/h and 32 km/h respectively for D1 and D2. The D2 average maximum speed is about 10 km/h higher, according to the speed profiles, but it can be stated that this maximum value represents a single isolated peak rather than a long high speed period. Thus, for these reasons, the specific energy consumption output is quite the same for both the groups, with a difference value of 0,80 kWh/100km. In addition to this, these values of autonomy are similar to the one indicated by the manufacturer.

4.4.2. Extra-urban

Different conditions are valid for the extra-urban section, which is characterised by high velocities and variable slope, as stated above. The two speed profiles are showed in

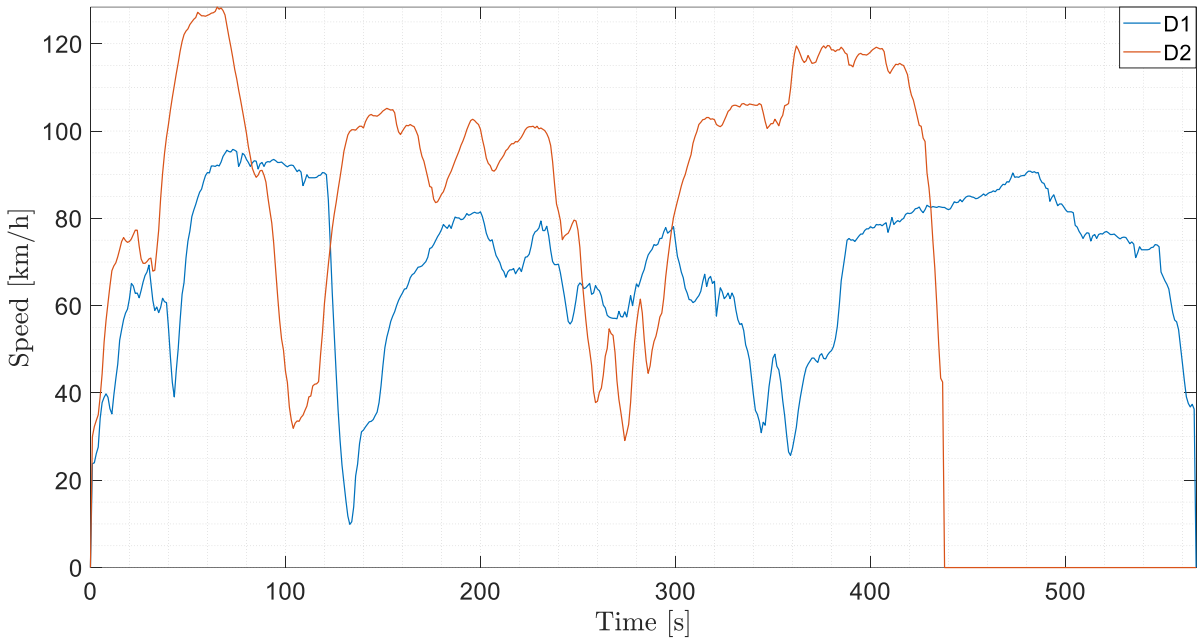

Figure 4.23. In this part of the road, the two groups present a very different behaviour. Even if the general trend is the same, because the route travelled is the same, the D2 velocity is always as high as possible, instead, the D1 eco-driving condition makes the maximum speed to be always lower than 110 km/h in this latter case. Also in this comparison, the simulation has been made for the same auxiliaries power level, considering as a reference the first sections of extra-urban road.

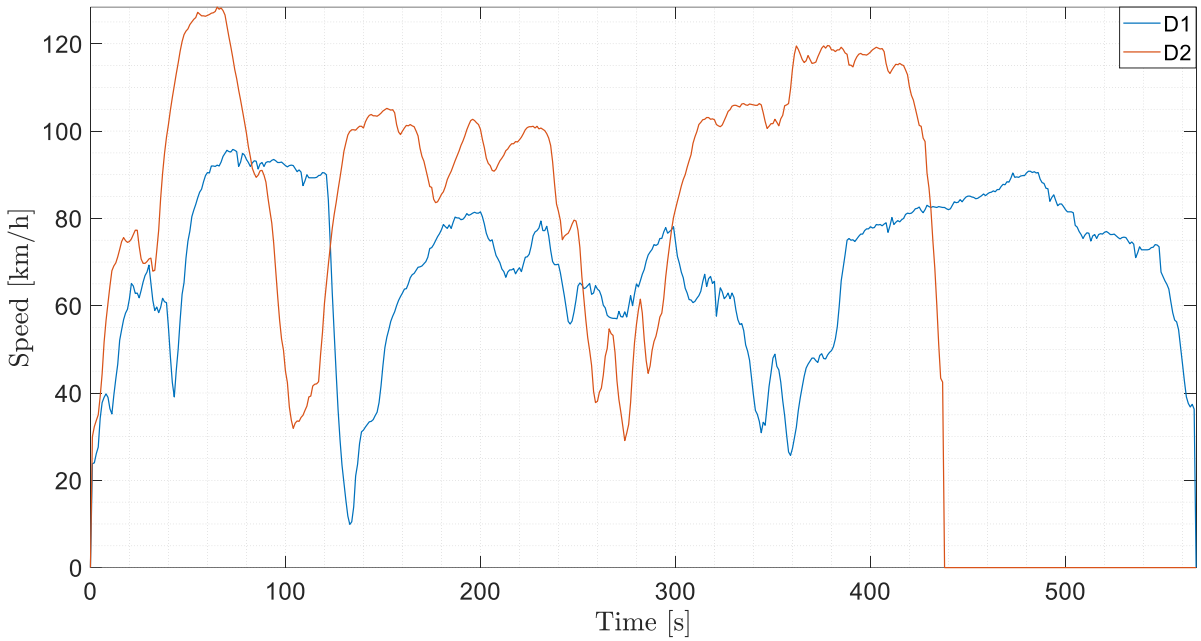

Figure 4.23: Comparison between D1 and D2 extra-urban sections.

The features and results of the simulations with an indication of the average values are reported in Table 4.16.

Table 4.16: Extra-urban results for D1 and D2.

	D1			D2		
N	**Maximum Speed [km/h]**	**Mean Speed [km/h]**	**Specific Energy Consumption [kWh/100km]**	**Maximum Speed [km/h]**	**Mean Speed [km/h]**	**Specific Energy Consumption [kWh/100km]**
1	99	74,4	13,76	106,8	70,6	14,18
2	98,5	73,3	13,38	124,8	72,7	15,34
3	102,7	70,4	13,30	126,3	77,3	17,14
4	90,3	67,5	12,55	137	72,7	18,61
5	104,6	72,1	13,69	127,5	78,2	16,68
6	92,4	60,4	11,64	128,4	70,3	16,19
7	95,9	67,8	12,90	128,2	78,6	17,13
8	98,2	62,2	12,72	134,0	86,3	18,42

9	107,8	81,4	15,74	136,6	83	18,53
10	106	72,3	14,06	136,8	86,6	18,02
11	106,5	72,7	14,43	124,6	74	16,37
12	105,5	74,9	14,29	131,2	74,3	15,54
13	103,8	73	14,33	133,4	81,9	17,94
14	97,5	64,6	12,56	124,9	83,7	17,52
15	96,5	66,7	12,48	130,5	83,8	17,85
16	106,3	69,13	13,19	123,3	91,9	19,59
17	104,9	68,8	13,09	125,2	77,1	16,92
18	102	62,5	12,89	128,7	68,4	15,43
19	99,9	67,9	12,68	137,6	90,3	20,32
20	107,5	70,4	13,40	125,1	78,6	16,06
21	95,8	68,5	12,95	128,4	89,6	18,86
22	108,7	69,6	13,10	127,8	79,5	16,84
23	98,1	69,7	12,70	108,5	79,3	15,57
24	96,5	63,9	11,91	119,1	67,2	16,01
25	103,1	70	13,00	126,9	77,8	16,80
	101,1	**69,4**	**13,2**	**127,3**	**78,9**	**17,1**

In extra-urban condition instead, the effect of the mean and maximum speed on the energy consumption is much more important.

Firstly, a difference between specific consumptions of city and extra-urban conditions of D1 can be noted. Even if the average mean speed is much higher in the extra-urban case, it is also true that it does not have a huge value and so the vehicle is near to its best-efficiency operational point.

Furthermore, when the mean speeds increases, the specific energy consumption steeply increases too, with an average difference value of about 4kWh/100km for only 10km/h of mean speed difference. This is of course also due to the long periods in which the vehicle travelled at its maximum speed (around 130 km/h).

To conclude, it is important to notice how the difference value stated above of 4kWh/100km between D1 and D2 groups corresponds to a value of SOC of about 5% for the vehicle chosen and for the distance of high-speed road and this value is quite similar to the average difference between D1 and D2 tests. This is a further demonstration of the fact that the model can accurately estimate the behaviour of the vehicle.

Conclusion

In this work, a methodology for the design of an Electric Vehicle model is described and its validation on a real-world vehicle system is presented, with detailed analysis of the results.

The main parameters of the model are the route, which significantly affects the speed profile, the choice of the vehicle and the power consumption of the auxiliary system. Thus, the results will be analyzed according to these model parameters, considering that the vehicle has been the same for the whole duration of the experimental campaign. This is composed of fifty tests divided into two groups, called D1 and D2. This division has been done in order to consider all the possibilities of a real-world condition: the D1 represents an eco-driving behavior, and thus with low velocities and limited maximum speed; instead, D2 characteristics are quite the opposite, and so high mean velocity and a maximum speed that is limited only by the vehicle one. For these reasons, a comparison between these two groups would be meaningless, even if a yardstick has been found.

Generally, the model accurately estimates the experimental outputs, since the average error between the two results is quite small, with a maximum error values of 1,16% and 0,88% respectively for D1 and D2, and the values of specific energy consumption are similar to the one of the manufacturer. Anyway, some outbounds were present for both groups: it has been noticed how the energy consumption for the tests starting with a full charged battery was significantly small, far below the average specific energy consumptions. Thus, the model has been modified in order to match the experimental results in these specific particular cases.

After the full-charged-battery correction, the average errors drop to values of -0,37% and 0,18% respectively for D1 and D2; in this way, the model better estimates the experimental results. This is also confirmed by the comparison done with the same level of the auxiliaries power. It has been established how the auxiliary system affects the energy consumption: simulations with similar speed profile characteristics, if have the same power of auxiliaries, will give also similar results, i.e., energy output. This is another evidence of the fact that velocities and the power of the auxiliary system are the main parameter of the model. In particular, this dependances has been explored analyzing the results of the two groups.

As regard D1 group, it has been found that the contribution of the power of the auxiliaries is more significant. For low velocities indeed, the mean speed gives a smaller contribution to the output than the power of auxiliaries and the time at high speed: the energy consumption is affected more by these two parameters rather than the mean speeds, since they are quite low. In case of D2 group, instead, a correlation between the mean speed and the difference in SOC can be found: when the speed is higher, so it is the energy consumption. Thus, at high velocities, mean and maximum speed are the most important parameters.

Lastly, a further comparison has been made. This time, the two groups were compared, according to the type of road. Indeed, the fixed route is composed mainly of two sections: a city zone, with limited velocities and frequent stops and fast accelerations, and an extra-urban road, characterized by high mean and maximum speeds. It has been found that for the urban zone, since the speed profiles are quite similar, the energy output are similar too. The opposite is valid for the extra-urban zone: the difference in mean and maximum speeds makes the energy consumption to significantly increase.

To conclude, this EV model seems to accurately estimate the energy consumption and so the State of Charge of a chosen vehicle. In the context of this thesis, future possible developments and modifications could be a more accurate evaluation of the power consumption of the auxiliary system and a more appropriate estimation of the efficiency of the vehicle using the efficiency map, since these two are very significant and case-dependent parameters.

Bibliography

[1] United Nations, "The sustainable development goals." https://www.un.org/sustainabledevelopment/sustainable-development-goals/ (accessed Feb. 10, 2023).

[2] R. A. Lacis,Andrew A.; Schmidt,Gavin A. Rind,David ; Ruedy, "Atmospheric CO2: Principal Control Knob Governing Earth's Temperature," no. October 2010, pp. 356–360, 2011, doi: 10.1126/science.1190653.

[3] "Emissions by sector." https://ourworldindata.org/emissions-by-sector#energy-electricity-heat-and-transport-73-2.

[4] "Greenhouse gas emissions." https://ourworldindata.org/greenhouse-gas-emissions.

[5] European Environment Agency, "Total greenhouse gas emission trends and projections in Europe (8th EAP)." https://www.eea.europa.eu/ims/total-greenhouse-gas-emission-trends.

[6] European Environment Agency, "Greenhouse gas emissions from transport in Europe." https://www.eea.europa.eu/ims/greenhouse-gas-emissions-from-transport.

[7] E. Zammit, A. Covello, C. Leone, M. Longo, W. Yaici, and F. Foiadelli, "Cost and Emission Comparison of Long-Distance Travel and Life-Cycle for EV and ICE Vehicle: a Case Study," *2022 IEEE Int. Conf. Environ. Electr. Eng. 2022 IEEE Ind. Commer. Power Syst. Eur. EEEIC / I CPS Eur. 2022*, 2022, doi: 10.1109/EEEIC/ICPSEurope54979.2022.9854748.

[8] "Electricity Maps." https://app.electricitymaps.com/zone/IT.

[9] G. Bieker, "A new life-cycle assessment of the greenhouse gas emissions of combustion engine and electric passenger cars in major markets," *Int. Counc. Clean Transp.*, no. July, 2021, [Online]. Available: https://theicct.org/publication/a-global-comparison-of-the-life-cycle-greenhouse-gas-emissions-of-combustion-engine-and-electric-passenger-cars/.

[10] M. Zoller, "ICE vehicles vs Electric Vehicles: An Analysis of Lifetime Carbon Emissions," 2019. .

[11] C. Leone, M. Longo, and L. M. Fernández-Ramírez, "Optimal size of a smart ultra-fast charging station," *Electron.*, vol. 10, no. 23, 2021, doi:

10.3390/electronics10232887.

[12] J. Liu, "Research on electric vehicle fast charging station billing and settlement system," *2017 2nd IEEE Int. Conf. Intell. Transp. Eng. ICITE 2017*, pp. 223–226, 2017, doi: 10.1109/ICITE.2017.8056913.

[13] M. Woodward, "Electric Vehicles," pp. 295–320, [Online]. Available: https://www2.deloitte.com/us/en/insights/focus/future-of-mobility/electric-vehicle-trends-2030.html.

[14] International Energy Agency (IEA), "Global EV Outlook 2021 - Accelerating ambitions despite the pandemic," *Glob. EV Outlook 2021*, p. 101, 2021, [Online]. Available: https://iea.blob.core.windows.net/assets/ed5f4484-f556-4110-8c5c-4ede8bcba637/GlobalEVOutlook2021.pdf.

[15] European Council, "'Fit for 55': Council adopts regulation on CO2 emissions for new cars and vans." https://www.consilium.europa.eu/en/press/press-releases/2023/03/28/fit-for-55-council-adopts-regulation-on-co2-emissions-for-new-cars-and-vans/.

[16] International Energy Agency (IEA), "Global EV Outlook 2022 - Securing supplies for an electric future," *Glob. EV Outlook 2022*, p. 221, 2022, [Online]. Available: https://www.iea.org/reports/global-ev-outlook-2022%0Ahttps://iea.blob.core.windows.net/assets/ad8fb04c-4f75-42fc-973a-6e54c8a4449a/GlobalElectricVehicleOutlook2022.pdf.

[17] "Drive Cycle Source." https://it.mathworks.com/help/autoblks/ref/drivecyclesource.html (accessed Apr. 12, 2023).

[18] J. Larminie and J. Lowry, *Electric Vehicle Technology Explained: Second Edition*. 2012.

[19] S. Alegre, J. V. Míguez, and J. Carpio, "Modelling of electric and parallel-hybrid electric vehicle using Matlab/Simulink environment and planning of charging stations through a geographic information system and genetic algorithms," *Renew. Sustain. Energy Rev.*, vol. 74, no. January 2016, pp. 1020–1027, 2017, doi: 10.1016/j.rser.2017.03.041.

[20] "MathWorks Student Competitions Team 2021. MATLAB and Simulink Racing Lounge: Vehicle Modeling." [Online]. Available: https://github.com/mathworks/vehicle-modeling/releases/tag/v4.1.1.

[21] "Calculating Rolling Resistance with a Parametrical Equation." https://simulation-blog.technia.com/simulation/calculating-rolling-resistance-with-a-parametrical-equation.

[22] M. Arat and E. O. Bolarinwa, "Rolling Resistance Effect of Tire Road Contact in Electric Vehicle Systems," *SAE Tech. Pap.*, vol. 2015-April, no. April, 2015, doi:

10.4271/2015-01-0624.

[23] The Engineering ToolBox, "Rolling friction and Rolling resistance." https://www.engineeringtoolbox.com/rolling-friction-resistance-d_1303.html.

[24] A. Kumar, A. Chandekar, P. W. Deshmukh, and R. T. Ugale, "Development of electric vehicle with permanent magnet synchronous motor and its analysis with drive cycles in MATLAB/Simulink," *Mater. Today Proc.*, vol. 72, no. xxxx, pp. 643–651, 2023, doi: 10.1016/j.matpr.2022.08.304.

[25] A. O. Kıyaklı and H. Solmaz, "Modeling of an Electric Vehicle with MATLAB/Simulink," *Int. J. Automot. Sci. Technol.*, vol. 2, no. 4, pp. 9–15, 2019, doi: 10.30939/ijastech..475477.

[26] J. A. Cabrera, J. J. Castillo, J. Pérez, J. M. Velasco, A. J. Guerra, and P. Hernández, "A procedure for determining tire-road friction characteristics using a modification of the magic formula based on experimental results," *Sensors (Switzerland)*, vol. 18, no. 3, 2018, doi: 10.3390/s18030896.

[27] I. Miri, A. Fotouhi, and N. Ewin, "Electric vehicle energy consumption modelling and estimation—A case study," *Int. J. Energy Res.*, vol. 45, no. 1, pp. 501–520, 2021, doi: 10.1002/er.5700.

[28] A. Adegbohun, F.; von Jouanne, A.; Phillips, B.; Agamloh, E.; Yokochi, "High Performance Electric Vehicle Powertrain Modeling, Simulation and Validation.," *Energies*, vol. 14, 1493, 2021, doi: 10.1007/978-3-319-40718-0_8.

[29] I. Evtimov, R. Ivanov, and M. Sapundjiev, "Energy consumption of auxiliary systems of electric cars," vol. 06002, pp. 2–6, 2017, doi: 10.1051/matecconf/201713306002.

[30] A. G. Martin Murnane, "A Closer Look at State of Charge (SOC) and State of Health (SOH) Estimation Techniques for Batteries," *Analog devices*, 2017, [Online]. Available: http://www.analog.com/media/en/technical-documentation/technical-articles/A-Closer-Look-at-State-Of-Charge-and-State-Health-Estimation-Techniques-....pdf.

[31] K. Movassagh, A. Raihan, B. Balasingam, and K. Pattipati, "A critical look at coulomb counting approach for state of charge estimation in batteries," *Energies*, vol. 14, no. 14, pp. 1–33, 2021, doi: 10.3390/en14144074.

[32] J. Schenk, F. Tankstelle, and S. Stang, "Renault Twingo," pp. 62050000–62050000, 2009, [Online]. Available: https://cdn.group.renault.com/ren/it/transversal-assets/brochures/X071VEVP2WE/brochure.pdf.

[33] "Chargemap," [Online]. Available: https://chargemap.com/map.

[34] "Google Maps." https://www.google.it/maps/place/Istituto+di+Istruzione+Secondaria+Superior

e+%22Presta-Columella%22/@40.3708596,18.1252148,12z/data=!4m27!1m20!4m19!1m6!1m2!1s0x13442a02d2adb43d:0xf0c0c07153455392!2sVia+Calvario,+58c,+73019+Trepuzzi+LE!2m2!1d18.0599354!2d4.

[35] "TrackAddict App." https://www.hptuners.eu/product/trackaddict-app/.

[36] "Renault Twingo E-Tech 100% Electric," [Online]. Available: https://cdn.group.renault.com/ren/it/transversal-assets/brochures/X071BMVP2W3/brochure.pdf.

[37] Electric Vehicle Database, "Renault Twingo Electric." https://ev-database.org/car/1270/Renault-Twingo-Electric.

[38] E. Wilhelm, L. Rodgers, and R. Bornatico, "Real-time electric vehicle mass identification," *2013 World Electr. Veh. Symp. Exhib. EVS 2014*, pp. 1–6, 2014, doi: 10.1109/EVS.2013.6914840.

[39] A. D'Hooge, L. Rebbeck, R. Palin, Q. Murphy, J. Gargoloff, and B. Duncan, "Application of Real-World Wind Conditions for Assessing Aerodynamic Drag for On-Road Range Prediction," *SAE Tech. Pap.*, vol. 2015-April, no. April, 2015, doi: 10.4271/2015-01-1551.

[40] Renault Group, "The energy efficiency of an electric car motor." https://www.renaultgroup.com/en/news-on-air/news/the-energy-efficiency-of-an-electric-car-motor/.

[41] Renault Group, "'The best of driving comfort for Twingo Electric with B Mode.'" https://www.renaultgroup.com/en/news-on-air/news/the-best-of-driving-comfort-for-twingo-electric-with-b-mode/.

[42] J. A. Sanguesa, V. Torres-Sanz, P. Garrido, F. J. Martinez, and J. M. Marquez-Barja, "A review on electric vehicles: Technologies and challenges," *Smart Cities*, vol. 4, no. 1, pp. 372–404, 2021, doi: 10.3390/smartcities4010022.

[43] S. Farhad and A. Nazari, "Introducing the energy efficiency map of lithium-ion batteries," *Int. J. Energy Res.*, vol. 43, no. 2, pp. 931–944, 2019, doi: 10.1002/er.4332.

[44] X. Liu, J. Wu, C. Zhang, and Z. Chen, "A method for state of energy estimation of lithium-ion batteries at dynamic currents and temperatures," *J. Power Sources*, vol. 270, pp. 151–157, 2014, doi: 10.1016/j.jpowsour.2014.07.107.

List of Figures

List of Tables